

---

Masters Theses

Student Theses and Dissertations

---

Fall 2022

**LITHOFACIES CHARACTERIZATION OF MARINE SHELF SHALE AND IMPLICAITONS ON DEPOSITIONAL CONDITIONS AND PROCESSES ON THE CONTINENTAL SHELF – A CASE STUDY OF THE UPPER-CRETACEOUS TUSCALOOSA MARINE SHALE IN LOUISIANA AND MISSISSIPPI, U.S.A.**

Efren Mendez Jr  
*Missouri University of Science and Technology*

Follow this and additional works at: [https://scholarsmine.mst.edu/masters\\_theses](https://scholarsmine.mst.edu/masters_theses)



Part of the [Geology Commons](#)

Department:

---

**Recommended Citation**

Mendez Jr, Efren, "LITHOFACIES CHARACTERIZATION OF MARINE SHELF SHALE AND IMPLICAITONS ON DEPOSITIONAL CONDITIONS AND PROCESSES ON THE CONTINENTAL SHELF – A CASE STUDY OF THE UPPER-CRETACEOUS TUSCALOOSA MARINE SHALE IN LOUISIANA AND MISSISSIPPI, U.S.A." (2022). *Masters Theses*. 8146.  
[https://scholarsmine.mst.edu/masters\\_theses/8146](https://scholarsmine.mst.edu/masters_theses/8146)

This thesis is brought to you by Scholars' Mine, a service of the Missouri S&T Library and Learning Resources. This work is protected by U. S. Copyright Law. Unauthorized use including reproduction for redistribution requires the permission of the copyright holder. For more information, please contact [scholarsmine@mst.edu](mailto:scholarsmine@mst.edu).

LITHOFACIES CHARACTERIZATION OF MARINE SHELF SHALE AND  
IMPLICATIONS ON DEPOSITIONAL CONDITIONS AND PROCESSES ON THE  
CONTINENTAL SHELF — A CASE STUDY OF THE UPPER-CRETACEOUS  
TUSCALOOSA MARINE SHALE IN LOUISIANA AND MISSISSIPPI, U.S.A.

by

EFREN MENDEZ JR

A THESIS

Presented to the Graduate Faculty of the  
MISSOURI UNIVERSITY OF SCIENCE AND TECHNOLOGY

In Partial Fulfillment of the Requirements for the Degree  
MASTER OF SCIENCE IN GEOLOGY AND GEOPHYSICS

2022

Approved by:

Wan Yang, Co-Advisor  
David Borrok, Co-Advisor  
David Wronkiewicz

© 2022

Efren Mendez Jr

All Rights Reserved

## ABSTRACT

The Upper Cretaceous Tuscaloosa Marine Shale (TMS) is an unconventional shale reservoir deposited on the continental shelf of the northern Gulf of Mexico Basin. Previous studies have focused on sequence stratigraphy, thermal modeling, and well-log correlations. However, a limited understanding of the stratigraphic heterogeneity of the TMS is yet to be studied. This study aims to characterize the stratigraphic heterogeneity of the TMS using core, petrographic, and well-log analyses to better understand the depositional conditions and processes that occur on the continental shelf. The TMS has been classified into four lithofacies of very fine sands – coarse silts (LF1), medium-fine silt (LF2), fine silt–clay (LF3), and microbial-algal deposits (LF4). LF1 is characterized by an erosional base and well-developed stratification, indicating tractional deposition by density currents. LF3 is characterized by a sharp or gradational base and sub-mm planar laminations, interpreted as pelagic deposits. LF2 is transitional between LF1 and 3. LF4 is characterized by a sharp or gradational base and discontinuous, poorly defined, pyrite and calcite replaced wavy laminations, interpreted as biogenically influenced deposits or organic. XRD analyses suggests variations in minerals, such as quartz, calcite, and total clay in all LF. The variability in mineralogy and sedimentary fabrics suggests that conditions on the continental shelf were oxygenated and later became anoxic, depositing organic-rich shales. Weak relationships in LF and wireline logs were found, suggesting challenges in identifying LF in wireline log signatures. The results of this study can improve the LF classification of the TMS and the understanding of depositional processes and conditions on the continental shelf.

## ACKNOWLEDGMENTS

I would like to thank Dr. Wan Yang, my advisor, for his guidance and philosophical views in science and life. His mentorship made me a better scientist and a better person. I would also like to thank my other committee members, Dr. David Wronkiewicz for his guidance. As well Dr. David Borrok who provided me the opportunity to pursue a graduate degree and work in a fun and complex project! To Dr. Mokhtari and Philip Wortman from University of Louisiana Lafayette I would like to thank them for allowing me to be part of the project. I would like to thank my lab mates and friends who helped me throughout my degree and had fun times outside of class.

I would like to thank Dr. David Moss, my undergraduate advisor at Sam Houston State University, who pushed me and believed in me to pursue a graduate degree.

I would like to give a huge thanks to my industry mentors during my internships at Pioneer Natural Resources and Chevron who gave me the opportunity of a lifetime to learn new skills and explore my curiosity. Rachelle Roper and Caitlin Leslie and David Wheatley and Christopher Johnson who all guided me to become a better geologist and work on fun and technical projects.

Finally, I would like to thank my parents and sister for their unconditional support throughout my time at Missouri S&T. As a first-generation college graduate of immigrant parents I couldn't have done it without them. As we say in Mexico, "*¡Sí se puede, Sí se pudo!*"

## TABLE OF CONTENTS

	Page
ABSTRACT.....	iii
ACKNOWLEDGMENTS .....	iv
LIST OF ILLUSTRATIONS.....	viii
LIST OF TABLES.....	xi
NOMENCLATURE .....	xii
 SECTION	
1. INTRODUCTION.....	1
1.1 SHALE REVOLUTION .....	1
1.2 HISTORY OF TUSCALOOSA MARINE SHALE .....	1
1.3 RESEARCH GAP .....	3
1.4 RESEARCH OBJECTIVE.....	4
2. GEOLOGICAL SETTING.....	5
2.1 STRUCTURAL FRAMEWORK.....	5
2.2 STRATIGRAPHY AND SEDIMENTOLOGY.....	7
2.2.1. Lower Tuscaloosa Formation .....	7
2.2.2. Lower Tuscaloosa - Massive Member .....	8
2.2.3. Lower Tuscaloosa - Stringer Sand .....	8
2.2.4. Lower Tuscaloosa - Pilot Sand.....	8
2.2.5. Tuscaloosa Marine Shale.....	9
2.2.6. Upper Tuscaloosa.....	9

3. DATA AND METHODOLOGY .....	11
3.1 DATA.....	11
3.2 METHODOLOGY.....	12
3.2.1. Core Descriptions .....	14
3.2.2. Scanning Electron Microscopy (SEM).....	14
3.2.3. Elemental Mapping.....	15
3.2.4. Thin Section Microscopy.....	15
4. RESULTS.....	17
4.1 TYPES OF LITHOFACIES.....	17
4.1.1. Bedload Lithofacies (LF1).....	18
4.1.2. Mixed Lithofacies (LF2) .....	20
4.1.3. Pelagic Lithofacies (LF3) .....	23
4.1.4. Organic Lithofacies (LF4) .....	23
4.2 TUSCALOOSA MARINE SHALE FACIES MODEL.....	27
4.3 LITHOFACIES DISTRIBUTIONS .....	27
4.4 MINERALOGY AND ORGANIC CONTENT LITHOFACIES CHARACTERIZATION.....	28
4.4.1. Bedload Facies (LF1) .....	30
4.4.2. Mixed Facies (LF2) .....	30
4.4.3. Pelagic Facies (LF3).....	31
4.4.4. Organic Facies (LF4).....	31
4.5 RESULTS OF SCANNING ELECTRON MICROSCOPY AND ENERGY DISPERSIVE X-RAY SPECTROSCOPY ANALYSES .....	36
4.5.1. Sample TMS-1-S1 .....	36

4.5.2. Sample TMS-7-S1 .....	40
4.6 WELL LOG SIGNATURES OF LITHOFACIES .....	41
4.6.1. Gamma Ray (GR).....	41
4.6.2. Deep Resistivity .....	42
5. DISCUSSION .....	46
5.1 GENERAL STATEMENT.....	46
5.2 DEPOSITIONAL PROCESSES .....	46
5.2.1. Tractional Deposits.....	46
5.2.2. Deposits of Wave-Enhanced Sediment-Gravity Flows .....	47
5.2.3. Fine-grained Turbidite Deposits .....	47
5.2.4. Tempestites.....	48
5.2.5. Current – Reworked .....	50
5.2.6. Pelagic Deposits .....	51
5.2.7. Biogenic Deposits.....	51
5.3 DEPOSITIONAL CONDITIONS.....	52
6. CONCLUSION .....	57
APPENDICES	
A. XRD AND TOC DATA.....	59
B. WIRELINE LOG DATA.....	66
C. LITHOFACIES DATA.....	99
BIBLIOGRAPHY .....	168
VITA .....	174

## LIST OF ILLUSTRATIONS

Figure	Page
1.1 Map of the United States shale plays and basins. ....	2
1.2 Regional map showing coverage of the Tuscaloosa Marine Shale and location of studied wells.....	3
2.1 Paleogeographic maps of North America during the Mesozoic.....	6
2.2 Generalized Cretaceous stratigraphic columns in Louisiana and Mississippi. ....	7
3.1 Regional map showing locations of cored wells with mineralogical and TOC data used in this study.....	12
3.2 Lithofacies classification and nomenclature for the Tuscaloosa Marine Shale from core descriptions and observations. ....	13
3.3 Lithofacies logs of all cored wells .....	13
3.4 Example of a core log from core #6.....	16
4.1 Photographs of core lithofacies from left to right (Bedload Facies, Mixed Facies, Pelagic Facies, and Organic Facies). ....	17
4.2 Photograph of Core #11 of a LF1 rich interval.....	19
4.3 On the left is a core image of LF1 rich interval and the sample location of the thin section taken (red box).....	20
4.4 On the left is a core photograph of LF1 and the sample location of the thin section taken (red box) photomicrograph of bedload lithofacies, modified from Weatherford Laboratories. ....	21
4.5 Core image of LF2 from Core #1 with a yellow box representing thin section sample.....	22
4.6 Core image of LF2 from Core #1 with a purple box representing thin section sample.....	22
4.7 Photograph of Core #5 of vertical and horizontal fractures in the TMS. ....	24

4.8 Core image of a LF3 interval from Core #1 and thin section sample (yellow box). ..	25
4.9 Core image of a LF3 interval from Core #1 with a yellow box representing the thin section sample.....	25
4.10 Core image of a LF3 interval from Core #5 with a white box representing the thin section sample.....	26
4.11 Typical TMS facies model based on core observations.....	28
4.12 Pie charts of lithofacies distribution of cored wells.....	29
4.13 Core lithofacies classification scheme for organic-rich shales for all five cores.....	30
4.14 Box plots showing the mineralogy and TOC content in all cored wells .....	32
4.15 Mineralogy data obtained through X-ray diffraction analysis of core samples for the wells in the study.....	33
4.16 (A) SEM image of a LF3 and microfacies 3a sample from Core #1.....	37
4.17 Elemental maps for Sample TMS-1-S1 from Core #1.....	38
4.18 Energy Dispersive X-Ray Spectrum (EDS) analysis for Point 1 in Sample TMS-1-S1 from Core #1.....	39
4.19 Energy Dispersive X-Ray Spectrum (EDS) analysis for Point 2 in Sample TMS-1-S1 from Core #1.....	39
4.20 SEM images of LF4 from Core #7 (C) Point 3 SEM-EDS analysis.....	40
4.21 Energy Dispersive X-Ray Spectrum (EDS) analysis for Point 3 in sample TMS-7-S1 from Core #7.....	41
4.22 Photograph of Core #7 of a LF4 rich interval.....	43
4.23 Histograms showing the gamma ray values of lithofacies.....	44
4.24 Histograms showing the range of resistivity values of lithofacies. ....	45
4.25 Photographs from Core #6 of wave-enhanced sediment gravity flows (WESGF)...	48
4.26 Photograph of Core #11 near the base of the core, showing multiple fine-grained turbidite packages in a LF1 interval.....	49

4.27 Photograph of Core #11 near the base of the core of multiple turbidite packages in a LF1 interval.....	50
4.28 Photographs showing examples of tempestites from Core #1.....	51
4.29 Photograph of Core #5 and current – reworked deposits lamina sets.....	53
4.30 Photograph showing an example of algal/microbial laminae (yellow arrows) in a LF4-rich interval in Core #7 .....	54
4.31 Photograph of Core #7, showing wavy, irregular, and wrinkly laminations of a biogenic origin. ....	55
4.32 Photographs showing heavily bioturbated LF1 intervals near the base of Core #11.....	56

**LIST OF TABLES**

Table	Page
3.1 Data availability of cores. ....	11
4.1 Lithofacies and Microfacies Summary. ....	26
4.2 Compiled statistics of mineralogy and TOC by lithofacies . ....	34

**NOMENCLATURE**

Symbol	Description
TMS	Tuscaloosa Marine Shale
GOM	Gulf of Mexico basin
HRZ	High Resistivity Zone
USGS	United States Geological Survey
TOC	Total Organic Carbon
LF	Lithofacies
LF1	Bedload Lithofacies
LF2	Mixed Lithofacies
LF3	Pelagic Lithofacies
LF4	Organic Lithofacies
SEM	Scanning Electron Microscopy
BSE	Back scattered electrons
EDS	Energy Dispersive X-ray spectroscopy
wt%	Weight Percentage
WESGF	Wave Enhanced Sediment Gravity Flows
SHSU	Sam Houston State University
Missouri S&T	Missouri University of Science and Technology

## **1. INTRODUCTION**

### **1.1 SHALE REVOLUTION**

Organic-rich shales are generally source rocks for hydrocarbons in conventional reservoirs. However, at the beginning of the 21st century, the advancement in drilling and hydraulic fracking sparked a new era for the oil and gas industry. Technological advances led to the production of hydrocarbons from tight organic-rich shales. Although technology has advanced, shale sedimentology and stratigraphy has not yet caught up. In the past decade, shale research and reservoir characterization have become an active research subject in the geosciences to understand the hydrocarbon potential of shale reservoirs. Research has been done on prolific shale plays in the United States, such as the Barnett Shale, Eagle Ford Shale and Wolfcamp formation in Texas, the Bakken Shale in the Northern United States, and the Marcellus Shale in the Northeastern United States (Figure 1.1; U.S. Energy Information Administration, 2016).

### **1.2 HISTORY OF TUSCALOOSA MARINE SHALE**

The Tuscaloosa Marine Shale (TMS) is a prospective unconventional shale reservoir located in the southern central gulf coast of the United States (Figure 1.2). Alfred C. Moore was one of the earliest geoscientists to suggest that the TMS has a hydrocarbon potential (Borrok et al., 2019). In 1997, John et al. (1997) labeled the TMS as a significant potential unconventional play with an “unproven” estimated seven-billion-barrel recoverable oil resource (Berch, 2013). A recent geologic assessment

conducted by the United States Geological Survey (USGS) suggests that the TMS has a technically recoverable reserve of 1.5 billion barrels of oil and 4.6 trillion cubic feet of gas (Figure 1.2; Hackley et al., 2018). Although it is not the original “seven-billion-barrel recoverable oil resource” John et al. (1997) suggested, the TMS serves as a potentially significant resource for shale oil and gas.

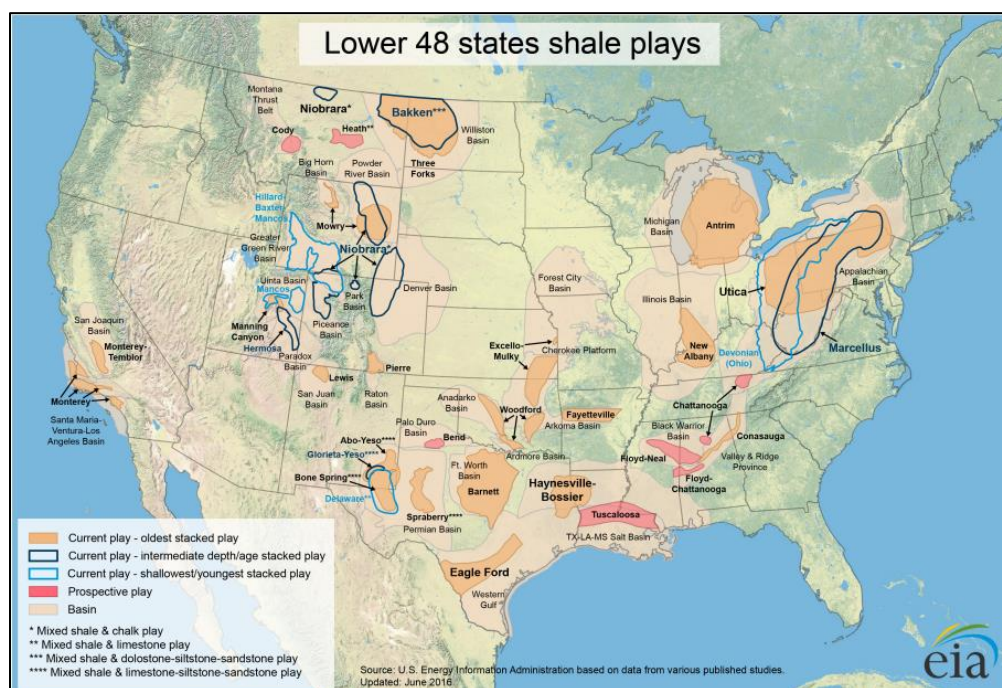


Figure 1.1: Map of the United States shale plays and basins (U.S. Energy Information Administration, 2016)

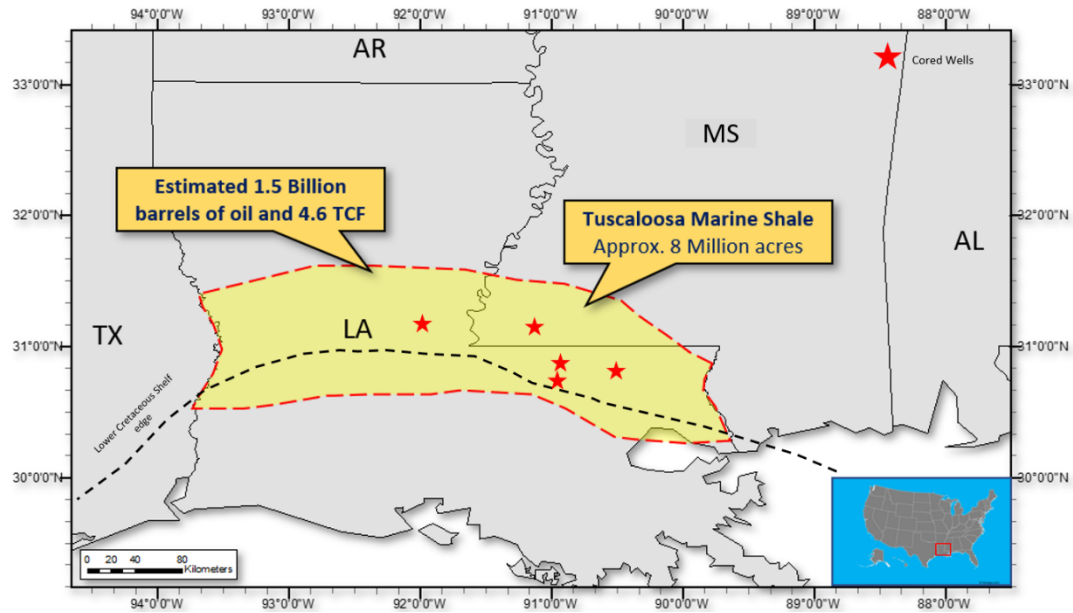


Figure 1.2: Regional map showing coverage of the Tuscaloosa Marine Shale and location of the studied wells.

### 1.3 RESEARCH GAP

Poor production results and limited understanding of the TMS relative to other shale plays (e.g., Marcellus Shale and Eagle Ford Shale) have led to low drilling activities in the past few years. The negative results can be attributed to the limited understanding of the stratigraphic heterogeneity in the TMS to identify hydrocarbon sweet spots. The challenge is, for example, the grain size of the shaly sediments. Shales are composed of clay - sized particles that are less than 4 microns and, therefore, are difficult to characterize without using high-power microscopes or geochemical analysis.

Previous work on the TMS has addressed issues on the sequence stratigraphy, production, thermal modeling, and geochemical characterization (Liu, 2005; Berch, 2013; Lohr et al., 2016; Pair, 2017; Borrok et al., 2019; Hackley et al., 2020; Lohr et al., 2020).

However, there is no lithofacies classification for the TMS to be used to describe cores from different locations, nor an attempt to quantify the stratigraphic heterogeneity using multi-scale datasets. Therefore, this study will use core, petrographic, and geochemical analyses will provide insight into the variations of texture, mineralogy, and petrophysical properties that can be used to understand the stratigraphic heterogeneity.

#### **1.4 RESEARCH OBJECTIVE**

This thesis research aims to characterize the TMS stratigraphic heterogeneity to better understand the depositional conditions and processes on the continental shelf.

## 2. GEOLOGICAL SETTING

### 2.1 STRUCTURAL FRAMEWORK

The TMS was deposited on the continental shelf of the Northern Gulf of Mexico basin (GOM; Warner 1993; Fearn, 2019). During the Late Triassic – Early Jurassic, rifting of Pangea led to two major episodes of rifting in the GOM (Berch, 2013; Weitkunat, 2015). The first episode occurred during the Early Jurassic, resulting in extensional faulting dominated the passive margin of the GOM (Figure 2.1A; Galloway, 2008; Mancini et al., 2008; Berch, 2013; Weitkunat, 2015; Pair, 2017). The second episode of rifting occurred in the Middle – Late Jurassic, leading to saline waters from the proto-Atlantic flooding the basin (Figure 2.1B; Scott, 2010; Pair, 2017). By the Early Cretaceous, rifting had halted and a waterway connecting the Atlantic Ocean and GOM known as the Cretaceous Interior Seaway formed.

A series of structural uplifts, such as the Wiggings Arch, Sabine Uplift, Monroe Uplift, and LaSalle Arch, Angelina-Caldwell Flexure and three depocenters such as the North Louisiana Salt Basin, the East Texas Basin, and Mississippi Interior Salt Basin had developed in south-central GOM during the two tectonic episodes. (Mancini et al., 2008; Fearn, 2019). These topographic features influenced the distribution and thickness of sedimentary units in the region (Mancini et al., 2008).

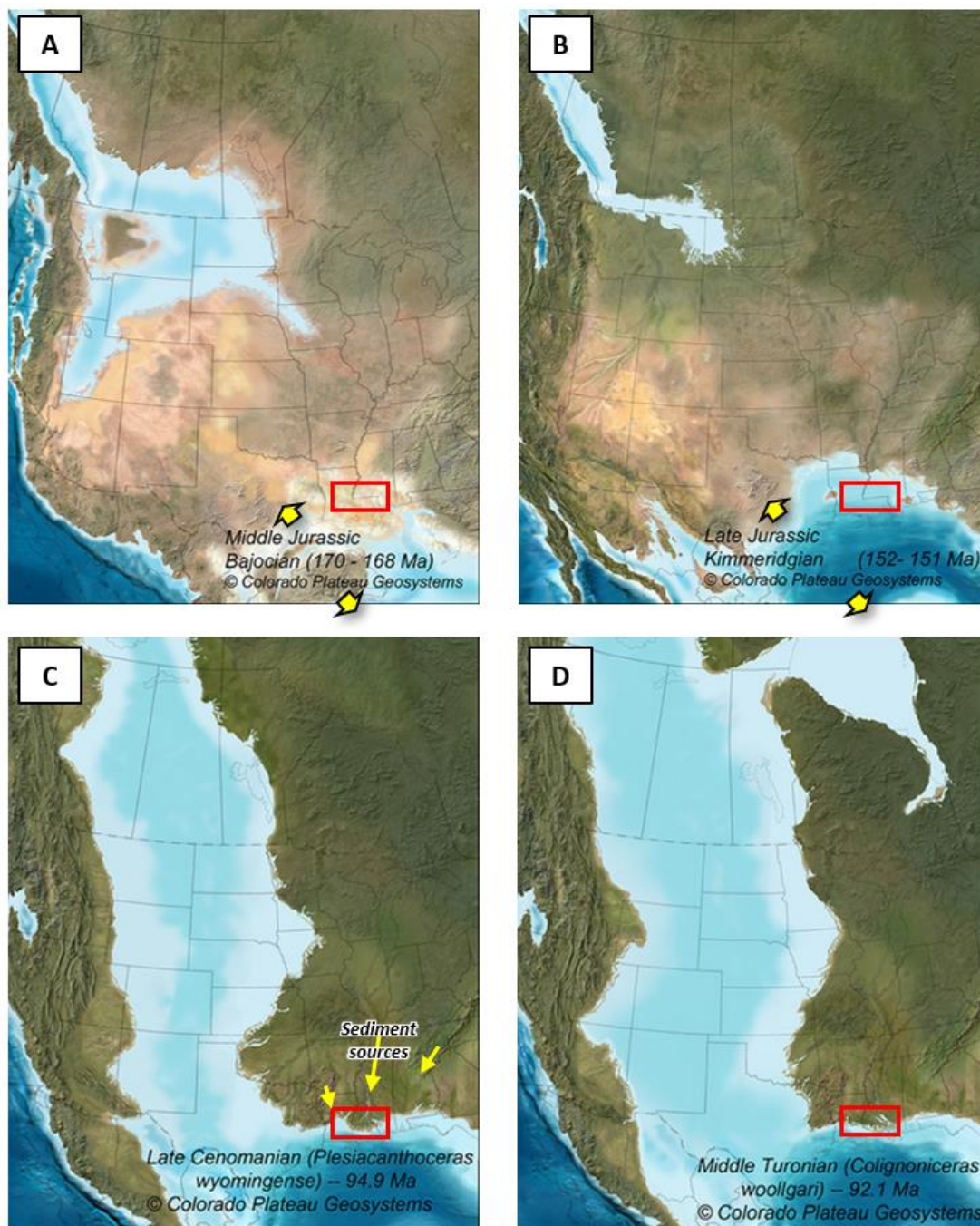


Figure 2.1 (A-D): Paleogeographic maps of North America during the Mesozoic. Red box highlights the study area (Modified from Colorado Plateau Geosystems)

## 2.2 STRATIGRAPHY AND SEDIMENTOLOGY

The Upper Cretaceous TMS is the middle of three formations in the Tuscaloosa Group (Spooner, 1964; Enomoto et al., 2017). The lower Tuscaloosa, middle Tuscaloosa or TMS, and the upper Tuscaloosa (Spooner, 1964; Dockery, 1996; John et al., 1997; Mancini and Puckett, 2003, 2005; Dockery and Thompson, 2016; Enomoto et al., 2017). The Tuscaloosa Group is representative of an entire transgressive-regressive cycle wherein the TMS was deposited during the transgression (Galloway, 2008).

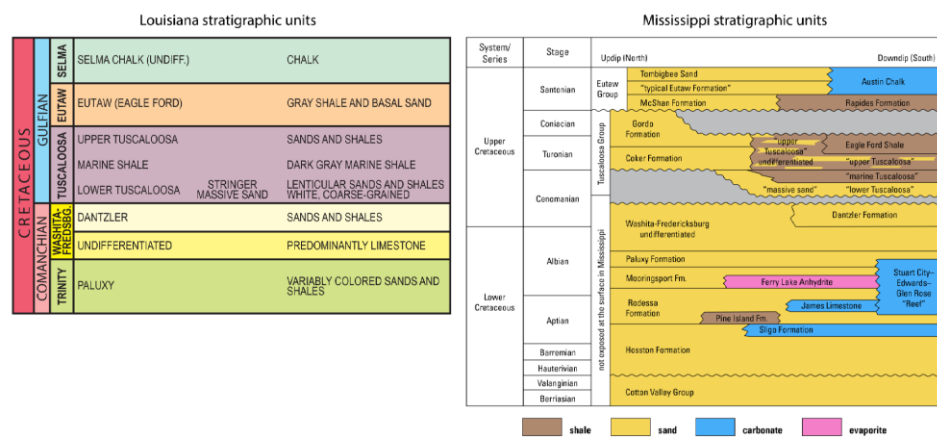


Figure 2.2: Generalized Cretaceous stratigraphic columns in Louisiana and Mississippi (Enomoto et al., 2017).

**2.2.1. Lower Tuscaloosa Formation.** The Lower Tuscaloosa basal unit was deposited in the early Cenomanian of the Late Cretaceous. Unconformably, it overlies the Albian-aged Dantzler Formation (Figure 2.2). The Lower Tuscaloosa trends in the subsurface from Southern Louisiana and Mississippi to Florida are exposed on outcrops

in Alabama. Thickness varies from 120 feet in outcrops to 2800 feet downdip in the subsurface due to faulting in the region (Parker, 1984; Corcoran et al., 1993).

Depositional environments of the Lower Tuscaloosa have been interpreted as fluvial – deltaic (Figure 2.1C; Karges, 1962; Gruebel, 1985; Minter et al., 1992). Additionally, Snedden et al. (2016), mapped deep-water sands identified as Lower Tuscaloosa in offshore Louisiana (Lowery et al., 2017).

**2.2.2. Lower Tuscaloosa - Massive Member.** The Lower Tuscaloosa can be further divided into the lowermost Massive, Stringer, and Pilot members (Figure 2.2; Mancini et al., 1980; Woolf, 2012). The Massive Member is dominated by fluvial channel fills consisting of basal pebble lags, cross-bedding, and mud drapes. (Berg and Cook, 1968; Chasteen, 1983; Woolf, 2012).

**2.2.3. Lower Tuscaloosa - Stringer Sand.** The overlying Stringer Sand is composed of grey shales interbedded with siltstone and sandstone with intense bioturbation and oyster fossils, indicating a nearshore environment and well-oxygenated condition for benthic organisms (Drennen, 1953; Chasteen, 1983; Woolf, 2012). However, these evident marine features are mostly present downdip where there was a stronger marine influence (Drennen, 1953; Chasteen, 1983 Woolf, 2012).

**2.2.4. Lower Tuscaloosa - Pilot Sand.** The uppermost member in the Lower Tuscaloosa, the Pilot Sand, is composed of reddish – white – light brown, massive to cross-bedded sandstone. It has been interpreted from well logs and cores to be deposited in the shoreface to proximal shelf environment (Berg and Cook, 1968; Mancini et al., 1980; Hamilton and Cameron, 1986; Woolf, 2012).

**2.2.5. Tuscaloosa Marine Shale.** Conformably overlying the Lower Tuscaloosa is the TMS (Figure 2.2). The TMS was deposited during a major transgression on the continental shelf of the GOM in the Cenomanian – Turonian ages (Figure 2.1D; Spooner, 1964; Dockery, 1996; John et al., 1997; Mancini and Puckett, 2003, 2005; Liu, 2005; Dockery and Thompson, 2016; Enomoto et al., 2017; Lowery et al., 2017). The TMS comprises of dark gray to black mm-sub-mm well-laminated shale and siltstone (Pair, 2017). Although the TMS is composed of dominantly organic-rich black shales, core observations suggest the TMS contains many tractional deposits.

An ocean anoxic event (OAE) refers to the occurrence of anoxic ocean bottom water in a short period, which is inferred by the preservation of a large amount of organic matter in the sediments and may be related to high concentration carbon dioxide (CO<sub>2</sub>) in the atmosphere due to increased volcanic activities (Dale et al., 2012; Stone, 2019). The increase in atmospheric CO<sub>2</sub> content leads to a warmer climate that enhances weathering on the continent. A high weathering rate would increase the nutrient and sediment influx into the ocean and increase the marine productivity, leading to an anoxia at the ocean bottom and preservation of a large amount of organic matter in the shales (Holmden et al., 2016; Lowery et al., 2017). The second event of OAE (OAE2) is interpreted to have occurred during the Cenomanian – Turonian time and correlates to the deposition of the Upper Cretaceous Eagle Ford Shale in Texas and TMS (Dale et al., 2011; Eldrett et al., 2015; Alnahwi and Loucks, 2019; Stone, 2019).

**2.2.6. Upper Tuscaloosa.** The uppermost unit, Upper Tuscaloosa, conformably overlies the TMS and unconformably underlies the Eutaw Formation or Austin Chalk in some regions (Figure 2.1). It is composed of bioturbated shales and regressive sandstones

(Spooner, 1964; Hogg 1988; Lohr et al., 2020). The Upper Tuscaloosa was deposited during a sea-level high-stand when the shoreline regressed, and sediment influx increased through outpouring sediments through deltaic sediments across the continental shelf (Barrel, 1997; Allen, 2013)

### 3. DATA AND METHODOLOGY

#### 3.1 DATA

Five cored wells were provided by Goodrich Petroleum Company, Devon Energy, and Halcon Resources (now Battalion Oil; Figure 3.1). Mineralogy, analyzed via X-ray diffraction (XRD), and total organic carbon (TOC) analyzed samples from cores were provided by the following laboratories: Weatherford®, OMNI Laboratories (now Weatherford), Core Laboratories®, GeoMark®, and TerraTek Inc. (now SLB). Thin sections of cores and some images were provided by Devon Energy and Weatherford®. Petrographic analyses were performed in the Advanced Materials Characterization Laboratory at Missouri University of Science and Technology. Table 3.1 summarizes the data availability of this study.

Table 3.1 Data availability of cores

Core Number	Mineralogy and TOC	SEM	Thin Sections	Wireline Logs
#1	X	X	X	X
#5	X		X	
#6	X		X	X
#7	X	X		X
#11	X			

### 3.2 METHODOLOGY

This study was conducted in two phases. The first phase consisted of describing five cores across Louisiana and Mississippi (Figure 3.1). Lithofacies were classified based on the percentage of tractional (sediment gravity and current flow) deposits and biogenic particles averaged over an interval (Figure 3.2; Yang et al., 2020). Lithofacies were classified, interpreted, and recorded. Facies logs were then imported into Petrel 2017 software for wireline log calibrations (Figure 3.3).

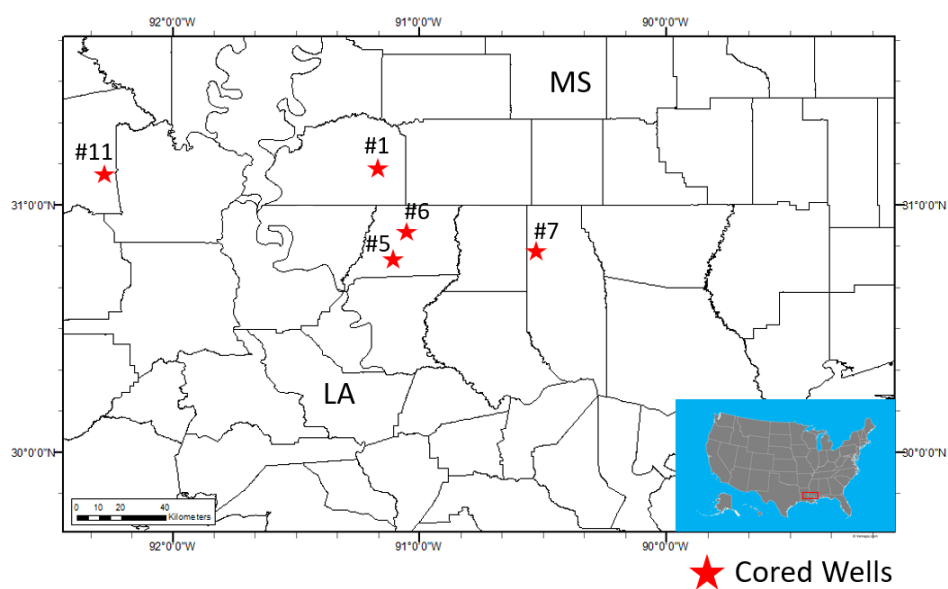


Figure 3.1: Regional map showing locations of cored wells with mineralogical and TOC data used in this study.

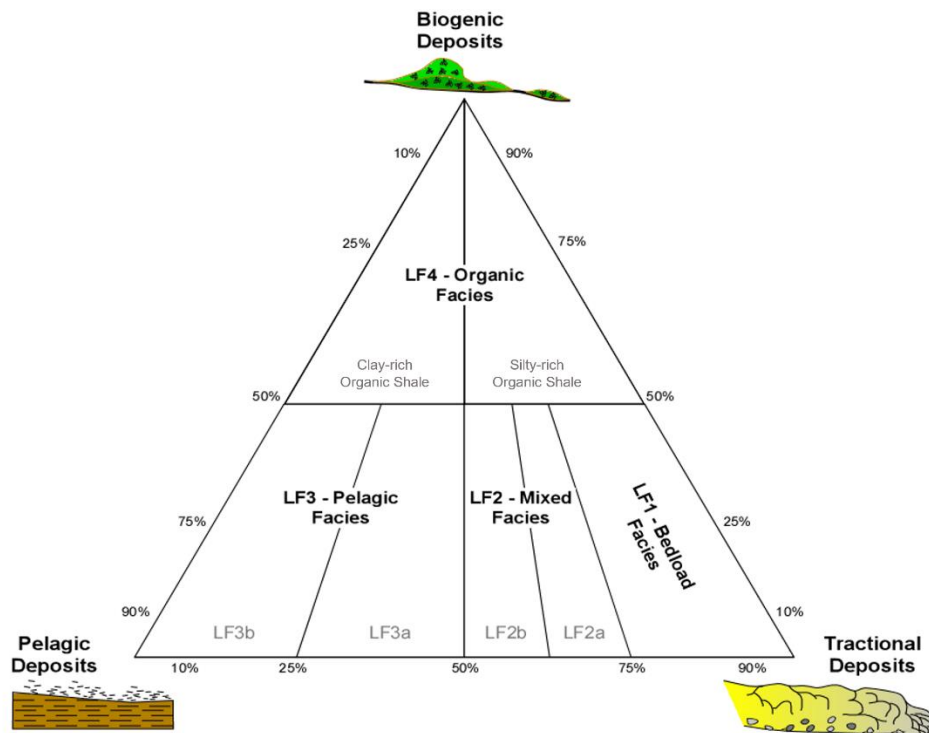


Figure 3.2: Lithofacies classification and nomenclature for the Tuscaloosa Marine Shale from core descriptions and observations (Modified from Yang et al., 2020).

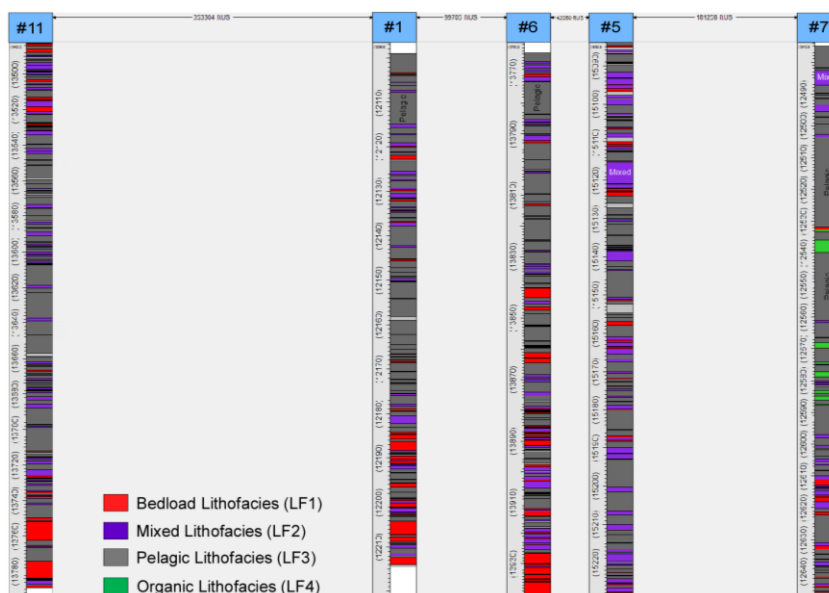


Figure 3.3: Lithofacies logs of all cored wells.

In the second phase, geochemical, mineralogical, petrographic and wireline log data were used to characterize the stratigraphic heterogeneity of the lithofacies and TMS. Thin sections and SEM images were used to further characterize the texture of microfacies and lithofacies. Mineralogical data and SEM-EDS elemental maps were used to characterize the elemental chemistry of different lithofacies.

**3.2.1. Core Descriptions.** A total of 975 ft (~297 m) of rock cores were described from five slabbed cores. Core descriptions included: parasequences, core images, type of contact, color, % of fine silt and clay, grain size, type of cement, thickness and geometry of laminations, sedimentary structures, bioturbation, mineralogy, fracture geometry, bed type, and depositional trends (Figure 3.4).

**3.2.2. Scanning Electron Microscopy (SEM).** SEM imaging was conducted on one core sample from Core #7 (TMS-7-S1) and a thin section from Core #1 (TMS-1-S1) using the PRISMA Variable Pressure SEM (FIGURE of SEM). Sample selection was based on efficiently capturing all facies and preventing further destruction of core and thin section samples. Core #7 was chosen due to its distal shelfward location, in order to best capture and characterize Lithofacies 4 (LF4). While Core #1 was selected due to its shelfward proximal location, in order to capture and characterize Lithofacies 3 (LF3). The samples were prepared by mounting them on a pin stub using a double-sided piece of tape. The samples were then braced by a long thin piece of copper tape that allowed the sample to be conductive enough. The samples were then placed into a Denton Desk V sputter coater for 45 seconds to be covered in a thin coating of Gold/Palladium (Au/Pd). The coating allows non-conductive materials to become conductive enough for SEM imaging. Both samples were inserted into the SEM and to be imaged and characterized to

identify and document the sedimentary texture and mineralogy. High-resolution imaging provided insights into the microscopic stratigraphic heterogeneity in mineral composition and texture of the samples.

**3.2.3. Elemental Mapping.** Elemental mapping was conducted using the Color SEM tool in the PRISMA Variable Pressure SEM in the AMCL at Missouri University of Science and Technology. This is to document type and distribution of various elements and inferred mineralogy in different facies. Energy Dispersive X-Ray Spectrum (EDS) was conducted on samples to quantify and identify the elemental composition of the minerals.

**3.2.4. Thin Section Microscopy.** A total of seven thin sections from Cores #1 and #5 were described and interpreted for mineralogic, textural, and structural characteristics of microfacies. High-resolution images were taken using a digital LECIA microscope. A petrographic microscope was also used to characterize grain size and shape, sedimentary structures, and fossils.

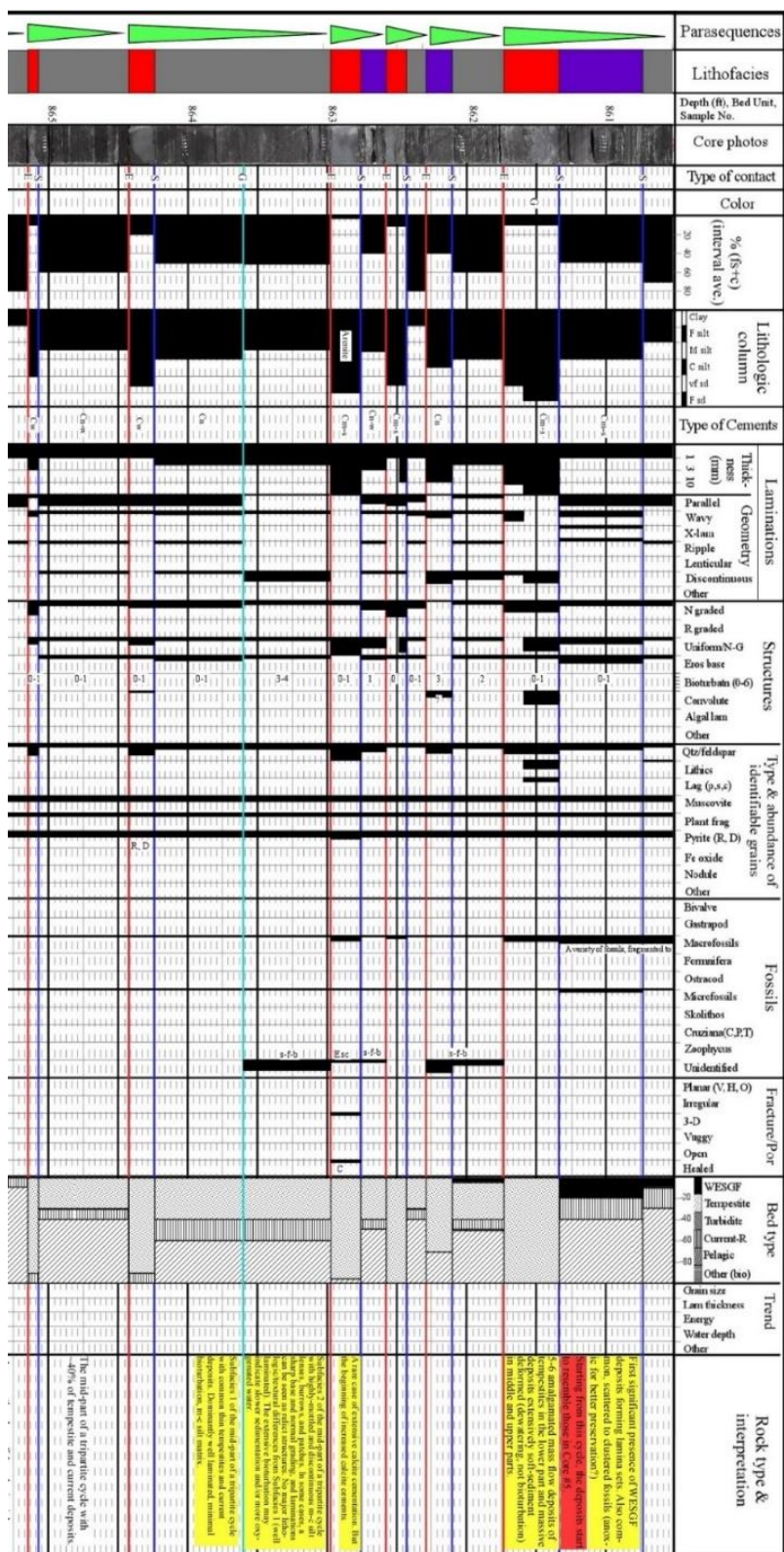


Figure 3.4: Example of a core log from core #6.

## 4. RESULTS

### 4.1. TYPES OF LITHOFACIES

Four lithofacies (LF) were recognized based on the average percentage of bedload deposits in a cored interval: 1) Bedload Facies (LF1); 2) Mixed Facies (LF2); 3) Pelagic Facies (LF3); 4) Organic Facies (LF4; Figure 4.1). LF1-3 are present throughout the entire cored intervals. However, LF4 was only documented in Core #7 and in a 50-ft interval near the base of the TMS, about 70 ft above the base of the core. The frequency and occurrence of facies indicate the changes in depositional conditions and sedimentary processes. Thin sections allowed to further characterize these changes. Table 4.1 is a summary of all lithofacies in the TMS.

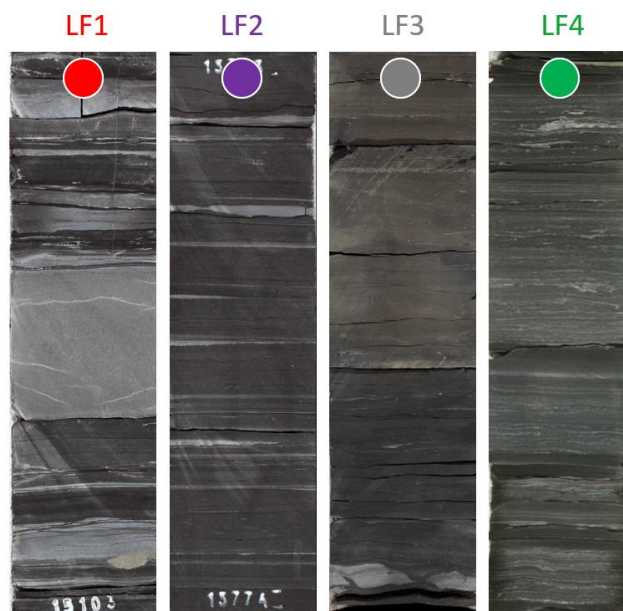


Figure: 4.1: Photographs of core lithofacies from left to right (Bedload Facies, Mixed Facies, Pelagic Facies, and Organic Facies).

**4.1.1. Bedload Lithofacies (LF1).** LF1 is an interval rich in siliciclastic siltstone and contains greater than 75% of tractional deposits (Figure 3.2; 4.1). The interval is 10 mm and up to 3 meters thick where amalgamated. LF1 is massive to well laminated. The laminations are parallel, cross laminated, climbing ripple laminated. It is commonly calcareous, and variably bioturbated. Individual tractional deposits are light gray to gray and centimeters thick. The lateral extent is limited by the width of the core, but mostly horizontal with a mm-cm relief. In thin sections, LF1 is composed of mostly quartz and calcite with traces of mudclast, foraminifera, and contain unevenly distributed framboidal pyrite. A typical LF1 has an erosional base and a sharp to gradational top. Normal grading is the most common type of bedding with the coarsest sediments at the base fining upwards. In addition, dewatering structures are present. Trace fossils are common near the base and top of the cores where coarse siltstones and very fine sandstones and are mainly *skolithos* and minor *cruziana* (Figure 4.2). This lithofacies is present throughout the cored intervals of all wells. It is abundant and up to 3 meters thick near the base of all cores and decreases in abundance and thickness upward from the base.

LF1 consists of two distinct microfacies: 1A) poorly laminated siltstone; 1B) massive siltstone. Both microfacies contain quartz-rich framework grains and a basal erosional boundary and an upper transitional to sharp boundary (Figure 4.3; 4.4).

Microfacies 1a is massive to poorly laminated, well sorted, and calcite cemented. The dominant mineralogy is quartz and calcite. A trace amount of muscovite and pyrite are present. Pyrite crystals form aggregates with a framboidal morphology. Microfacies 1B contains medium to coarse silts and laminated, loosely packed, and moderately sorted.

It is calcite cemented within the siltstone laminae. The dominant grains are quartz.

Secondary grain types are framboidal pyrite, muscovite, and foraminifera.

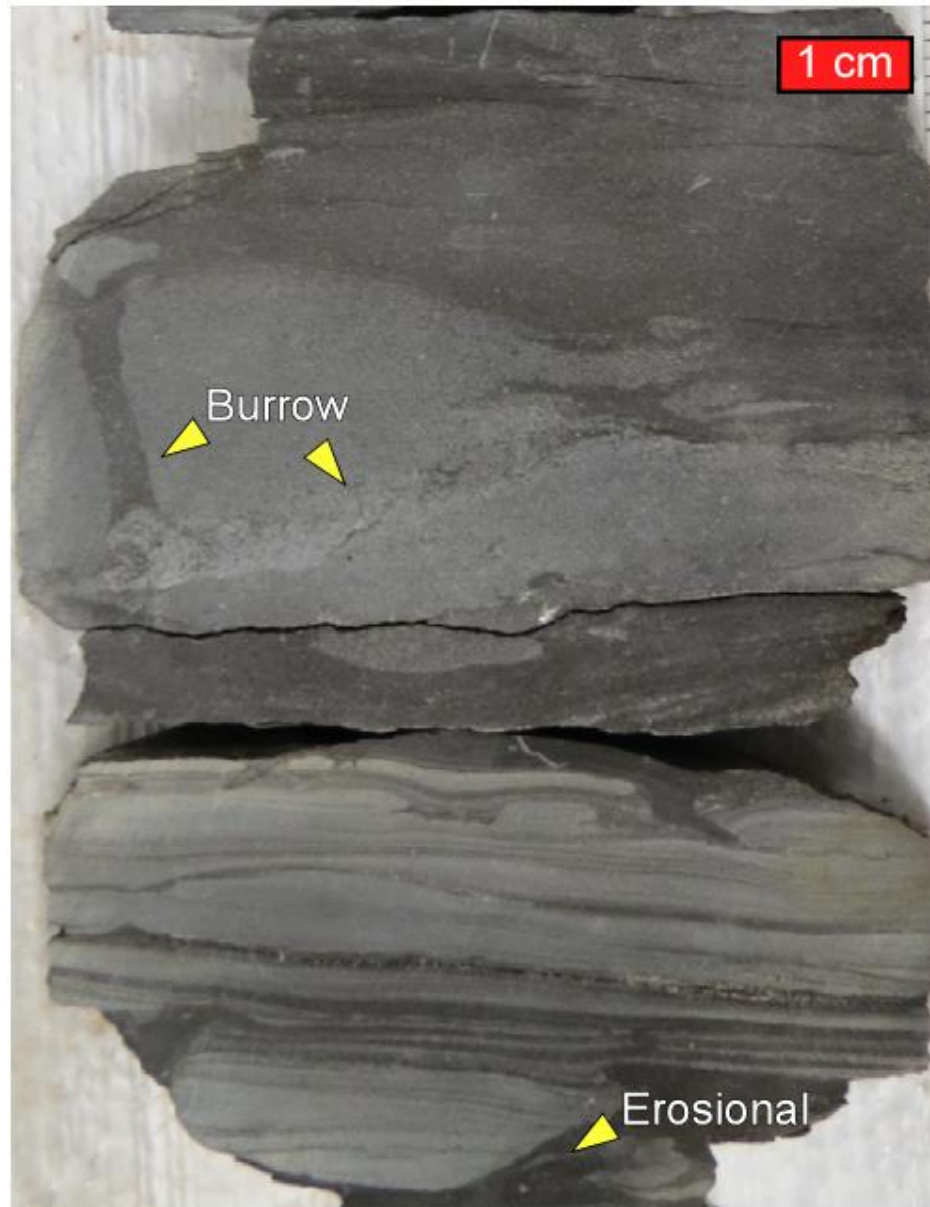


Figure 4.2: Photograph of Core #11 of a LF1 rich interval.

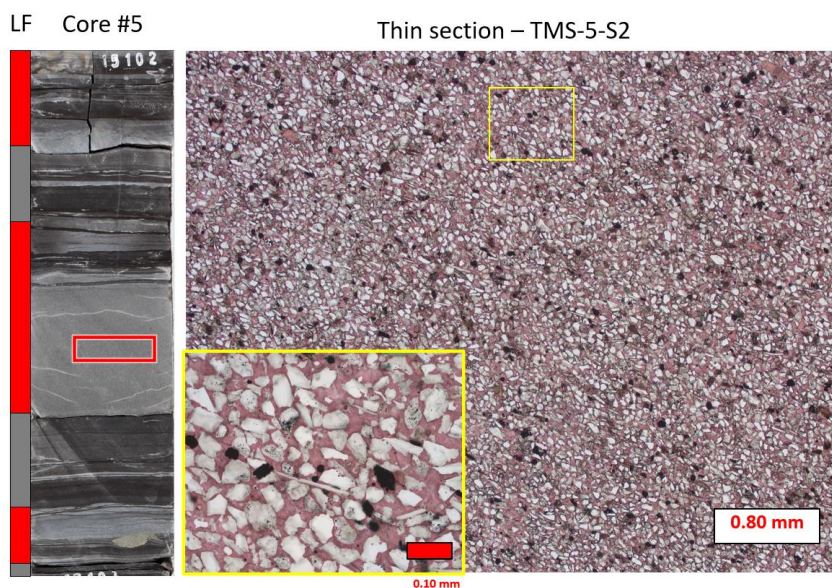


Figure 4.3: On the left is a core image of LF1 rich interval and the sample location of the thin section taken (red box). On the right is a photomicrograph of microfacies 1A modified from Weatherford Laboratories. Photomicrograph of microfacies 1a showing dominant sedimentary fabric and mineralogy. Sample TMS-5-S2, Tuscaloosa Marine Shale, Core #5.

**4.1.2. Mixed Lithofacies (LF2).** LF2 is defined as an interval of shale composed of 50–75% tractional deposits (Figure 3.2; 4.1). It is up to 5 ft (~150 cm) thick. It can be subdivided into LF2a and LF2b where they are composed of 62.5–75% and 50–62.5% tractional deposits, respectively. LF2 is well laminated with parallel, cross, climbing ripple, and lenticular laminations. It is calcareous to non-calcareous, and variable in degree of bioturbation. Bioturbation is not as common as in LF1. The tractional deposits in LF2 are light gray to gray, mm-sub-mm thick, laterally longer than 5 cm, and generally horizontal with a mm-scale relief at the base. In thin sections, the mineral composition of LF2 is similar to that of LF1. However, mudclasts tend to be less common. LF2 occurs throughout the cored intervals. It is abundant near the base of all cores and decreases in

abundance and thickness upsection. Trace fossils are common but variable; but *cruziana* can be seen throughout the core. Two microfacies, 2A and 2B, massive siltstone/claystone and an interlaminated siltstone were identified in LF2 (Figure 4.5; 4.6).

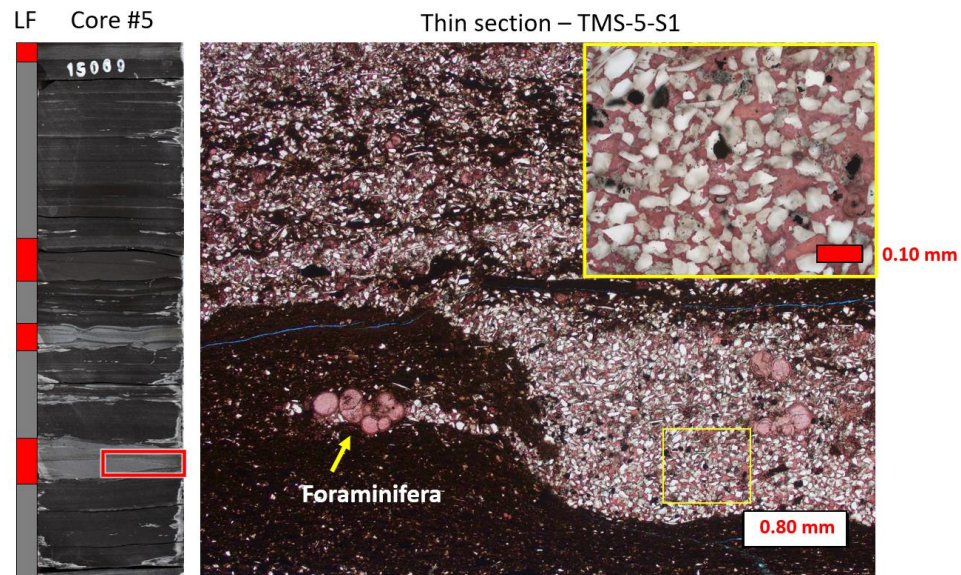


Figure 4.4: On the left is a core photograph of LF1 and the sample location of the thin section taken (red box) photomicrograph of bedload lithofacies, modified from Weatherford Laboratories. Photomicrograph of microfacies 1B showing lag deposits on top of a high relief erosional base. Sample TMS-5-S1, Tuscaloosa Marine Shale, Core #5.

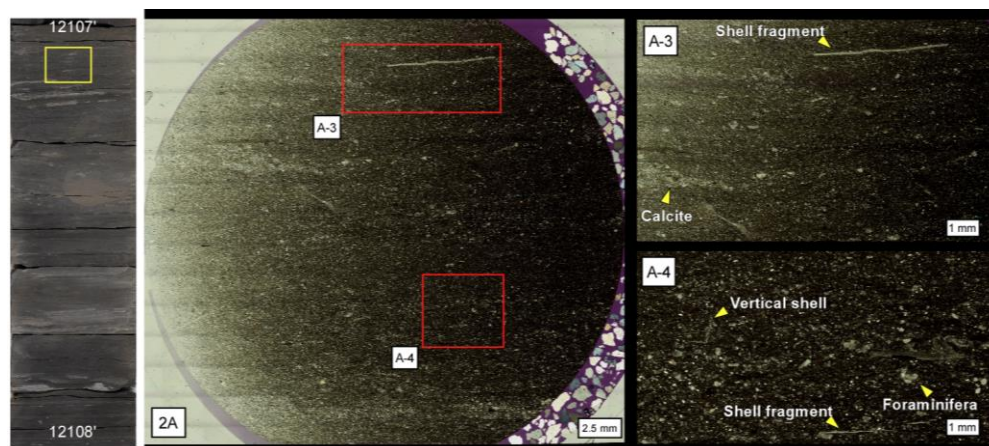


Figure 4.5: Core image of LF2 from Core #1 with a yellow box representing thin section sample. Photomicrographs of Mixed facies, as modified from Weatherford Laboratories. (2a) Photomicrograph of microfacies 2a showing dominant sedimentary fabric and mineralogy (yellow arrows). Sample TMS-1-S2, Tuscaloosa Marine Shale, Core #1

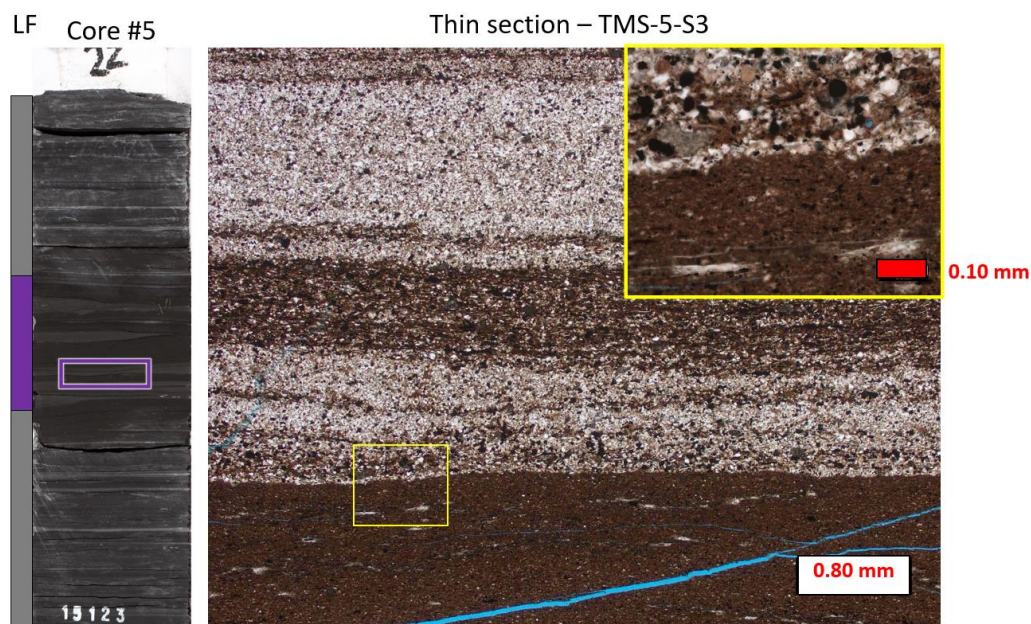


Figure 4.6: Core image of LF2 from Core #1 with a purple box representing thin section sample. Photomicrographs of Mixed facies, as modified from Weatherford Laboratories. Photomicrograph of microfacies 2b showing dominant sedimentary fabric and mineralogy (yellow arrows). Sample TMS-5-S3, Tuscaloosa Marine Shale, Core #5.

**4.1.3. Pelagic Lithofacies (LF3).** LF3 is defined as an interval of shale composed of claystone and fine siltstone or <50% of tractional deposits of medium and coarse-siltstone and very fine sandstone (Figure 3.2; 4.1). This lithofacies consists of two sub-facies: LF3a) is composed of 50 – 25% of tractional deposits and 30 ft (~9 m) thick. LF3b is composed of 0 – 25% of tractional deposits. LF3 is well laminated with mostly mm-sub-mm, planar laminations and millimeter thick silty planar laminations (Figure 4.1). Like LF2, cement varies from calcareous – non-calcareous. Bioturbation is rare but can be present near the top of the cores. Although rare, shell fossils can be found, but rarely concentrated. LF3 intervals are uncommon near the base of the cores but increase in abundance and thickness upsection. Trace fossil commonly found are *mantle and swirl* and *cruziana*. Vertical fractures are common in LF3 and up to ~10 ft (~3 m) long (Figure 4.7). LF3 consists of three distinct microfacies: 3A) Silt-rich laminated claystone; 3B) Clay-rich laminated claystone; 3C) Mottled claystone (Figure 4.8; 4.9; 4.10).

**4.1.4. Organic Lithofacies (LF4).** LF4 contains 5-40% particles of a possible biogenic origin and is 1-30 cm thick (Figure 3.2; 4.1). The particles are embedded in very fine silt and clay with abundant disseminated foraminifera tests. The LF is well laminated, calcareous, and rarely bioturbated. The laminae, however, are discontinuous. The particles are dark brown, elongate, mm-sub-mm thick, 0.1-5 cm long, wrinkly, and sub-horizontal, and wavy. In thin sections, they are opaque, amorphous, some calcite-replaced, and contain common and unevenly distributed framboidal pyrites. Some intervals contain sub-mm-size clots. The elongate particles are interpreted as algal mats; the clotted texture suggests microbial-influenced deposit; both types of biogenic deposits are interlaminated. No thin sections were taken from LF4 rich intervals.



Figure 4.7: Photograph of Core #5 of vertical and horizontal fractures in the TMS.

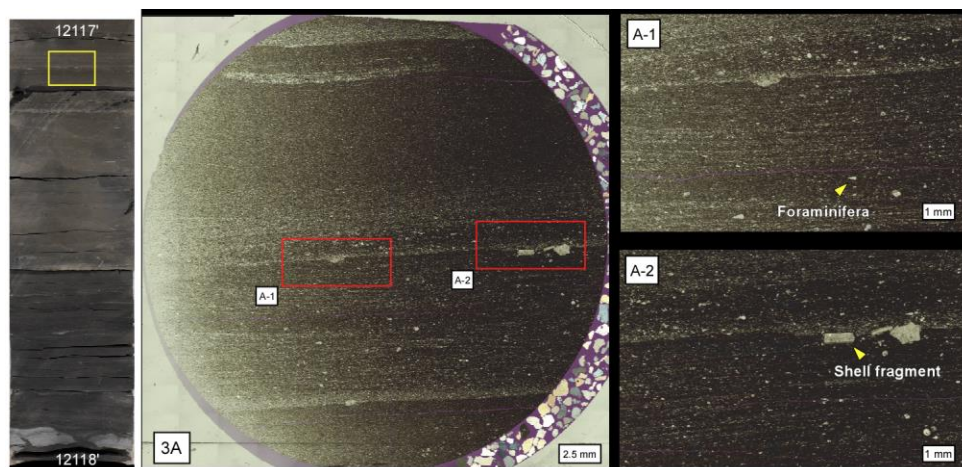


Figure 4.8: Core image of a LF3 interval from Core #1 and thin section sample (yellow box). Photomicrograph of LF3. (3A) Photomicrograph of microfacies 3a silt-rich laminated claystone. (A-1) Multiple mm-sub-mm silt-rich planar laminations with traces of foraminifera (yellow arrow). (A-2) Broken calcitic shell fragments at the base of a lamination (yellow arrows). Sample TMS-1-S1, Tuscaloosa Marine Shale, Core #1.

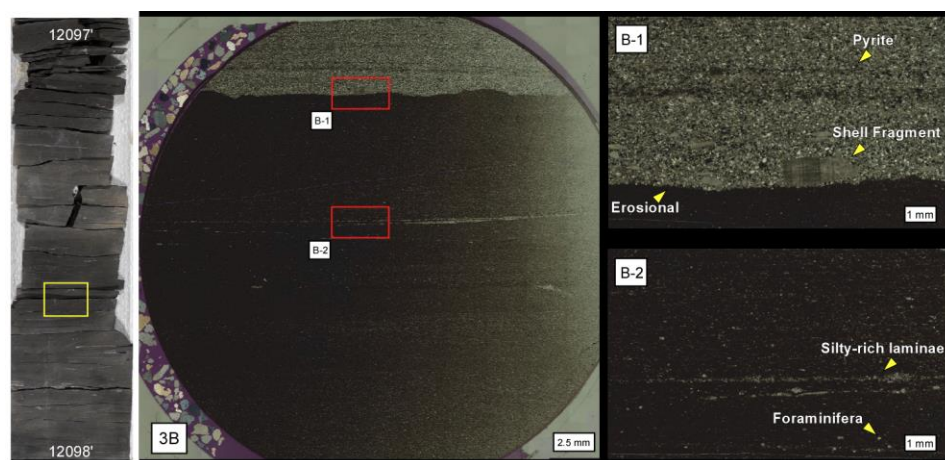


Figure 4.9: Core image of a LF3 interval from Core #1 with a yellow box representing the thin section sample. (3B) Photomicrograph of microfacies 3B clay-rich laminated shale. (B-1) An erosional surface separating the lower microfacies 3B and upper microfacies 1B. (B-2) Sub-mm silty-rich laminae. Sample TMS-1-S3, Tuscaloosa Marine Shale, Core #1.

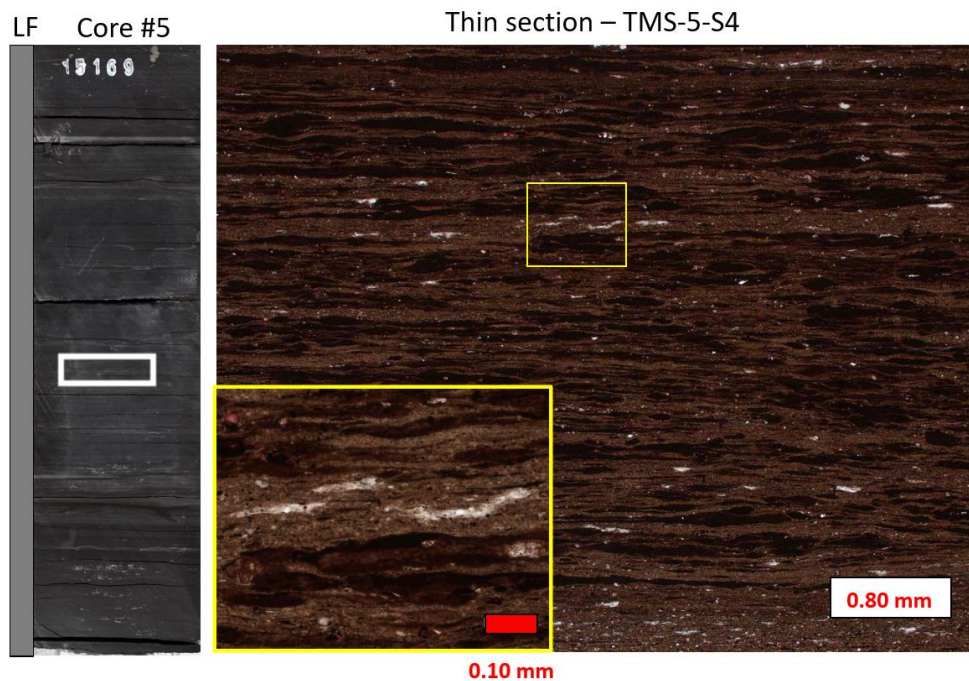


Figure 4.10: Core image of a LF3 interval from Core #5 with a white box representing the thin section sample. Photomicrograph of microfacies 3C mottled claystone. Plane polarized light. Sample TMS-5-S4, Tuscaloosa Marine Shale, Core #5.

Table 4.1 Lithofacies and Microfacies Summary

Lithofacies	Sub-facies	Microfacies
LF1	-	1A – Poorly laminated Siltstone
		1B – Massive Siltstone
LF2	LF2a	2A – Massive Siltstone/Claystone
	LF2b	2B – Interlaminated Siltstone
LF3	LF3a	3A – Silt-rich Claystone 3B – Claystone
	LF3b	3C- Mottled Claystone
LF4	-	-

## **4.2. TUSCALOOSA MARINE SHALE FACIES MODEL**

Lithofacies trends were recorded in the TMS. A typical facies model can be described from base to top: 1) A moderate to high-relief erosional base with a thick LF1 interval and a gradational or sharp top; 2) An interlaminated shale and siltstone LF2 with a gradational or sharp top; 3) Planar laminated claystone – fine siltstone LF3 interval and a gradational or sharp top; 4) Although rare, a LF4 interval rich in biogenic particles with an erosional top signifying the end and beginning of a cycle (Figure 4.11).

## **4.3. LITHOFACIES DISTRIBUTIONS**

The lithofacies distribution in cored wells was recorded (Figure 4.12). LF3 is the major lithofacies for all cored wells. LF4 was only recorded in Core #7, one of two distal shelfward cores, and makes up less than 10% of the total lithofacies distribution. In Core #7 the lithofacies distribution of the cored interval is LF1, 6%; LF2, 12%; LF3, 76%; and LF4, 6%. In Core #1, the most proximal shelfward core, the lithofacies distribution of the cored interval is LF1, 18%; LF2, 12%; LF3, 76%; LF4, 0%. In Core #6, the lithofacies distribution of the cored interval is LF1, 20%; LF2, 18%; LF3, 61%; LF4, 0%. In Core #5, the lithofacies distribution of the cored interval is LF1, 11%; LF2, 26%; LF3, 63%; LF4, 0%. In Core #11, the lithofacies distribution of the cored interval is LF1, 18%; LF2, 12%; LF3, 70%; LF4, 0%.

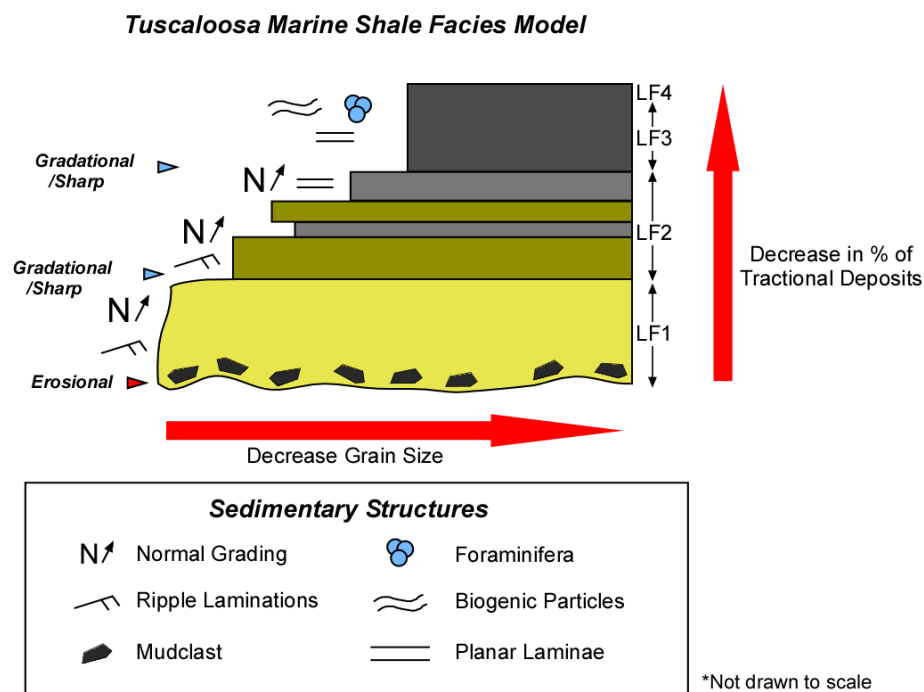


Figure 4.11: Typical TMS facies model based on core observations.

#### 4.4. MINERALOGY AND ORGANIC CONTENT LITHOFACIES CHARACTERIZATION

LF1-4 are mainly composed of quartz, calcite, and clay minerals. All clay minerals were summed up for this study and labeled as total clay. Mineralogy data were plotted by lithofacies in a ternary diagram to classify shales (Figure 4.13). LF1 data has an even wide distribution. Most LF2 data suggest claystone and silicate mineral-rich mudstones. Most LF3 data suggest clay-rich mudstone and argillaceous mixed mudstone. LF4 data suggest carbonate – rich mudstone to mixed carbonate mudstone. Boxplots were built to semi-quantify the mineralogy and TOC of each LF (Figure 4.14). Mineralogy logs were plotted for each core to see the vertical distribution of minerals in the TMS (Figure 4.15).

## Core Lithofacies Distributions

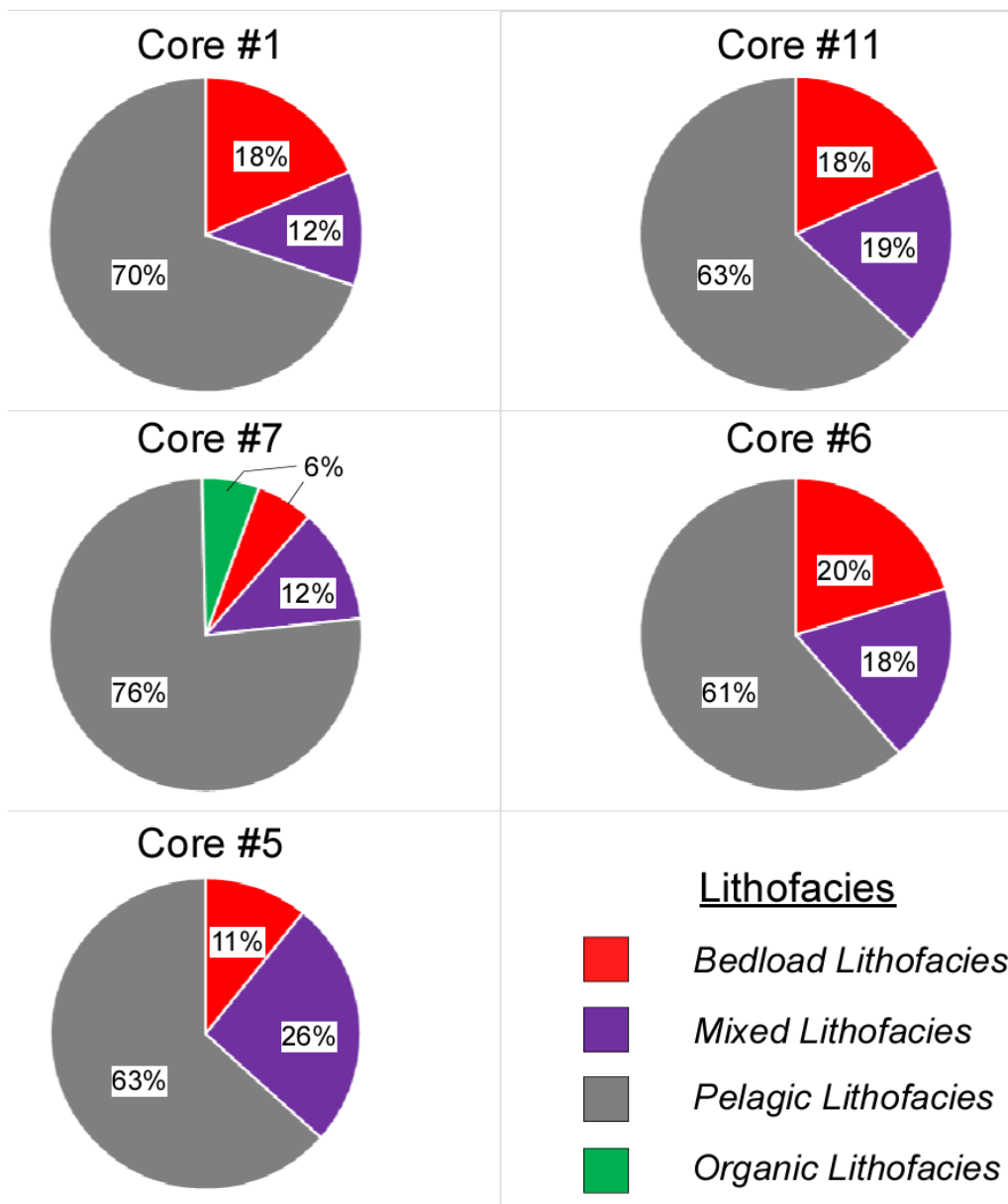


Figure 4.12: Pie charts of lithofacies distribution of cored wells.

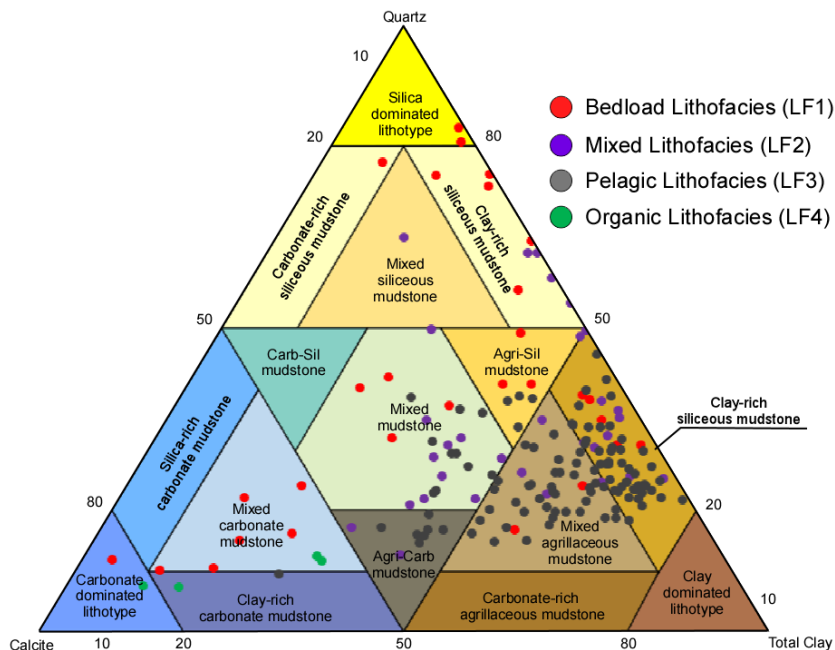


Figure 4.13: Core lithofacies classification scheme for organic-rich shales for all five cores. Modified from Gamero et al. (2012).

**4.4.1. Bedload Facies (LF1).** A total of 30 mineralogy and 35 pyrolysis samples were classified as LF1. The XRD results from five wells show that the composition of LF1 in the TMS includes primarily quartz, calcite, and clay, while pyrite, potassium feldspar, and plagioclase are secondary. The range of quartz varies from 9.3 to 70.8 wt% with an average value of 35.7 wt%, calcite from <1 to 78.8 wt% with an average value of 21.1%, clay minerals from 3.4 to 59.2 wt% with an average value of 28.1%, pyrite from 1.5 to 7.4 wt% with an average value of 3.8 wt%, potassium feldspar from <1 to 9.9 wt% with an average value of 4.4 wt%, and plagioclase from 0.9 to 8.1 wt% with an average value of 4.5%. In addition to mineralogy, the total organic carbon content (TOC) for LF1 ranges from 0.17 to 2.79 wt%.

**4.4.2. Mixed Facies (LF2).** A total of 31 mineralogy and 36 pyrolysis samples were classified as LF2. The mineral composition of LF2 includes quartz, calcite, and clay

as the primary minerals, while pyrite, potassium feldspar, and plagioclase are secondary minerals. The range of quartz varies from 12 to 54.6 wt% with an average value of 30.1 wt%, calcite from <1 to 44.3 wt% with an average value of 14.3 wt%, clay minerals from 14.0 to 59.4 wt% with an average value of 41.5 wt%, pyrite from 0.4 to 8.2 wt% with an average value of 3.2 wt%, potassium feldspar from <1 to 10.1 wt% with an average value of 4.1%, and plagioclase from <1 to 8.8 wt% with an average value of 4.3 wt%. The TOC content for LF2 ranges from 0.49 to 2.49 wt%.

**4.4.3. Pelagic Facies (LF3).** A total of 109 mineralogy and 99 pyrolysis samples were classified as LF3. The mineral composition of LF3 includes quartz, calcite, and clay minerals as the primary minerals, while pyrite, potassium feldspar, and plagioclase are secondary. The range of quartz varies from 8.8 to 39.3 wt% with an average value of 22.5 wt%, calcite from 0.4 to 56.6 wt% with an average value of 14 wt%, clay minerals from 25.1 to 68.5 wt% with an average value of 50.8 wt%, pyrite from <1 to 11 wt% with an average value of 3.6 wt%, potassium feldspar from <1 to 7.1 wt% with an average value of 1.6 wt%, and plagioclase from 0.6 to 10.1 wt% with an average value of 4.3 wt%. The TOC content for LF3 ranges from 0.11 to 3.19 wt%.

**4.4.4. Organic Facies (LF4).** A total of four mineralogy and pyrolysis samples were classified as LF4. The major composition of LF4 includes quartz, calcite, and clay minerals as the primary minerals, while pyrite, potassium feldspar, and plagioclase are secondary. The range of quartz varies from 7.0 to 12.0 wt% with an average value of 9.3 wt%, calcite from 51.0 to 74.0 wt% with an average value of 62.5 wt%, clay minerals from 9.0 to 30.0 wt% with an average value of 20.8%, pyrite from 2.0 to 6.0 wt% with an average value of 4.0 wt%, potassium feldspar from 1.0 to 2.0 wt% with an average value

of 1.5 wt%, and plagioclase from 2.0 to 3.0 wt% with an average value of 2.3 wt%. The TOC content for LF4 ranges from 1.97 to 2.72 wt%, with an average value of 2.41 wt%.

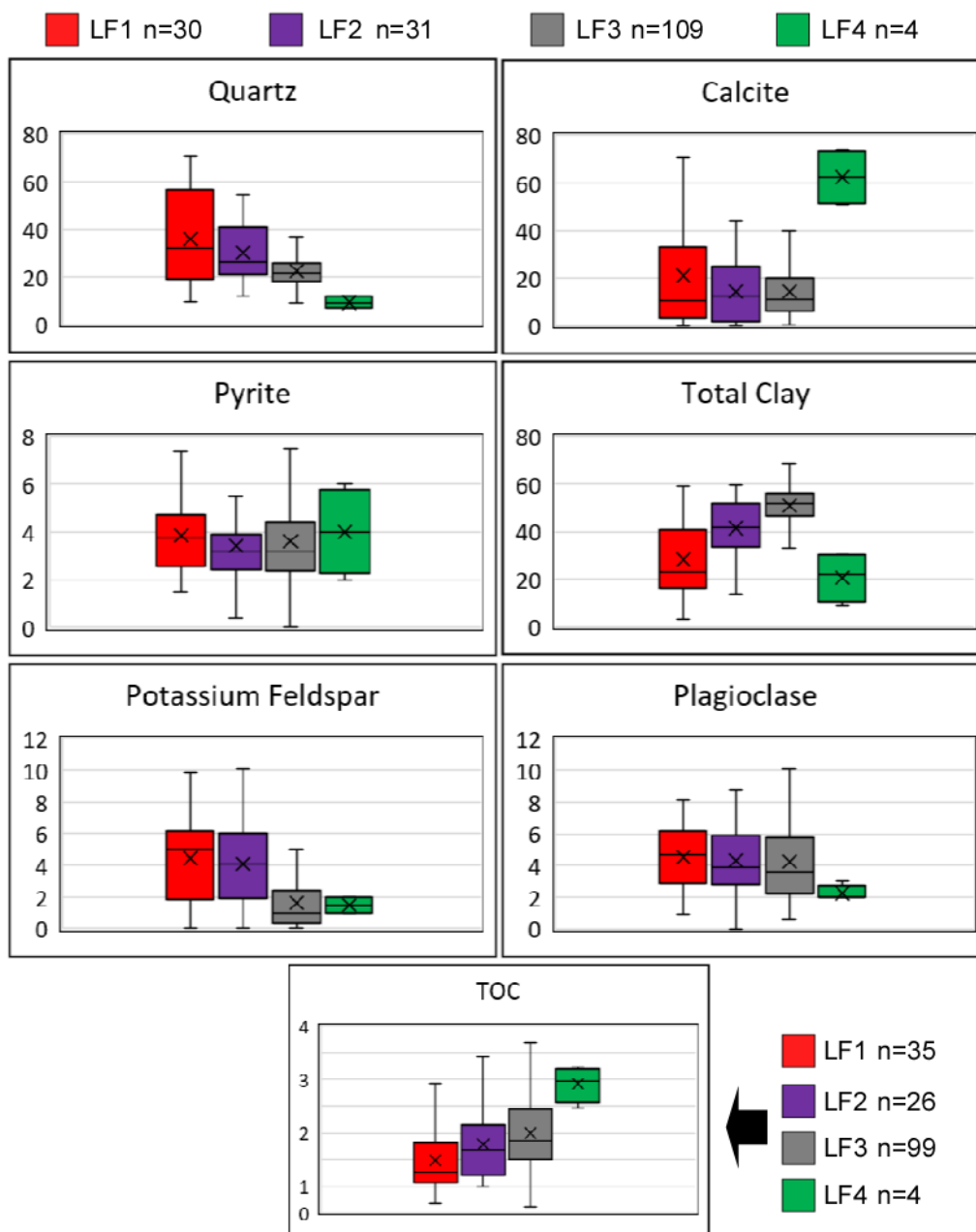


Figure 4.14: Box plots showing the mineralogy and TOC content in all cored wells. Note vertical axis is measured in wt%.

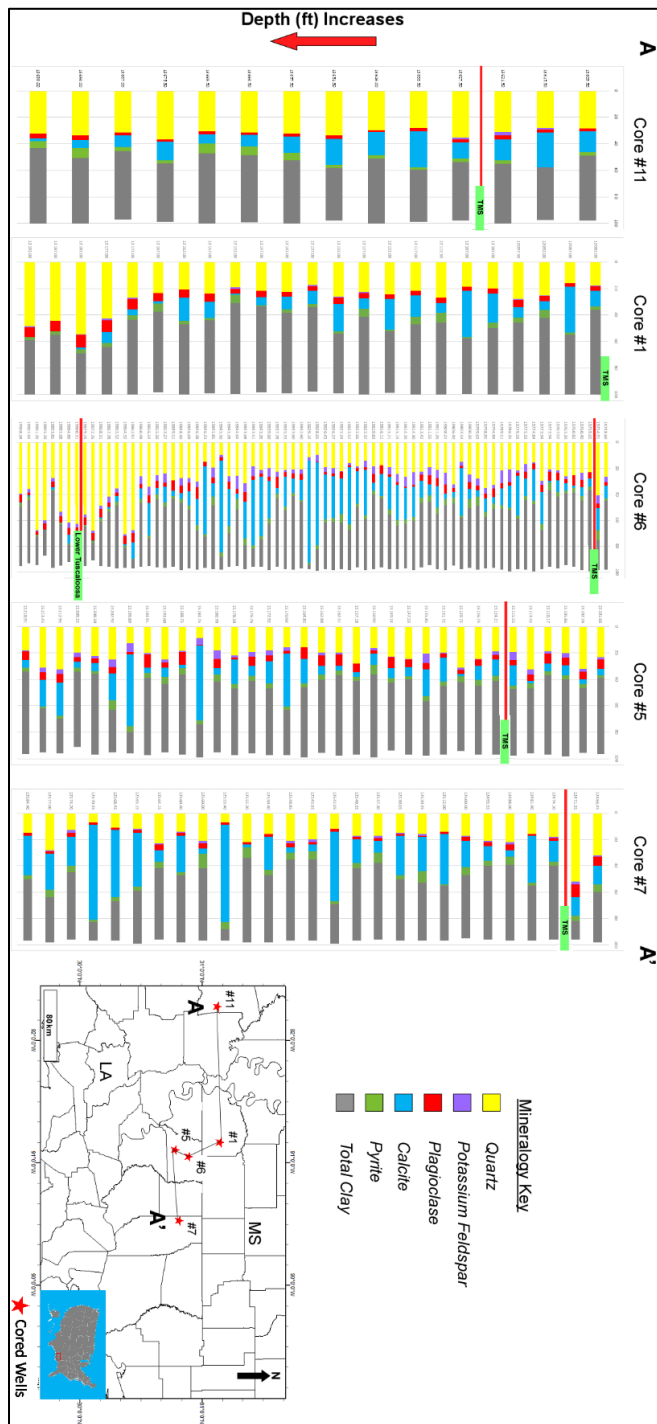


Figure 4.15: Mineralogy data obtained through X-ray diffraction analysis of core samples for the wells in the study. XRD Data from third party laboratories described in section 3.1. See Table 1.A in Appendix A for additional XRD data reference.

Table 4.2: Compiled statistics of mineralogy and TOC by lithofacies.

<b>Lithofacies (LF)</b>	<b>LF1</b>	<b>LF2</b>	<b>LF3</b>	<b>LF4</b>
Number of samples	30	31	109	4
<b>Quartz</b>				
Mean	35.8	30.2	22.5	9.3
Median	31.85	26.3	21.5	9
Std Dev	19.88	11.95	5.93	2.63
Kurtosis	-1.07	-0.49	0.08	-5.29
Skew	0.49	0.79	0.65	0.12
Range	61.50	42.60	30.50	5.00
Minimum	9.30	12.00	8.80	7.00
Maximum	70.80	54.60	39.30	12.00
<b>Calcite</b>				
Mean	21.1	14.3	14.1	62.5
Median	10.3	12.5	11.0	62.5
Std Dev	23.7	13.0	10.6	12.2
Kurtosis	0.1	-0.5	1.4	-5.7
Skew	1.1	0.7	1.2	0.0
Range	78.8	44.3	56.1	23.0
Minimum	0.0	0.0	0.4	51.0
Maximum	78.8	44.3	56.5	74.0
<b>Total Clay</b>				
Mean	28.1	41.5	50.8	20.8
Median	22.9	41.9	51.6	22.0
Std Dev	15.4	10.9	8.2	10.9
Kurtosis	-0.8	-0.1	0.5	-5.0
Skew	0.5	-0.3	-0.6	-0.2
Range	55.8	45.4	43.4	21.0
Minimum	3.4	14.0	25.1	9.0
Maximum	59.2	59.4	68.5	30.0
<b>Plagioclase</b>				
Mean	4.5	4.3	4.3	2.3
Median	4.7	3.9	3.6	2.0
Std Dev	2.0	2.3	2.3	0.5
Kurtosis	-1.1	-0.6	-0.2	4.0
Skew	0.0	0.3	0.7	2.0
Range	7.2	8.8	9.5	1.0
Minimum	0.9	0.0	0.6	2.0
Maximum	8.1	8.8	10.1	3.0

Table 4.2: Compiled statistics of mineralogy and TOC by lithofacies (cont.)

<b>Lithofacies (LF)</b>	<b>LF1</b>	<b>LF2</b>	<b>LF3</b>	<b>LF4</b>
<b>Pyrite</b>				
Mean	3.8	3.4	3.6	4.0
Median	3.8	3.2	3.2	4.0
Std Dev	1.6	1.7	2.0	1.8
Kurtosis	0.2	1.6	1.1	-3.3
Skew	0.7	1.0	1.0	0.0
Range	5.9	7.8	11.0	4.0
Minimum	1.5	0.4	0.0	2.0
Maximum	7.4	8.2	11.0	6.0
<b>KSPAR</b>				
Mean	4.4	4.1	1.7	1.5
Median	5.0	4.1	1.0	1.5
Std Dev	3.1	2.5	1.7	0.7
Kurtosis	-0.9	-0.4	1.4	NA
Skew	0.2	0.3	1.3	NA
Range	9.9	10.1	7.1	1.0
Minimum	0.0	0.0	0.0	1.0
Maximum	9.9	10.1	7.1	2.0
<b>Number of samples</b>	35	26	99	4
<b>TOC</b>				
Mean	1.0	1.3	1.5	2.4
Median	0.8	1.2	1.4	2.5
Std Dev	0.6	0.7	0.6	0.3
Kurtosis	0.8	0.7	-0.2	-0.6
Skew	1.1	1.1	0.5	-0.8
Range	2.6	2.4	3.1	0.8
Minimum	0.2	0.5	0.1	2.0
Maximum	2.8	2.9	3.2	2.7

#### **4.5. RESULTS OF SCANNING ELECTRON MICROSCOPY AND ENERGY DISPERSIVE X-RAY SPECTROSCOPY ANALYSES**

One thin section sample (TMS-1-S1) from Core #1 and one core sample from Core #7 was analyzed to capture the microscopic heterogeneity of LF3 and LF4, respectively. SEM and backscattered electrons (BSE) capture particle morphologies and variability in average atomic numbers, respectively. Generally, the brighter the BSE signal, the higher the average atomic number (Harding, 2002). Elemental point analyses were performed to screen for typical shale minerals: aluminum, sodium, and potassium (clay minerals); calcium (calcite); iron and sulfur (pyrite); and silicon and oxygen (quartz; Dubois, 2018).

**4.5.1. Sample TMS-1-S1.** LF3 and microfacies 3A are classified in this sample. Both BSE images show similar differences in BSE signals (Figure 4.16). The BSE signal in the similar concentrations of framboidal pyrite embedded in a fine-silt to clay sized framework. The differences in BSE signals are a proxy for variations in elemental composition. SEM-EDS point analyses were performed to confirm the inferred mineralogy of the framboidal pyrite and matrix. Elemental maps and spectrum analyses of point 1 show the presence of mostly iron and sulfur, confirming the occurrence of pyrite (Figure 4.17; 4.18; 4.19). Based on the elemental maps and spectrum analysis, the matrix mainly comprises oxygen, aluminum, and silicon, inferring a clay-siliceous rich matrix.

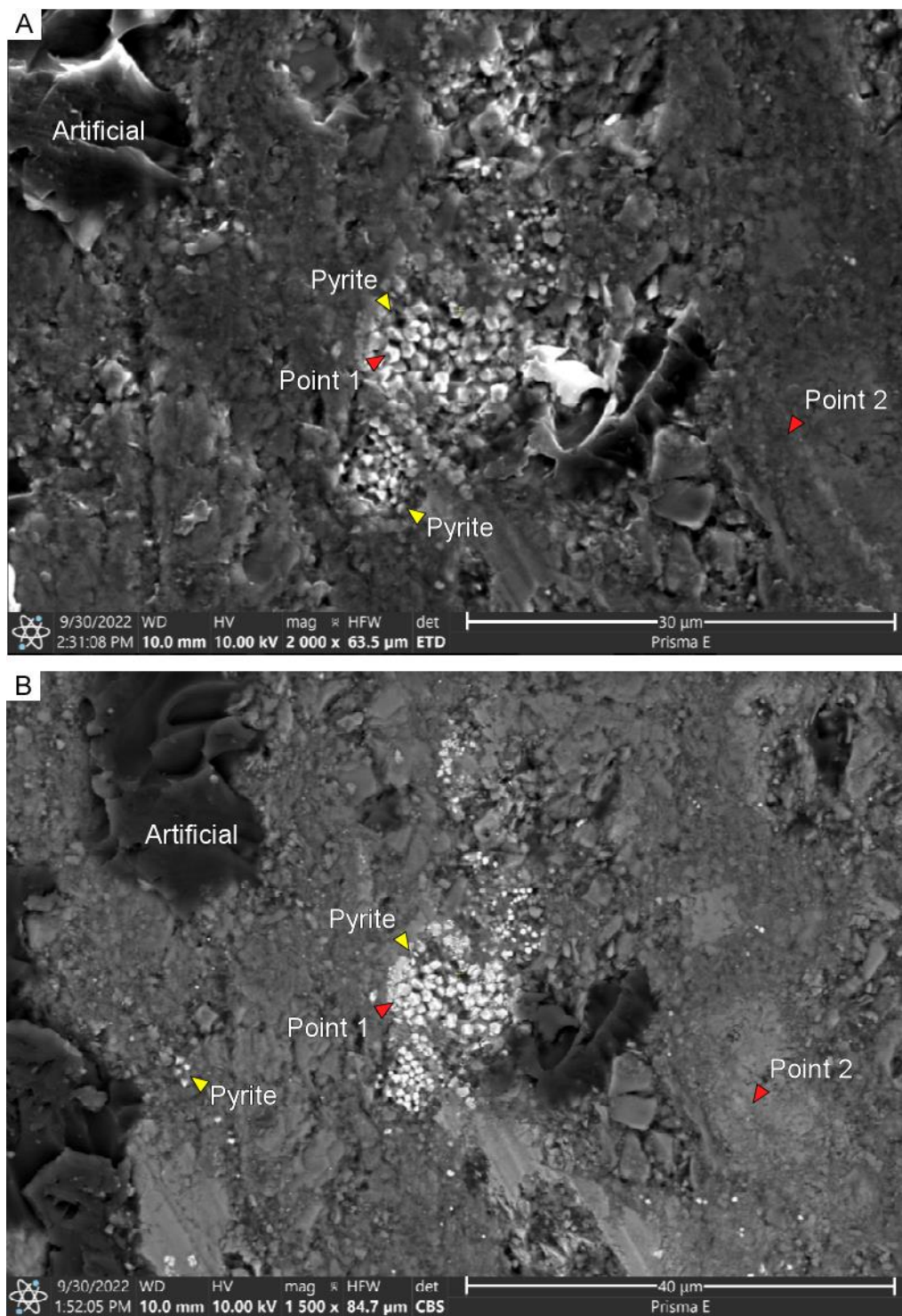


Figure 4.16: (A) SEM image of a LF3 and microfacies 3a sample from Core #1. (B) BSE image of the same area. Points 1 and 2 represent location of EDS point analyses (red triangles). Note scale change. See Figure 4.8 for location. Sample TMS-1-S1, Tuscaloosa Marine Shale, Core #1.

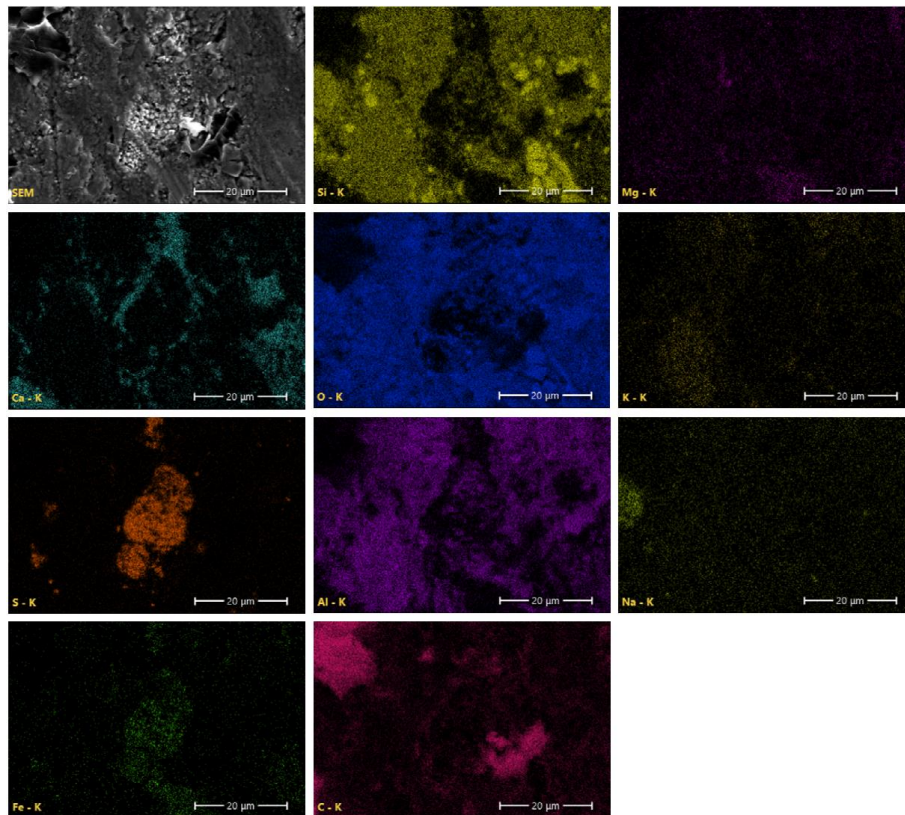


Figure 4.17: Elemental maps for Sample TMS-1-S1 from Core #1.

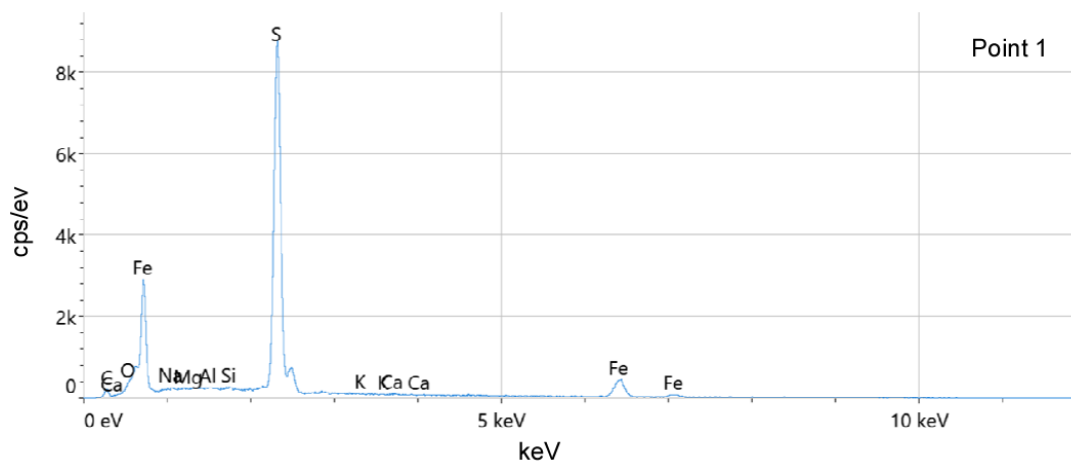


Figure 4.18: Energy Dispersive X-Ray Spectrum (EDS) analysis for Point 1 in Sample TMS-1-S1 from Core #1. See Figure 4.16 for location.

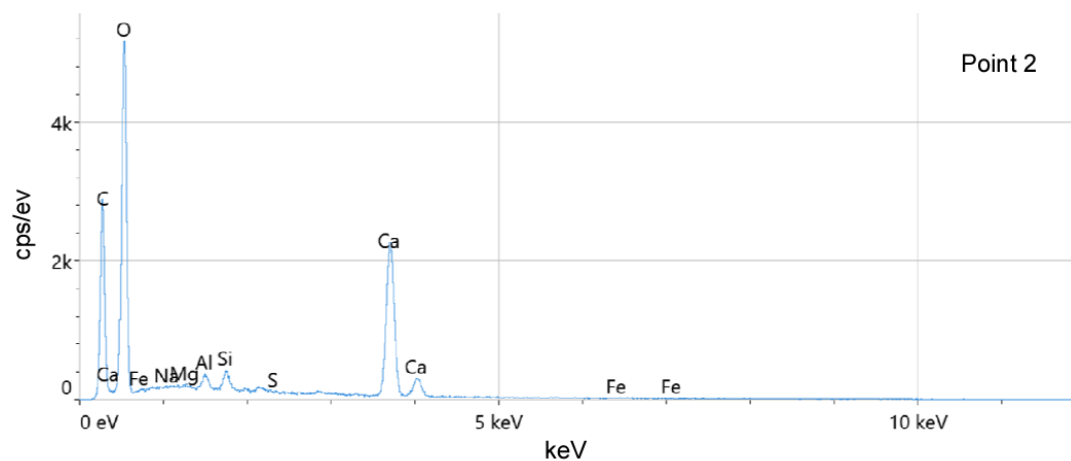


Figure 4.19: Energy Dispersive X-Ray Spectrum (EDS) analysis for Point 2 in Sample TMS-1-S1 from Core #1. See Figure 4.16 for location.

**4.5.2. Sample TMS-7-S1.** This sample was classified as LF4. SEM images show the presence of pyrite (Figure 4.20C). The matrix is mainly composed of flaky clay minerals and quartz. Target point analyses were analyzed in the phase of an inferred pyrite crystal. Spectrum analyses confirm the presence of iron; however, the signal of sulfur is slightly weak (Figure 4.21).

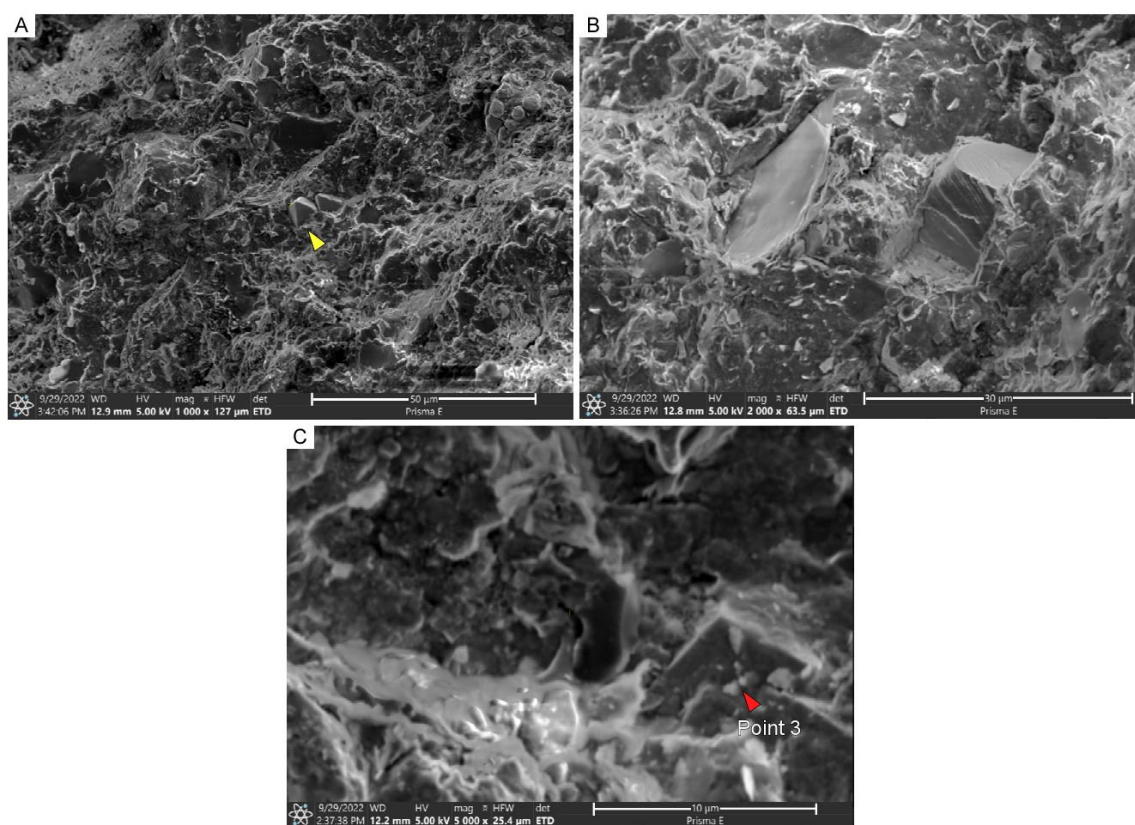


Figure 4.20 (A-C): SEM images of LF4 from Core #7 (C) Point 3 SEM-EDS analysis. See Figure 4.21 for spectral analysis.

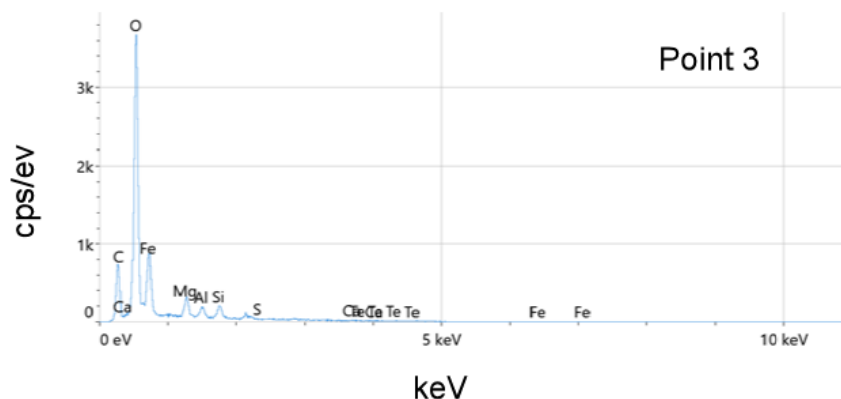


Figure 4.21: Energy Dispersive X-Ray Spectrum (EDS) analysis for Point 3 in sample TMS-7-S1 from Core #7. See Figure 4.20C for location.

#### 4.6. WELL LOG SIGNATURES OF LITHOFACIES

Core and well-log calibrations are a standard workflow to link core data to wireline logs. Commonly used well logs like gamma ray and resistivity can be proxies for lithology, radioactivity, and fluid types, respectively.

**4.6.1. Gamma Ray (GR).** Gamma-ray logs are the measure of the amount of radiation in rocks. The primary radiation sources come from the following elements: potassium, thorium, and uranium. Shales, especially organic-rich shales, are highly radioactive since most of the potassium is derived from clay minerals, and thorium and uranium are derived from organic matter (Guo et al., 2021).

LF1-3 has bi-modal distributions with a more prominent mode at 90-100 API and 100-110 API. The other minor mode is at 140-150 API. LF4 has only two bins, falling under 100-110 API and 110-120 API (Figure 4.23).

**4.6.2. Deep Resistivity.** Resistivity logs in unit of ohms are used widely in the industry to evaluate the formation fluid types and lithology. These logs measure the degree to which it can impede the flow of an electric current. Clay minerals have an impact on resistivity as they can conduct electricity, therefore, decrease the resistivity. Resistivity logs commonly have shallow, medium, and deep resistivity logs. This refers to the lateral extent of the measurement taken (Schlumberger Glossary).

Resistivity logs in unit of ohms are used widely in the industry to evaluate the formation fluid types and lithology. These logs measure the degree to which it can impede the flow of an electric current. Clay minerals have an impact on resistivity as they can conduct electricity, therefore, decrease the resistivity. Resistivity logs commonly have shallow, medium, and deep resistivity logs. This refers to the lateral extent of the measurement taken (Schlumberger Glossary).

LF1 has a bimodal distribution with a minor mode at 0-3 ohms and a prominent mode at 6-9 ohms. LF2 has a log-normal distribution where the most prominent mode is 3-6 ohms. LF3 has a positive skewed unimodal distribution with the most significant mode at 6-9 ohms. LF4 only has two bins from 3-6 ohms and 6-9 ohms (Figure 4.24).

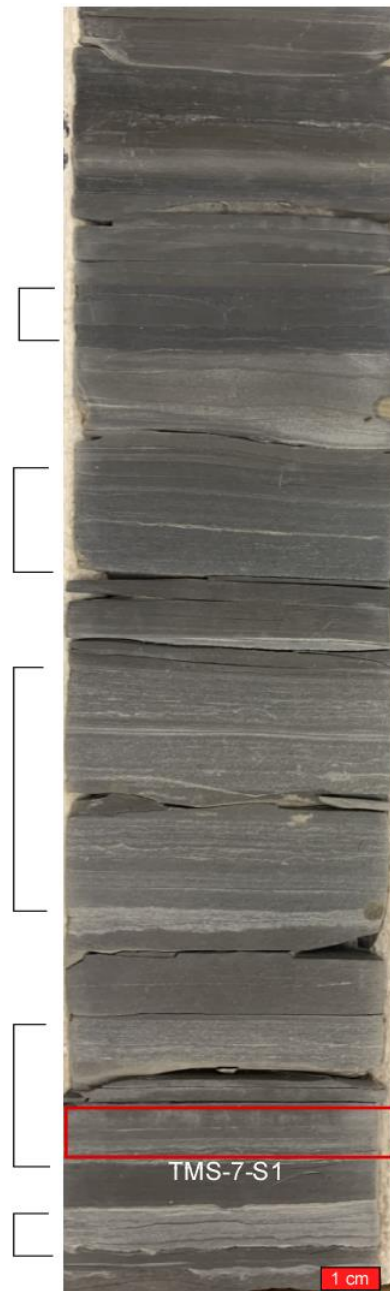


Figure 4.22: Photograph of Core #7 of a LF4 rich interval. Sample TMS-7-S1 was used for SEM and EDS analyses (Red box).

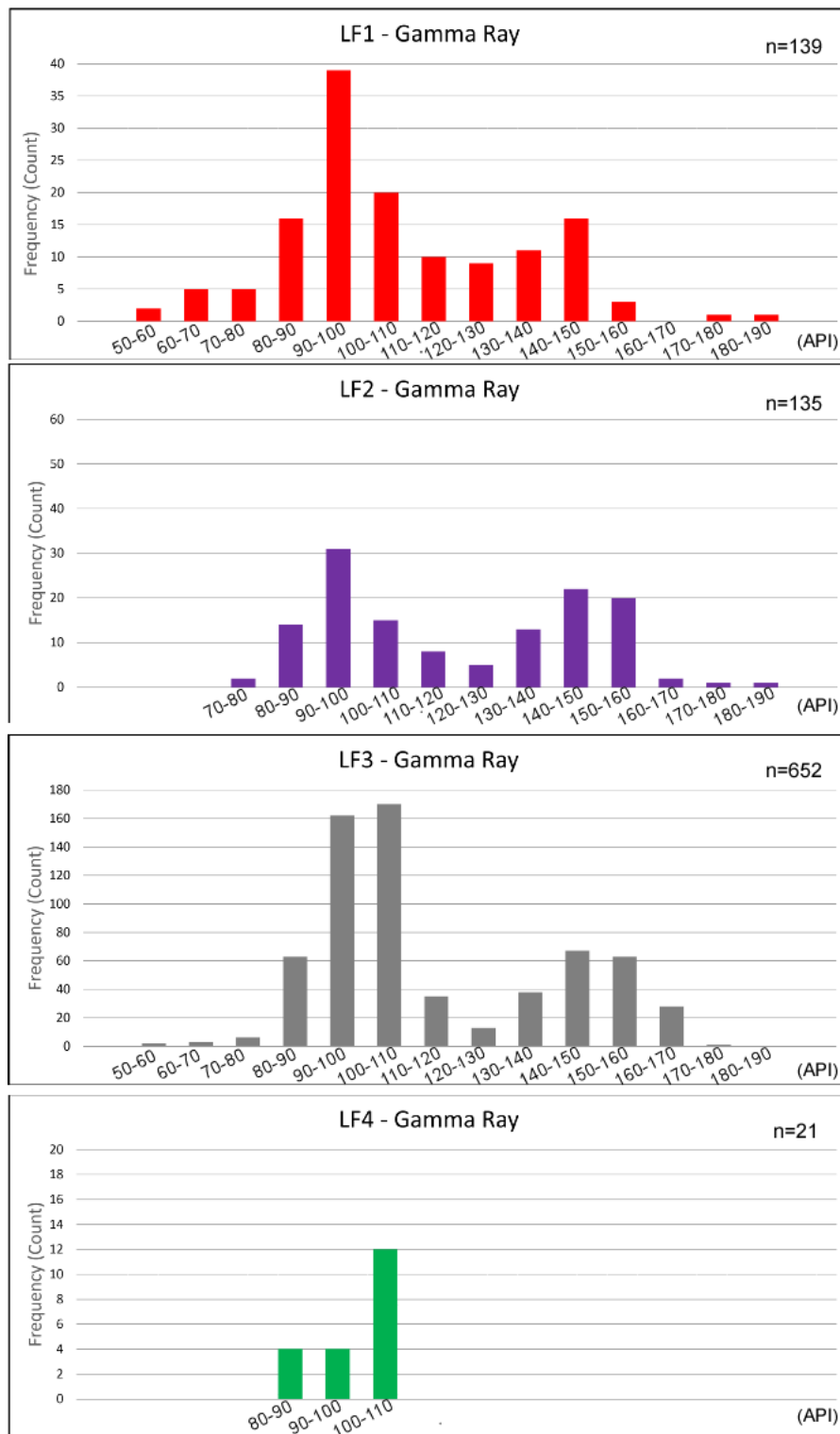


Figure 4.23: Histograms showing the gamma ray values of lithofacies. See Table 1.B in Appendix B for data reference.

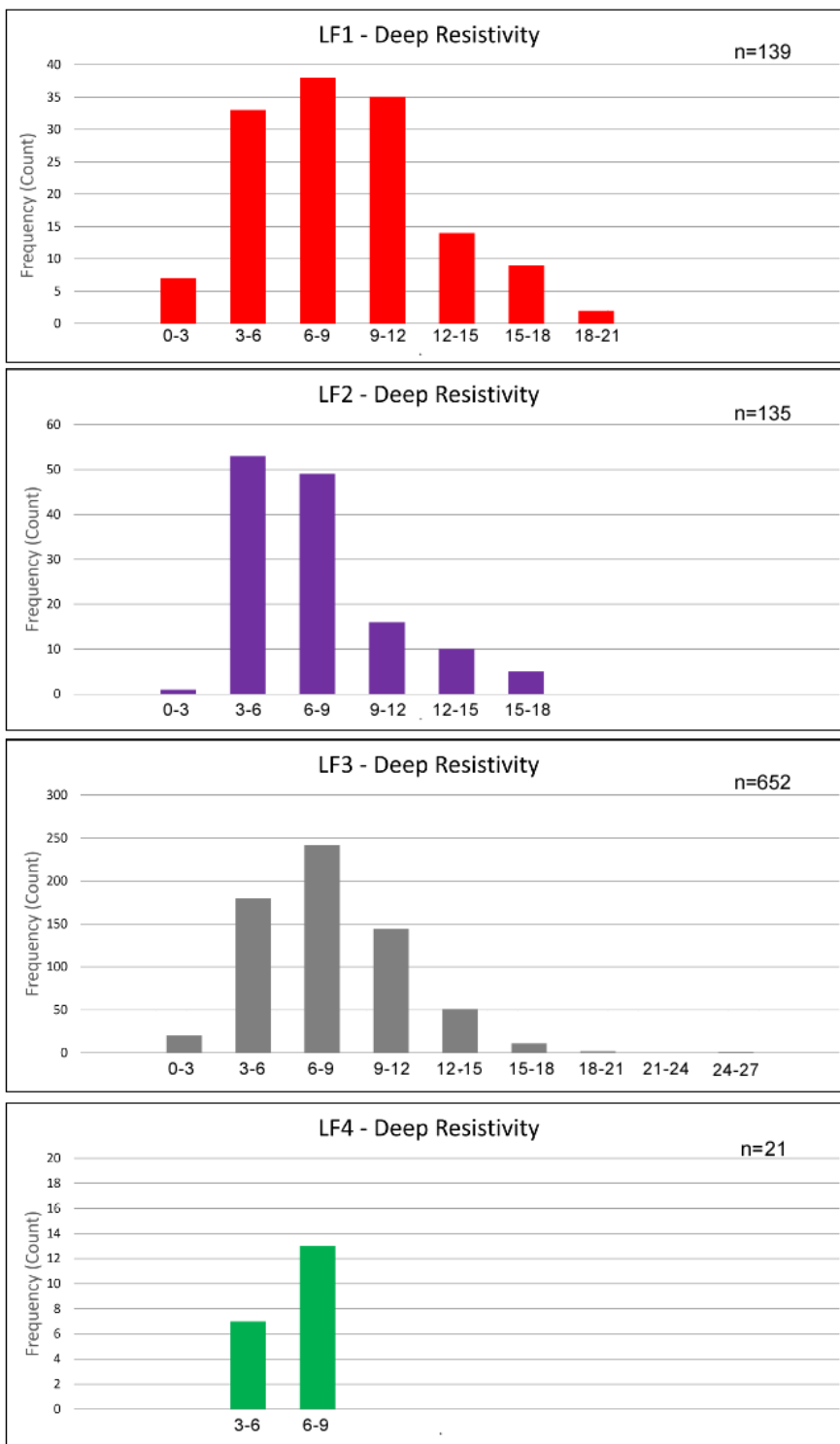


Figure 4.24: Histograms showing the range of resistivity values of lithofacies. See Table 1.B in Appendix B for data reference.

## 5. DISCUSSION

### 5.1. GENERAL STATEMENT

The various observations and interpretations as presented above are used to characterize the stratigraphic heterogeneity of the TMS in order to understand the depositional conditions and processes during the deposition of the TMS on the continental shelf of north-central Gulf of Mexico.

### 5.2. DEPOSITIONAL PROCESSES

Based on the results of the core observations, three different types of depositional processes were interpreted: 1) tractional; 2) pelagic; 3) biogenic. These processes produced distinctive mineral compositions, geochemical signatures, and sedimentary textures that provide insight into the depositional processes and conditions on the continental shelf.

**5.2.1. Tractional Deposits.** In the TMS, four types of tractional process were recognized: 1) wave-enhanced sediment-gravity flows (WESGF); 2) turbidity flows; 3) storm-induced flows; 4) undifferentiated bottom current flows (Macquaker et al., 2010; Lazar et al., 2015). They produced wave-enhanced sediment gravity flow deposit, turbidite, tempestite, and laminated medium-coarse siltstone. The various sedimentary textures and structures of these tractional deposits provide information on the shifts in sedimentary processes and conditions on the continental shelf.

### **5.2.2 Deposits of Wave-Enhanced Sediment-Gravity Flows (WESGF).**

WESGF are products of near wave-base or storm-enhanced wave agitations that suspend sediments in the water column and produce a density current that transports and deposits sediments downslope. Following the tractional transport and deposition, a waning episode of energy deposits the suspended clay to silt sized sediments (Macquaker et al., 2010; Lazar et al., 2015a; Lazar et al., 2015b).

These deposits are characterized by a low-relief erosional base with minor erosion and internal interlaminated grading lamina sets, and a top erosional or gradational surface marking the end of the event. The internal architecture is composed of 1) basal homogeneous siltstone-very fine sandstone; 2) single or multiple laminasets composed of silt or very fine sand grading upward to clay; 3) clay-rich laminasets that fine upwards. WESGF deposits are relatively common in some intervals in the cores, especially near the base of the cores (Figure 4.25).

The bases of the cores were sampled either in the Lower Tuscaloosa or in the transition zone between the TMS or the Lower Tuscaloosa. This suggests the occurrence of WESGF was in relatively shallow water, where sediments were influenced by wave action or major storms that induced density currents up slope.

**5.2.3. Fine-grained Turbidite Deposits.** First described by Bouma (1964), turbidites are deposited by episodic turbulent flows induced by storms, floods, and seafloor sediment collapses (Lazar et al., 2015a; Lazar et al., 2015b). Turbidites are common in the TMS. These turbidites contain medium siltstone – very fine sandstone in the basal part and fine upward to a fine siltstone and claystone (Figure 4.26; 4.27).

High-energy turbidity currents can cause severe erosion in the seafloor. The deposits are characterized by a high-relief erosional base with fossil fragments or mud clasts comprising a lag deposit. Above the lag is a variably cross laminated coarse to fine siltstone and very fine sandstone.

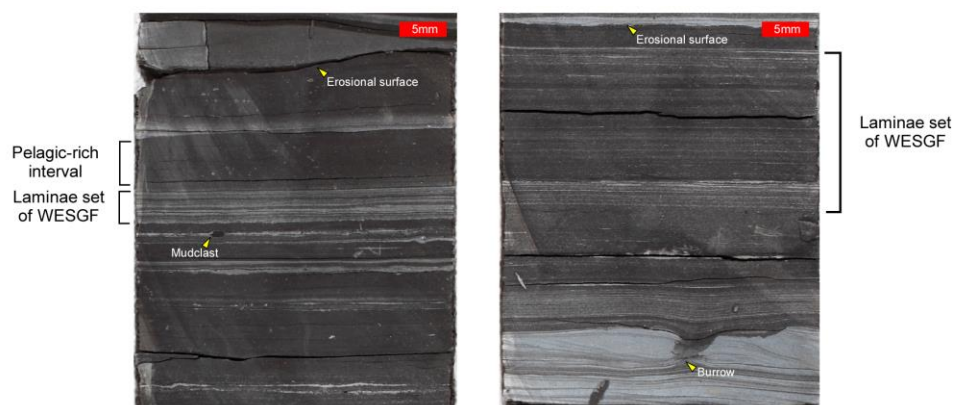


Figure 4.25: Photographs from Core #6 of wave-enhanced sediment gravity flows (WESGF).

**5.2.4. Tempestites.** Tempestites are depositional products of storm waves or return flows. Storms induced waves to suspend sediments in the water column and produced sediment-loaded currents and transport sediments down slope. The flow energy wanes, resulting in suspension settling (Lazar et al., 2015a; Lazar et al., 2015b).

Tempestites are depositional products of storm waves or return flows. Storms induced waves to suspend sediments in the water column and produced sediment-loaded currents and transport sediments down slope. The flow energy wanes, resulting in suspension settling (Lazar et al., 2015a; Lazar et al., 2015b).

These deposits can be characterized by a scouring, wavy, and relatively high relief erosional surface with sediment and fossil lags. The internal architecture is composed of poorly to moderate defined laminae sets near the base and moderately developed near the top. Grain size fines upwards to form a 'smoothly graded' appearance (Lazar et al., 2015a; Lazar et al., 2015b). The uppermost part is generally composed of planar laminae sets made up of clay-fine silt (Figure 4.28). Tempestites are widespread in the TMS. However, they are relatively common and thick near the base and top of the core.

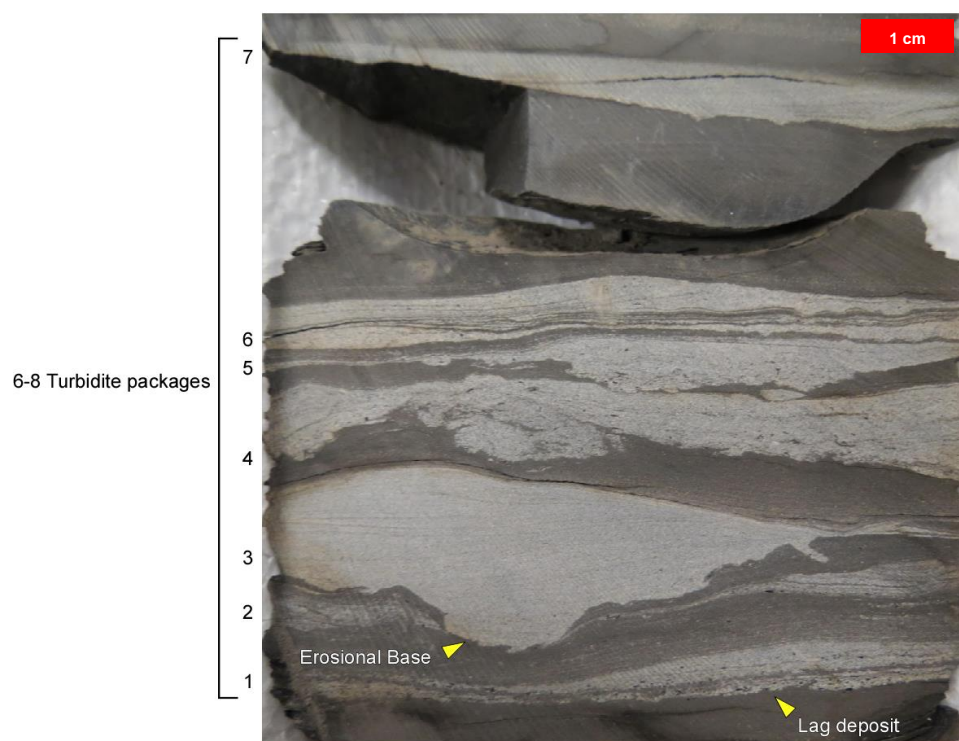


Figure 4.26: Photograph of Core #11 near the base of the core, showing multiple fine-grained turbidite packages in a LF1 interval.

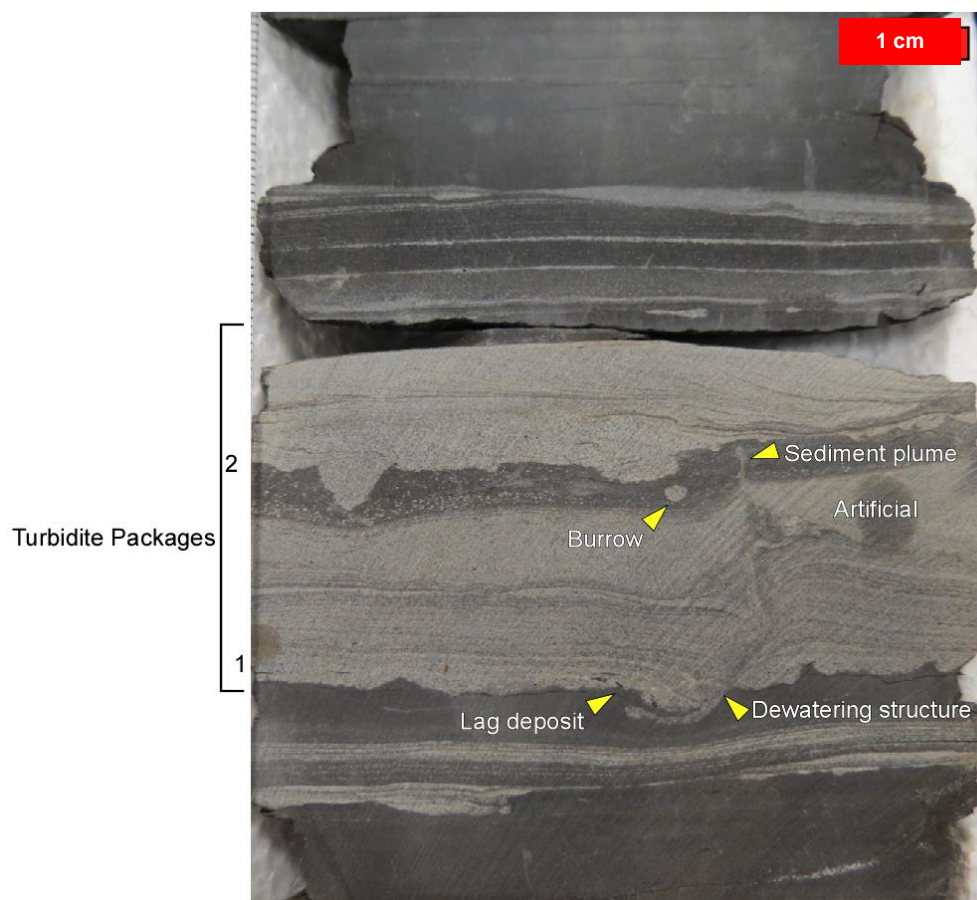


Figure 4.27: Photograph of Core #11 near the base of the core of multiple turbidite packages in a LF1 interval. Note saw marks crossing from bottom left to top right.

**5.2.5. Current – Reworked.** Current deposits are millimeter thick coarse to medium siltstone, forming 1-10 mm thick lamina sets (Figure 4.29). They are mainly parallel laminated and persistent. The basal and top contacts are sharp to gradational and commonly not erosional. It is speculated that the sediments were transported by water currents on the seafloor, not by density flows.



Figure 4.28: Photographs showing examples of tempestites from Core #1.

**5.2.6. Pelagic Deposits.** These deposits make up a majority of the TMS (Fig. 4.12). They are commonly planar laminated with little bioturbation. They are major component of LF3 and rich in clay minerals. It is interpreted that these fine silt and clay-size sediments were deposited by vertical settling.

**5.2.7. Biogenic Deposits.** Only in Core #7, one of two distal shelfward located cores, were biogenic deposits documented. Wavy, irregular, or wrinkly laminations are very distinct for biogenic deposits in LF4 (Figure 4.12). The laminae are mostly pyrite replaced, and some calcite replaced. The mineralogy and sedimentary texture of these deposits are different from those of the tractional and pelagic deposits (Figures 4.27; 4.28A-F). They are interpreted as benthic algal or microbial mats (O'Brien, 1990).

### 5.3. DEPOSITIONAL CONDITIONS

Evidence for oxygenated bottom water conditions is present near the base and top of the cores. Near the base of the core where LF1 is dominant, trace fossils, such as

*skolithos*, are very common. Bioturbation can be very intense and destroyed sedimentary structures (Figure 4.32).

Evidence for anoxic/dysoxic bottom water is restricted to distal shelfward settings. Anoxic conditions in the TMS are dominant. Evidence includes: 1) preservation of biogenically-influenced algal and microbial deposits; 2) absence of bioturbation; 3) abundance in pyrite. Biogenic deposits in LF4 are commonly pyrite replaced (Figure 4.29 C-D). These wavy laminae have been interpreted as algal/microbially trapped particles. The preservation and growth of algal/microbial mats on the seafloor suggest that the conditions are anoxic. The condition also resulted in a low degree of bioturbations. The lack of grazing by animals facilitated and promoted the preservation of organic biogenic particles. In addition, the presence and abundance of pyrite serve as a proxy for anoxic conditions. Although these biogenic deposits are only found in one core, LF3-rich intervals poor in bioturbation may also be indicative of bottom water anoxia. A strong anoxia will promote algal and microbial growth.

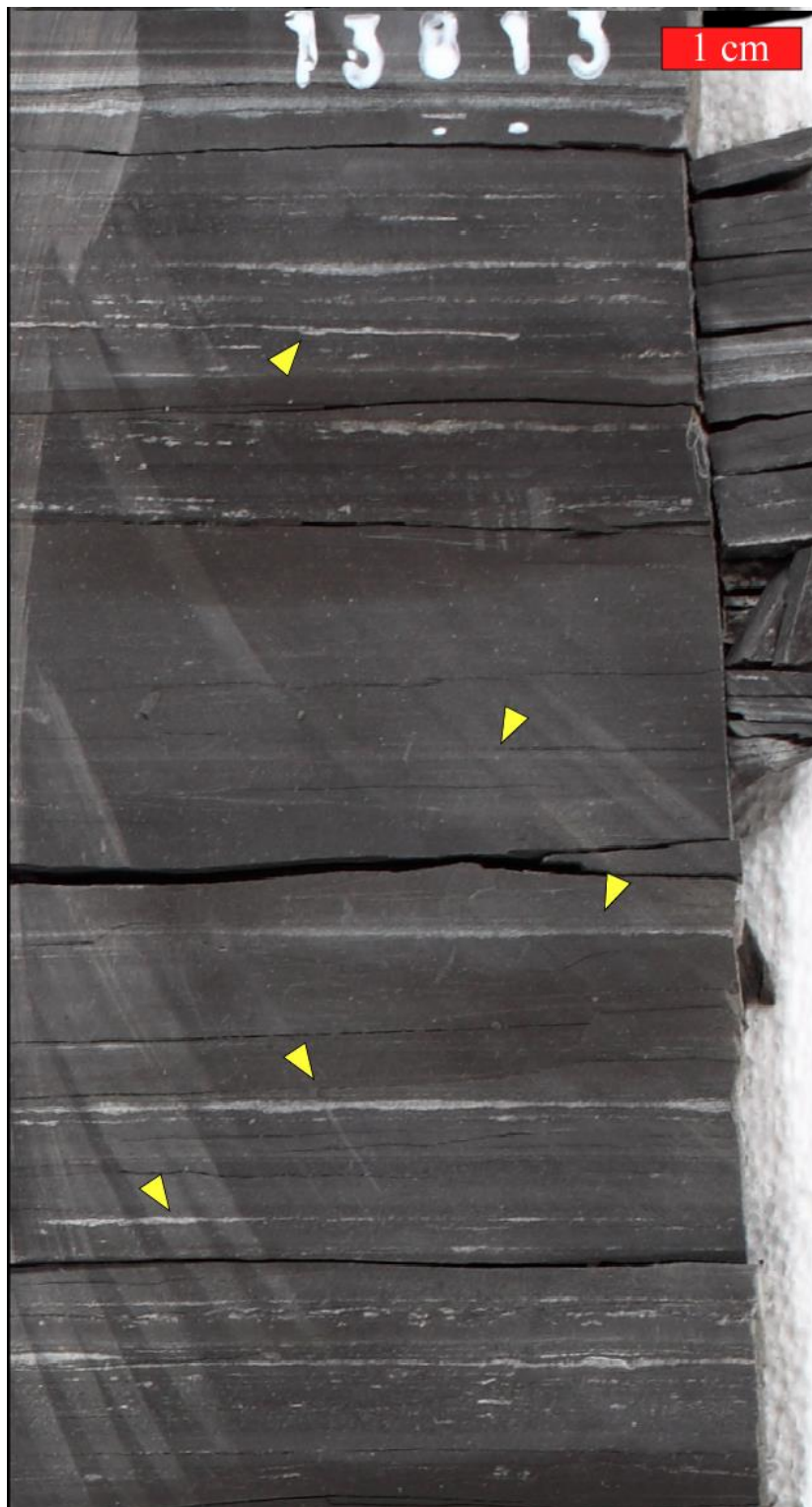


Figure 4.29: Photograph of Core #5 and current – reworked deposits lamina sets.



Figure 4.30: Photograph showing an example of algal/microbial laminae (yellow arrows) in a LF4-rich interval in Core #7.

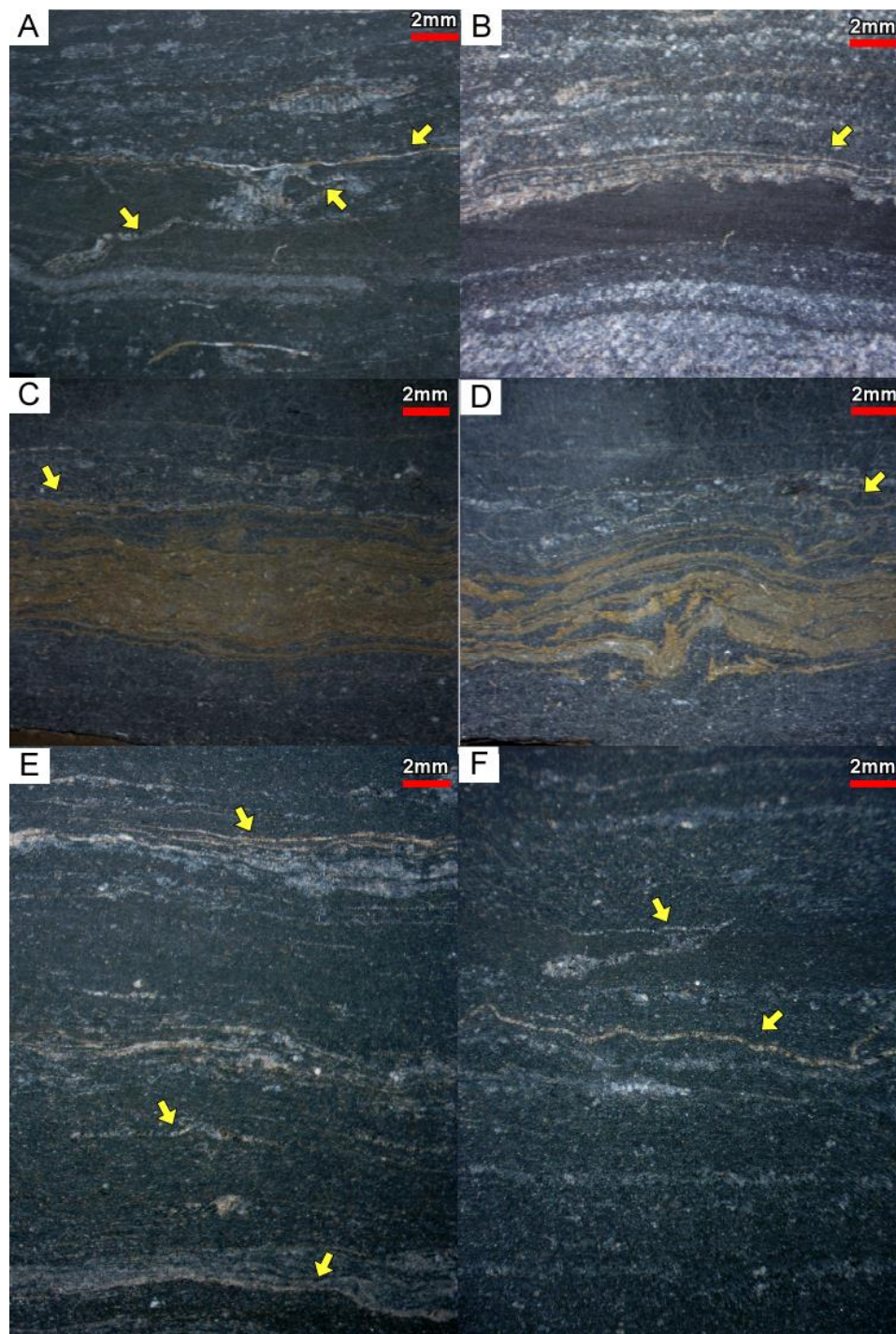


Figure 4.31 (A-F): Photograph of Core #7, showing wavy, irregular, and wrinkly laminations of a biogenic origin.

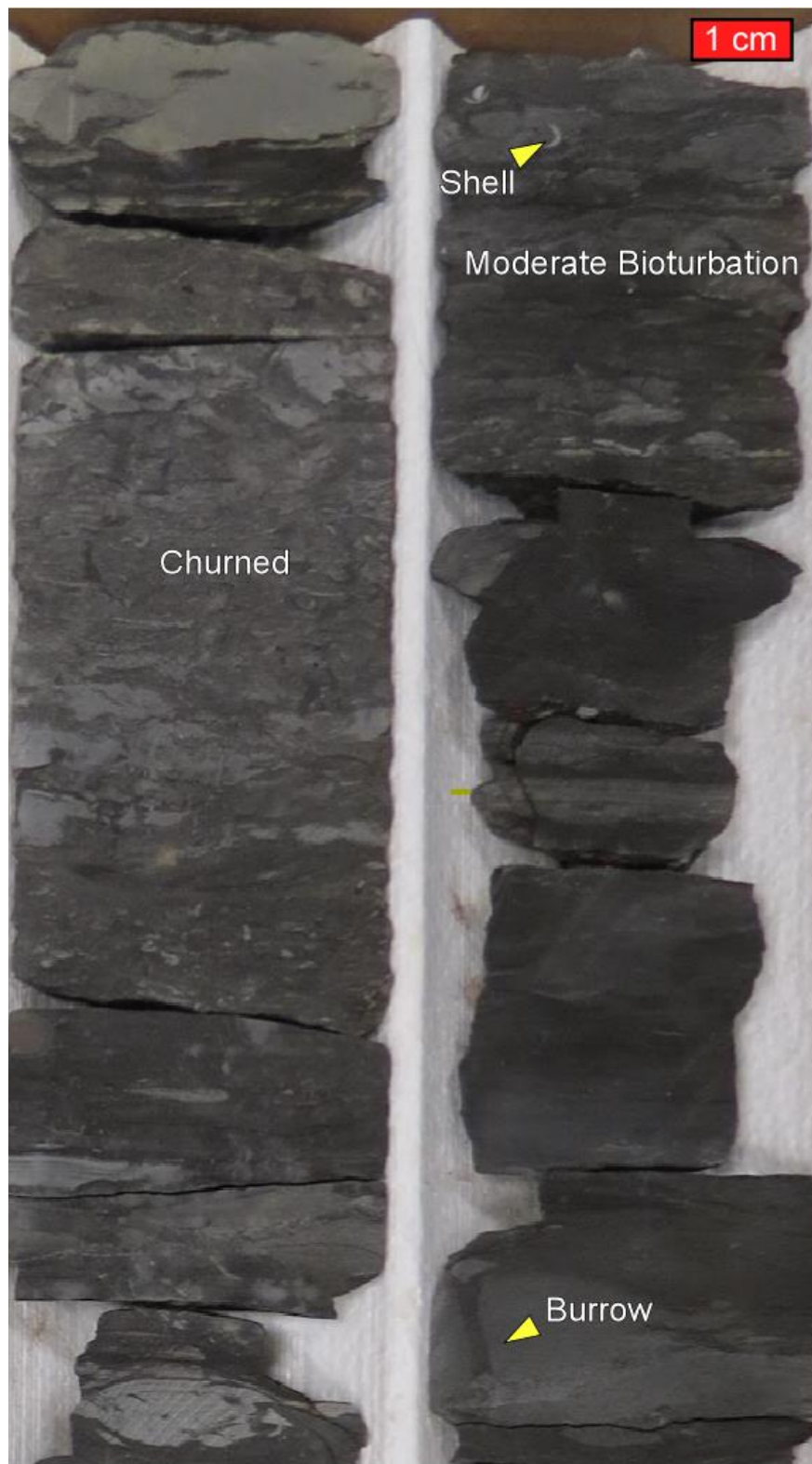


Figure 4.32: Photographs showing heavily bioturbated LF1 intervals near the base of Core #11.

## 6. CONCLUSIONS

Three types of depositional processes were interpreted from sedimentary characteristics through core observations: 1) tractional transport and deposition; 2) pelagic settling; 3) biogenic production and trapping. All lithofacies are present in both distal and proximal shelf settings. However, changes in abundance and thickness occur. The depositional processes are interpreted from data of micro- and lithofacies, and SEM and geochemical analyses. Four distinct lithofacies were documented in five cores across the TMS: 1) bedload lithofacies (LF1); 2) mixed lithofacies (LF2); 3) pelagic lithofacies (LF3); 4) biogenic lithofacies (LF4; Figure 4.1). The average mineral content in each lithofacies indicates that the dominant minerals are quartz, clay minerals, and calcite. LF1 is mostly composed of quartz with various amounts of clay and calcite. LF2 and LF3 are mostly composed of clay minerals and various amounts of calcite and quartz. LF4 is mostly dominated by calcite and various amount of clay minerals. Average TOC content shows large variations: LF1, 0.98 wt% TOC; LF2, 1.29 wt% TOC; LF3, 1.49 wt% TOC; LF4, 2.41 wt% TOC. LF1 is organic poor, while LF4 is organic-rich. Evidence in core observations and petrographic observations suggests the depositional conditions on the continental shelf and during deposition of the TMS went through anoxic, dysoxic, and oxic phases on the seafloor.

The depositional conditions present on the continental shelf can vary from oxic to anoxic/dysoxic. Evidence in core observations and petrographic observations sugg

Microscopic heterogeneities are reflected by two microfacies in LF1, two microfacies in LF2, three microfacies in LF3. Framboidal pyrite is embedded in a clay-silicate

mineral-rich framework in many samples. In addition, SEM images and point EDS analysis suggests the presence of framboidal pyrite.

Core-log calibrations suggest that it is difficult to distinguish lithofacies based on signatures of gamma-ray and resistivity wireline logs.

Future work to better quantify the heterogeneity includes the use of petrophysical data to establish porosity and permeability relationships in different types of lithofacies. Additional samples of LF4 should be analyzed to better describe the mineralogy and sedimentary texture of biogenic deposits. Poor calibration results between wireline log signatures and lithofacies can be attributed to resolution of data or variation of data values. Further use of other wireline logs such as neutron density, scratch curves, and high-resolution spectral gamma could be used to find a viable calibration of wireline log signatures and lithofacies.

**APPENDIX A.**

**XRD and TOC DATA**

Table A.1. XRD and TOC data collated from samples for wells 1, 5-7, and 11. The samples are from conventional and rotary sidewall cores. Wells 1-11 were previously published by (Borrok, et al., 2019; Beitel, 2021). The data was modified and added a lithofacies column. The following XRD and TOC values are included in the table: quartz, calcite, total clay, pyrite, plagioclase, k-feldspar, pyrite, TOC, and lithofacies.

Table A.1 XRD and TOC data from samples for wells 1, 5-7 &amp; 11.

Well #	Core Depth	Quartz	Calcite	Total Clay	Pyrite	KSPAR	PLAG	TOC	Lithofacies
	(ft)	(%)	(%)	(%)	(%)	(%)	(%)	(%)	
1	12082	17.6	11.9	63.7	6.0	0.0	5.8	1.24	3
1	12087	16.2	34.6	45	3.7	0.8	7.6	1.19	3
1	12092	25.2	6.9	57.6	3.1	1.1	8.9	2.21	3
1	12097.5	27.9	8	52.1	2.7	0.5	9.5	1.59	3
1	12102	19.8	21.9	50.1	2.6	0.0	7.7	2.43	3
1	12107	18.7	35.1	41.6	2.2	0.7	7.4	0.91	3
1	12112.5	27.1	7.5	54.2	7	8	4	1.83	2
1	12117	21.9	16	52.9	3	4	5	3.10	3
1	12122	24.4	23.3	46.1	4	2	5	1.15	3
1	12127	22.5	8	58.5	2	2	7	1.92	3
1	12132	26.3	20.3	44.9	2	0	3	1.64	2
1	12137	17.4	10.4	64	3	2	6	1.64	3
1	12142	22.4	9.7	60.8	3	4	6	2.06	3
1	12147	21.9	6.1	64.7	3	2	7	1.82	3
1	12152	19.3	0.6	68.5	4	4	5	1.75	3
1	12157	23.8	12.3	55.3	3	6	4	2.23	3
1	12162	20.8	17.3	53	4	5	9	1.83	2
1	12167	23.6	1.9	60.9	4	3	4	2.23	3
1	12172	27.1	4.6	56.2	4	8	1	0.59	1
1	12177	42.8	8.1	36	4	6	2	1.53	1
1	12182	54.6	1.5	31.2	4	4	7		2
1	12187	44.6	0	45.1	3	6	6		2
1	12192	48.6	0	41.1	2	0	8		2
5	15101.66	48.3	5.2	32.1	4	6	2		1
5	15102.26	35.8	14	37.6	2	0	7	0.57	1
5	15105.86	23	4.7	57.8	4	0	5	0.82	3
5	15110.17	32	3.2	48.9	3	7	3	0.71	2
5	15113.55	19.9	7.6	58.3	4	2	3	1.28	3
5	15115.55	18.6	5.6	60.1	4	1	3	1.00	3
5	15124.21	32.4	1.7	49.3	4	7	5	0.82	3
5	15126.73	19.3	15.1	50.2	3	1	6	1.15	3
5	15129.72	18.9	12.2	55.9	3	1	9	1.11	3
5	15131.72	24.5	10.7	52.2	8	2	3	1.67	3
5	15135.85	31.2	1.9	52.2	4	5	5	0.79	2
5	15147.53	19.8	18.2	51.8	3	0	7	1.09	3

Table A.1 XRD and TOC data from samples for wells 1, 5-7 &amp; 11 (cont.).

5	15149.24	20.4	20.1	41.1	4	1	9	1.42	3
5	15150.92	24.5	7	56.7	4	2	8	1.99	3
5	15157.18	22.6	7.5	51.6	3	0	9	1.39	3
5	15162.51	16.1	8.4	62.4	3	3	2	0.86	3
5	15162.88	27.8	3.5	55.8	4	4	4	0.91	3
5	15164.85	19.7	3.5	60.8	4	4	7	1.30	3
5	15170.94	19.5	6.5	55.3	4	2	1	1.43	3
5	15172.92	15.5	18.4	53	5	7	7	1.36	3
5	15176.76	15.6	39.8	34.2	3	5	1	1.90	3
5	15178.2	17.8	17.1	50.8	5	1	10	1.79	3
5	15180.7	19	7.6	54.8	5	2	4	1.36	3
5	15184.75	22	18.8	50.1	4	1	10	1.55	3
5	15188.75	18	4.7	53.6	4	6	2	0.87	3
5	15193.6	8.8	56.5	25.1	7	6	5	2.10	3
5	15194.91	18.2	2.8	60.5	2	2	4	1.21	3
5	15199.89	25.1	6.9	52.1	3	4	3	1.32	3
5	15202.92	20	3.8	58.2	2	4	6	1.21	3
5	15208.5	12.7	54.5	16.4	3	6	7	1.47	1
5	15209.22	24.7	20.2	32.3	2	7	6		2
5	15212.95	22.1	6.2	60.9	1	3	6	0.76	3
5	15213.45	19.7	4.5	57	3	1	6	0.69	3
5	15218.91	32.5	25	26.5	6	1.00	7.00	0.74	3
5	15220.8	31	20.3	33.2	4	2.00	10.00	0.75	3
5	15223.85	18.1	5.8	62.4	3	1.00	2.00	0.88	3
6	13748.60	26.4	9.8	53	3	3	3	1.32	3
6	13754.91	40.7	17.3	23	3	5	2	0.97	2
6	13759.65	22.8	6.3	63	3	5	4	0.81	3
6	13760.40	23.3	6.8	54	2	2	7	0.86	3
6	13760.82	25	1.8	57	1	2	6	0.95	3
6	13763.20	25.8	5.6	55	1	3	6	0.95	3
6	13767.07	21.3	8.8	56	3	1	2	0.63	2
6	13773.94	29.7	24.9	30	4	2	2	0.63	2
6	13773.94	20.6	1.2	59	6	0	6	1.55	2
6	13774.84	15.4	24.1	52	2	0	3	1.02	1
6	13775.33	16.7	13.2	54	1	2	6	1.51	3
6	13779.59	21.3	30.9	39	1	4	5	2.53	3
6	13786.35	20.7	17.2	47	1	3	5	2.07	3

Table A.1 XRD and TOC data from samples for wells 1, 5-7 &amp; 11 (cont.).

6	13789.51	21.5	13	47	1	3	4	1.09	3
6	13794.84	32.6	4.9	46	7	6	4	1.19	1
6	13798.85	34.8	10.2	40	3	0	5	0.79	1
6	13799.63	27.7	4.9	49	1	3	5	1.23	3
6	13800.20	24.6	7.5	46	3	4	2	2.80	2
6	13803.53	14.8	36.5	40	1	1	3	1.28	3
6	13806.40	32.3	4.5	48	3	5	6	1.21	1
6	13808.22	23.2	3.9	50	2	3	2	0.51	3
6	13811.26	21	16.5	42	3	4	2	1.15	2
6	13811.55	18.7	8.5	49	2	1	6	0.90	3
6	13813.42	22.4	13.1	50	2.7	0.0	2.3	1.51	3
6	13814.30	22.9	23	38	0.0	1.5	2.0	1.21	3
6	13814.70	26.2	24.2	34	3	5	0	1.30	2
6	13815.13	24.4	26.7	34	1	3	0	1.47	2
6	13815.71	18.9	25.1	42	2	4	4	2.74	2
6	13816.11	17.4	16.8	53	2.8	2.6	3.0	1.95	3
6	13819.83	18.3	6.4	57	2.6	1.2	2.2	2.40	3
6	13822.37	14	34.7	39	1.4	0.0	2.7	1.37	3
6	13822.66	18.4	25.3	47	2.8	0.0	1.6	1.66	3
6	13823.57	15.7	44.3	31	2	3	4	1.07	2
6	13825.24	22	27.2	36	3	2	4	0.74	2
6	13826.27	19.6	32.2	37	4	4	9	1.69	2
6	13826.43	18.6	34.3	36	4	7	3	1.20	2
6	13828.65	9.6	63.8	17	4	0	8	0.55	1
6	13829.14	11.2	78.8	3	2	3	3	2.79	1
6	13832.60	20.4	15.6	52	2.4	0.0	2.3	2.01	3
6	13833.60	20.6	11.2	57	5.6	0.0	2.0	1.70	3
6	13835.33	21	22.8	45	6.5	0.0	1.9	0.98	3
6	13837.78	22.2	4.7	52	7.6	0.0	2.3	1.94	3
6	13839.60	19.6	29.3	36	2.4	0.0	1.6	1.06	3
6	13843.39	21.2	45.7	21	4	2	6	1.77	1
6	13843.51	18.4	50.4	14	6	2	7	0.94	1
6	13843.68	31.4	28	18	5	3	5	0.79	1
6	13844.64	25.6	3.8	44	3	1	5	1.85	1
6	13845.28	25.9	28.7	26	3	6	5	0.55	1
6	13845.50	9.3	70.6	10	2	2	2	0.62	1
6	13845.85	19.1	10.4	49	2	10	3	1.17	1

Table A.1 XRD and TOC data from samples for wells 1, 5-7 &amp; 11 (cont.).

6	13846.23	15	52.3	24	3	10	4	0.62	1
6	13846.38	30	20.2	30	4	3	6	0.62	1
6	13846.69	27.2	10.9	45	3.0	0.0	2.2	0.57	3
6	13848.50	27.2	4.8	52	3	2	3	0.64	2
6	13849.51	28.9	4	52	7.2	0.0	3.5	1.07	3
6	13853.27	23.8	12	48	5.3	0.0	3.1	0.78	3
6	13855.50	25.2	5	52	2.7	0.8	3.3	1.24	3
6	13856.54	34	25.2	22	4	5	4	2.17	1
6	13860.48	25.8	7.9	49	1.6	0.0	2.6	0.11	3
6	13862.91	67.6	12.6	7	7	6	3	0.76	1
6	13864.32	70.8	1.6	15	7	6	5	0.67	1
6	13865.52	35.3	4.4	49	6.1	0.6	3.6	0.77	3
6	13867.78	41.4	1.2	42	3	7	3	0.49	2
6	13868.31	48.6	0.5	34	6	7	8	0.57	2
6	13872.76	68.1	0.7	13	2	3	2	0.38	1
6	13879.74	55.3	0.3	30	5	3	3	0.21	1
6	13880.31	62.8	1.4	21	5	9	8	0.17	1
6	13884.80	61.7	6.6	14	5	7	6	0.37	1
6	13885.68	53.4	0.3	32	8	10	4	0.68	2
6	13893.85	27.2	1.6	59	5	7	7	0.19	1
6	13895.70	59.8	0.4	19	4	2	5	0.30	1
6	13901.70	67.7	0	22	3	10	1	0.60	1
6	13907.44	36	1.1	49	3.7	0.9	5.1	0.42	3
6	13908.28	39.3	0.4	46	4.1	0.0	4.1		3
7	12466.45	32	14	38	2		1.00	1.31	3
7	12471.35	52	14	14	3	6	4	0.94	2
7	12474.1	18	16	56	6	2.00	4.00	1.55	3
7	12481.4	16	36	42	4	1.00	3.00	1.26	3
7	12488	22	5	58	0	2	7	1.19	2
7	12493.55	21	11	56	6	1.00	3.00	1.63	3
7	12500	17	20	48	1		2.00	2.02	3
7	12512	14	38	42	9	1.00	1.00	2.02	3
7	12520.35	16	26	44	3	1.00	1.00		3
7	12530.05	15	30	47	8	2.00	2.00	1.25	3
7	12537.2	17	9	58	4	1.00	2.00	0.83	3
7	12540.35	17	18	55	2		2.00	2.41	3
7	12542.05	12	53	30	2		2.00	2.62	4

Table A.1 XRD and TOC data from samples for wells 1, 5-7 &amp; 11 (cont.).

7	12545.65	20	5	62	6	2.00	2.00	1.19	3
7	12548.85	21	4	62	5	2.00	3.00	2.41	3
7	12550.4	16	25	51	4		2.00	1.58	3
7	12552.2	22	2	64	8		2.00	1.76	3
7	12553.4	7	74	9	5	2.00	3.00	1.97	4
7	12560	21	4	55	5		2.00	1.13	3
7	12560.4	14	28	51	11	2.00	4.00	2.55	3
7	12564.15	23	9	54	2	1.00	2.00	2.22	3
7	12565.15	12	41	40	1	1	6		2
7	12568.45	11	51	30	6	1.00	2.00	2.34	4
7	12570.45	7	72	14	3		2.00	2.73	4
7	12574.7	13	22	51	5	1.00	4.00	2.60	3
7	12577	28	27	34	3	1.00	2.00	2.19	3
7	12584.4	15	30	47	3		2.00	3.20	3
11	13609.50	28.4	15.7	48.8	1.1	0.0	2.9		3
11	13615.50	27.8	26.4	39.8	7.5	0.0	3.7		3
11	13621.50	30.9	15.9	44.8	5.7	0.0	3.5		3
11	13627.50	35.5	12	44.5	1.4	0.0	3.3		3
11	13633.50	28	27.1	39.5	6.4	0.8	3.9		3
11	13646.00	29.6	17.1	48.9	1.8	0.7	5.0	1.55	3
11	13651.50	33.8	19.7	39.7	2.0	0.7	3.5	2.71	3
11	13657.50	32.4	12.5	47.5	5	4	6	1.77	2
11	13663.50	31.3	8.8	50.6	2.5	0.0	3.6	2.93	3
11	13669.50	30.4	6.9	52.8	0.9	0.0	4.5	2.21	3
11	13675.50	36.8	13.9	43.9	6.3	1.1	3.6	1.94	3
11	13687.00	31.4	8.8	51.7	1.7	0.0	6.2	2.19	3
11	13693.00	33.4	6.4	49.5	2.8	0.0	6.2	2.32	3
11	13699.00	32.5	2.4	56.7	4	2	3	1.35	2

**APPENDIX B.  
WIRELINE LOG DATA**

Table B.1. Gamma ray and deep resistivity data collated from wells 1, 6, and 7. The data comes from wireline logs. The following values are included in the table: deep resistivity, gamma ray, and lithofacies.

Table B.1 Gamma Ray and Deep Resistivity data from wells 1, 6 &amp; 7.

Well Number	Core Depth (ft)	Lithofacies	Deep Resistivity (ohm)	Gamma Ray (API)
1	12099.0	3	7.4959	94.25
1	12099.5	3	7.5842	95.03
1	12100.0	3	7.7275	108.01
1	12100.5	3	7.7503	106.45
1	12101.0	3	7.6679	107.13
1	12101.5	3	7.5128	101.67
1	12102.0	3	7.3866	104.92
1	12102.5	3	7.3816	106.22
1	12103.0	3	7.2441	103.38
1	12103.5	1	7.1106	98.08
1	12104.0	1	7.0658	95.51
1	12104.5	3	7.3138	95.42
1	12105.0	3	7.882	95.91
1	12105.5	2	8.4731	94.84
1	12106.0	3	9.0792	92.98
1	12106.5	3	9.4065	92.59
1	12107.0	3	9.5135	88.16
1	12107.5	2	9.526	90.21
1	12108.0	3	9.5627	95.19
1	12108.5	3	9.7479	102.64
1	12109.0	3	9.8484	102.64
1	12109.5	3	9.6286	99.91
1	12110.0	3	9.4448	99.03
1	12110.5	3	9.1468	100.59
1	12111.0	3	9.0612	99.81
1	12111.5	3	8.956	101.14
1	12112.0	3	8.9324	99.58
1	12112.5	3	9.0725	99.78
1	12113.0	3	9.052	97.67
1	12113.5	3	8.9797	97.47
1	12114.0	3	8.765	99.42
1	12114.5	3	8.7401	102.64
1	12115.0	3	8.337	103.72
1	12115.5	2	8.1346	102.55
1	12116.0	3	7.9726	102.06
1	12116.5	3	7.836	99.72
1	12117.0	3	7.6151	98.27

Table B.1 Gamma Ray and Deep Resistivity data from wells 1, 6 &amp; 7 (cont.).

1	12117.5	3	7.6682	98.96
1	12118.0	3	7.9537	100.22
1	12118.5	3	8.3239	100.59
1	12119.0	3	8.7165	99.03
1	12119.5	2	9.1207	93.47
1	12120.0	1	9.6531	89.76
1	12120.5	3	10.1844	88.98
1	12121.0	3	10.4328	93.96
1	12121.5	3	10.264	96.89
1	12122.0	1	9.9077	92.89
1	12122.5	1	9.5239	89.45
1	12123.0	3	9.2126	86.01
1	12123.5	3	9.0055	85.62
1	12124.0	3	8.8872	83.89
1	12124.5	3	8.837	87.62
1	12125.0	3	8.9245	85.86
1	12125.5	3	9.0518	88.11
1	12126.0	2	9.153	88.89
1	12126.5	3	9.3751	94.16
1	12127.0	3	9.5847	93.28
1	12127.5	2	9.8139	91.13
1	12128.0	3	10.1369	89.35
1	12128.5	3	10.5062	87.71
1	12129.0	3	11.0689	86.63
1	12129.5	2	11.511	88.8
1	12130.0	3	11.9382	95.12
1	12130.5	3	12.2025	104.16
1	12131.0	2	12.7056	102.31
1	12131.5	1	13.0116	99
1	12132.0	1	12.6373	93.19
1	12132.5	3	10.5105	98.41
1	12133.0	3	9.5885	107.87
1	12133.5	3	8.3468	112.65
1	12134.0	3	7.4337	115.43
1	12134.5	3	7.019	113.86
1	12135.0	3	7.1839	111.52
1	12135.5	3	7.9472	110.84
1	12136.0	1	8.7866	106.45
1	12136.5	3	9.5582	106.06

Table B.1 Gamma Ray and Deep Resistivity data from wells 1, 6 &amp; 7 (cont.).

1	12137.0	1	9.5615	99.23
1	12137.5	2	8.7371	104.4
1	12138.0	3	7.8949	105.57
1	12138.5	3	7.2309	111.75
1	12139.0	3	6.9384	108.92
1	12139.5	3	6.9531	103.05
1	12140.0	3	7.1444	97.91
1	12140.5	3	7.3105	96.4
1	12141.0	3	7.2726	101.78
1	12141.5	3	7.2166	103.86
1	12142.0	3	7.2068	107.61
1	12142.5	2	7.0433	106.06
1	12143.0	3	7.1025	103.52
1	12143.5	3	7.4075	99.81
1	12144.0	3	7.7649	102.94
1	12144.5	3	8.2922	108.6
1	12145.0	3	8.7452	108.89
1	12145.5	1	9.1963	110.35
1	12146.0	3	9.6689	111.03
1	12146.5	3	10.1413	114.74
1	12147.0	3	10.7632	109.18
1	12147.5	3	10.8958	99.62
1	12148.0	3	10.1346	93.31
1	12148.5	3	8.7711	95.17
1	12149.0	3	7.666	102.43
1	12149.5	3	6.9209	106.34
1	12150.0	2	6.5864	110.65
1	12150.5	3	6.518	110.04
1	12151.0	3	6.5224	109.13
1	12151.5	3	6.5158	105.21
1	12152.0	3	6.6372	100.69
1	12152.5	3	6.8253	98.37
1	12153.0	3	7.1325	96.91
1	12153.5	3	7.5268	100.24
1	12154.0	3	7.9645	102.06
1	12154.5	3	8.5404	102.61
1	12155.0	3	9.2999	103.88
1	12155.5	3	9.8436	106.03
1	12156.0	3	9.9644	110.64

Table B.1 Gamma Ray and Deep Resistivity data from wells 1, 6 &amp; 7 (cont.).

1	12156.5	3	10.0204	116.11
1	12157.0	3	10.2149	119.13
1	12157.5	3	10.393	119.92
1	12158.0	3	10.6213	116.2
1	12159.5	3	10.0146	104.11
1	12160.0	3	9.8303	101.77
1	12160.5	3	9.6299	103.23
1	12161.0	3	9.4891	103.81
1	12161.5	3	9.2717	107.81
1	12162.0	3	9.0437	105.67
1	12162.5	3	8.9352	102.35
1	12163.0	3	9.0151	96.4
1	12163.5	3	9.1168	94.55
1	12164.0	3	9.0397	91.72
1	12164.5	3	8.899	93.76
1	12165.0	3	8.854	96.5
1	12165.5	1	9.0179	104.79
1	12166.0	3	9.1145	106.25
1	12166.5	3	9.2891	103.03
1	12167.0	3	9.4802	96.69
1	12167.5	3	9.9858	97.68
1	12168.0	1	10.3342	101.78
1	12168.5	1	10.3665	105.68
1	12169.0	3	10.1283	106.64
1	12169.5	3	10.076	109.47
1	12170.0	3	9.6527	110.35
1	12170.5	3	9.6111	108.99
1	12171.0	3	10.1097	107.03
1	12171.5	3	10.568	107.91
1	12172.0	3	10.8991	107.91
1	12172.5	3	10.4762	105.96
1	12173.0	3	9.8678	104.6
1	12173.5	1	9.3857	103.33
1	12174.0	3	8.7497	100.98
1	12174.5	3	8.2107	99.13
1	12175.0	3	7.6151	99.72
1	12175.5	1	7.0439	103.62
1	12176.0	3	6.7515	102.74
1	12176.5	3	6.7748	99.55

Table B.1 Gamma Ray and Deep Resistivity data from wells 1, 6 &amp; 7 (cont.).

1	12177.0	3	7.0821	95.16
1	12177.5	3	7.0621	99.46
1	12178.0	2	7.1041	104.11
1	12178.5	3	7.2628	101.28
1	12179.0	1	7.3458	94.74
1	12179.5	1	7.5422	86.06
1	12180.0	3	7.5795	85.51
1	12180.5	3	7.5494	80.61
1	12181.0	2	7.4801	81.58
1	12181.5	2	7.3315	81.68
1	12182.0	2	7.4501	81.81
1	12182.5	3	8.1034	75.3
1	12183.0	3	9.3297	64.52
1	12183.5	3	10.7958	55.93
1	12184.0	3	11.8289	58.15
1	12184.5	1	13.1406	65.18
1	12185.0	1	14.8467	67.13
1	12185.5	1	15.7307	63.52
1	12186.0	3	15.0487	62.64
1	12186.5	1	13.1835	75.23
1	12187.0	1	11.3324	83.86
1	12187.5	1	9.8212	90.01
1	12188.0	1	9.0118	90.3
1	12188.5	2	8.7441	92.89
1	12189.0	1	8.8327	91.13
1	12189.5	3	9.0242	91.36
1	12190.0	1	9.3107	91.94
1	12190.5	2	9.1837	96.53
1	12191.0	1	8.2841	104.2
1	12191.5	2	7.5369	107.91
1	12192.0	2	6.7766	115.82
1	12192.5	3	6.2625	109.28
1	12193.0	3	6.1929	111.97
1	12193.5	3	6.4378	106.22
1	12194.0	3	6.634	104.85
1	12194.5	3	6.8845	102.25
1	12195.0	3	6.992	105.77
1	12195.5	3	6.796	113.57
1	12196.0	1	6.6184	114.94

Table B.1 Gamma Ray and Deep Resistivity data from wells 1, 6 &amp; 7 (cont.).

1	12196.5	1	6.505	108.93
1	12197.0	3	6.5873	101.13
1	12197.5	3	7.1529	91.96
1	12198.0	3	7.7631	87.33
1	12198.5	3	8.4169	82.91
1	12199.0	3	8.5623	84.08
1	12199.5	1	8.1131	88.08
1	12200.0	2	7.3624	90.25
1	12200.5	1	6.8031	91.12
1	12201.0	2	6.5421	91.02
1	12201.5	2	6.495	91.41
1	12202.0	2	6.5394	93.18
1	12202.5	2	6.6157	89.67
1	12203.0	3	6.7276	91.03
1	12203.5	3	6.8716	87.62
1	12204.0	3	7.1205	90.15
1	12204.5	1	7.3268	90.31
1	12205.0	1	7.3496	91.87
1	12205.5	1	7.3147	91.68
1	12206.0	1	7.3208	90.25
1	12206.5	1	7.486	88.3
1	12207.0	1	7.7564	84.98
1	12207.5	2	7.9204	82.54
1	12208.0	1	7.7493	84.98
1	12208.5	1	7.3046	90.35
1	12209.0	3	6.9713	92.36
1	12209.5	3	6.4627	88.94
1	12210.0	2	6.4719	81.53
1	12210.5	3	6.3821	74.06
1	12211.0	3	6.6452	70.64
1	12211.5	3	6.466	69.36
1	12212.0	2	5.3697	77.55
1	12212.5	1	4.2312	90.34
1	12213.0	1	3.5274	104.6
1	12213.5	1	2.9835	114.16
1	12214.0	1	2.7413	113.18
6	13763.5	3	12.1688	148.05
6	13764.0	3	9.1559	148.55
6	13764.5	3	8.7301	148.97

Table B.1 Gamma Ray and Deep Resistivity data from wells 1, 6 &amp; 7 (cont.).

6	13765.0	3	9.3364	148.27
6	13766.5	2	7.07	150.25
6	13766.0	3	8.0426	147.67
6	13766.5	2	7.07	150.25
6	13767.0	3	6.8846	148.36
6	13767.5	2	7.3992	154.37
6	13768.0	2	7.8498	153.73
6	13768.5	2	7.7696	156.55
6	13769.0	3	7.7433	152.13
6	13769.5	2	7.8403	149.55
6	13770.0	3	7.4867	150.95
6	13770.5	1	7.2299	147.39
6	13771.0	1	7.0476	145.27
6	13771.5	2	6.9551	144.05
6	13772.0	2	7.2731	150.87
6	13772.5	2	7.8257	147.04
6	13773.0	3	7.4834	145.2
6	13773.5	3	7.811	146.42
6	13774.0	3	7.856	156.04
6	13774.5	3	7.4018	161.23
6	13775.0	3	6.5941	155.15
6	13775.5	3	6.4682	149.63
6	13776.0	3	6.6688	143.74
6	13776.5	3	6.9382	147.86
6	13777.0	3	7.0971	156.46
6	13777.5	3	6.9955	166.66
6	13778.0	3	6.6213	169.04
6	13778.5	3	6.2772	164.89
6	13779.0	3	6.2455	160.92
6	13779.5	3	7.1262	159.2
6	13780.0	3	7.9446	157.06
6	13780.5	3	8.2362	157.43
6	13781.0	3	9.4029	154.98
6	13781.5	3	10.5556	155.78
6	13782.0	3	10.3618	151.85
6	13782.5	3	9.8376	156.52
6	13783.0	3	8.5427	161.07
6	13783.5	2	7.6064	164.39
6	13784.0	3	8.0177	162.3

Table B.1 Gamma Ray and Deep Resistivity data from wells 1, 6 &amp; 7 (cont.).

6	13784.5	3	8.7784	159.13
6	13785.0	3	9.1183	152.33
6	13785.5	2	7.9901	148.7
6	13786.0	3	7.0027	148.75
6	13786.5	2	7.1226	144.13
6	13787.0	3	8.0006	139.55
6	13787.5	3	8.4747	129.36
6	13788.0	3	9.5722	134.87
6	13788.5	3	9.3793	138.77
6	13789.0	3	8.6533	151.24
6	13789.5	3	8.3598	148.64
6	13790.0	1	8.2468	148.76
6	13790.5	2	7.7055	136.98
6	13791.0	2	6.8385	144.42
6	13791.5	2	6.8405	146.39
6	13792.0	2	8.3697	150.12
6	13792.5	1	11.1354	142.86
6	13793.0	3	11.6902	142.69
6	13793.5	3	9.7846	150.8
6	13794.0	3	8.2395	159.37
6	13794.5	3	8.5526	157.51
6	13795.0	3	9.5599	149.37
6	13795.5	1	10.0642	145.56
6	13796.0	3	11.4419	139.25
6	13796.5	3	13.9875	137.94
6	13797.0	3	12.3645	131.31
6	13797.5	3	10.0628	133.64
6	13798.0	3	9.1745	132.64
6	13798.5	3	6.9265	134.92
6	13799.0	3	5.4309	132.84
6	13799.5	3	5.9119	138.14
6	13800.0	3	7.1567	142.24
6	13800.5	3	7.7919	147.84
6	13801.0	3	8.4199	141.44
6	13801.5	3	10.8313	134.93
6	13802.0	2	10.4732	133.45
6	13802.5	2	10.1201	136.98
6	13803.0	3	9.0712	134.28
6	13803.5	3	8.424	129.54

Table B.1 Gamma Ray and Deep Resistivity data from wells 1, 6 &amp; 7 (cont.).

6	13804.0	3	8.1584	131.38
6	13804.5	3	8.3214	138.53
6	13805.0	3	8.5071	140.12
6	13805.5	3	8.7185	141.46
6	13806.0	3	8.1248	137.99
6	13806.5	3	7.9655	147.21
6	13807.0	3	8.0858	151.63
6	13807.5	3	7.5484	157.52
6	13808.0	3	7.4877	154.32
6	13808.5	3	7.9013	152.66
6	13809.0	3	8.3516	152.9
6	13809.5	1	8.8605	152.17
6	13810.0	3	10.3772	147.2
6	13810.5	3	9.2064	142.25
6	13811.0	3	8.1986	144.59
6	13811.5	3	7.1699	145.5
6	13812.0	1	7.4073	146.9
6	13812.5	3	8.557	139.38
6	13813.0	1	11.7318	137.78
6	13813.5	3	18.1867	138.52
6	13814.0	3	24.4582	141.94
6	13814.5	3	17.016	143.98
6	13815.0	3	10.5936	145.47
6	13815.5	3	8.5515	147.96
6	13816.0	3	10.8835	148.87
6	13816.5	3	12.9145	147.45
6	13817.0	3	15.4823	148.18
6	13817.5	3	15.5569	147.57
6	13818.0	3	15.5473	144.85
6	13818.5	3	14.4263	138.59
6	13819.0	3	12.358	135.97
6	13819.5	3	12.2972	136.66
6	13820.0	3	13.8604	134.69
6	13820.5	3	15.2047	125.75
6	13821.0	3	15.6275	119.24
6	13821.5	3	14.505	113.71
6	13822.0	3	12.9598	119.9
6	13822.5	3	12.1905	129.7
6	13823.0	3	10.4536	138.29

Table B.1 Gamma Ray and Deep Resistivity data from wells 1, 6 &amp; 7 (cont.).

6	13823.5	3	9.6697	141.07
6	13824.0	3	10.9043	147.57
6	13824.5	3	11.9972	156.9
6	13825.0	3	11.182	161.14
6	13825.5	3	9.7785	152.81
6	13826.0	3	9.5256	151.09
6	13826.5	3	9.9969	152.64
6	13827.0	3	11.1307	155.22
6	13827.5	3	12.3982	153.72
6	13828.0	2	13.2586	151.82
6	13828.5	3	12.9807	147.67
6	13829.0	3	12.1647	146.2
6	13829.5	3	11.1002	149.31
6	13830.0	3	11.6155	160.36
6	13830.5	3	12.1594	166.23
6	13831.0	3	12.1479	162.42
6	13831.5	3	11.893	153.94
6	13832.0	3	11.267	144.16
6	13832.5	2	10.8554	141.6
6	13833.0	2	10.5836	142.83
6	13833.5	2	10.976	148.95
6	13834.0	3	11.4938	157.86
6	13834.5	3	12.3539	154.05
6	13835.0	2	12.9674	151.84
6	13835.5	3	13.3733	141.94
6	13836.0	3	11.9232	145.01
6	13836.5	3	10.1672	147.96
6	13837.0	3	7.8428	156.48
6	13837.5	3	5.884	160.65
6	13838.0	3	5.8931	158.63
6	13838.5	3	8.0132	155.75
6	13839.0	3	10.7413	147.76
6	13839.5	3	13.7239	144.31
6	13840.0	3	15.3273	138.32
6	13840.5	1	15.9914	137.1
6	13841.0	1	15.437	133.5
6	13841.5	1	13.0631	136.32
6	13842.0	1	11.503	140.12
6	13842.5	1	10.0462	149.82

Table B.1 Gamma Ray and Deep Resistivity data from wells 1, 6 &amp; 7 (cont.).

6	13843.0	1	9.8063	148.85
6	13843.5	3	10.1241	144.29
6	13844.0	3	10.9183	136.44
6	13844.5	3	12.1087	131.95
6	13845.0	2	12.6319	131.83
6	13845.5	3	12.2385	118.85
6	13846.0	3	14.8095	109.32
6	13846.5	1	18.4345	112.5
6	13847.0	1	17.496	130.4
6	13847.5	3	15.8574	145.53
6	13848.0	3	13.8799	142.65
6	13848.5	3	12.4114	133.05
6	13849.0	3	10.11	126.42
6	13849.5	3	10.2259	131.71
6	13850.0	3	10.948	136.01
6	13850.5	3	12.1043	142.23
6	13851.0	3	12.2627	141.8
6	13851.5	3	10.3448	150.14
6	13852.0	3	9.3123	150.49
6	13852.5	1	9.5859	145.56
6	13853.0	3	10.1497	145.21
6	13853.5	3	11.4711	150.31
6	13854.0	3	12.3835	159.13
6	13854.5	3	13.6268	158.62
6	13855.0	3	14.8453	159.11
6	13855.5	3	16.2676	161.99
6	13856.0	3	19.0836	163.24
6	13856.5	3	17.2973	158.43
6	13857.0	3	11.7555	150.44
6	13857.5	1	10.6152	145.21
6	13858.0	3	10.6898	145.84
6	13858.5	3	10.5459	154.04
6	13859.0	3	11.3287	147.25
6	13859.5	2	12.9687	133.13
6	13860.0	3	14.5186	120.26
6	13860.5	3	14.1402	117.64
6	13861.0	3	13.3074	118.38
6	13861.5	1	13.9056	106.84
6	13862.0	1	16.6187	96.89

Table B.1 Gamma Ray and Deep Resistivity data from wells 1, 6 &amp; 7(cont.).

6	13862.5	1	16.0264	90.1
6	13863.0	1	13.2274	89.12
6	13863.5	1	11.1507	87.86
6	13864.0	1	12.5134	94.63
6	13864.5	3	13.3121	100.71
6	13865.0	3	13.4666	107.51
6	13865.5	3	12.3698	115.88
6	13866.0	3	12.2913	132.11
6	13866.5	3	12.519	148.92
6	13867.0	3	13.1267	155.88
6	13867.5	3	12.8076	155.55
6	13868.0	3	12.7253	147.95
6	13868.5	2	13.1091	140.11
6	13869.0	3	14.8826	138.82
6	13869.5	2	16.948	143.38
6	13870.0	2	12.877	152.6
6	13870.5	2	9.9379	153.12
6	13871.0	3	9.304	158.77
6	13871.5	3	10.1848	151.06
6	13872.0	3	11.6659	140.62
6	13872.5	3	12.5204	128.34
6	13873.0	3	11.5705	134.67
6	13873.5	3	11.5926	142.55
6	13874.0	3	11.4417	149.47
6	13874.5	2	11.9105	148.5
6	13875.0	2	12.2342	148.35
6	13875.5	3	12.6915	145.85
6	13876.0	3	13.1169	136.46
6	13876.5	3	14.4677	129.47
6	13877.0	1	15.9832	128.74
6	13877.5	3	12.0949	127.84
6	13878.0	3	11.3469	132.88
6	13878.5	3	8.8614	133.8
6	13879.0	2	8.9981	133.06
6	13879.5	1	9.8459	124.19
6	13880.0	3	9.0044	118.95
6	13880.5	1	11.3511	132.67
6	13881.0	3	8.6773	151.51
6	13881.5	3	7.7197	163.89

Table B.1 Gamma Ray and Deep Resistivity data from wells 1, 6 &amp; 7(cont.).

6	13882.0	3	6.9572	165.74
6	13882.5	3	6.3908	162.06
6	13883.0	3	6.1064	162.75
6	13883.5	3	5.588	160.56
6	13884.0	3	4.5731	163.83
6	13884.5	3	3.3959	178.25
6	13885.0	1	3.0861	187.8
6	13885.5	2	4.4521	182.93
6	13886.0	2	7.3531	150.4
6	13886.5	2	7.4631	123.69
6	13887.0	1	8.1711	115.22
6	13887.5	3	7.8526	127.34
6	13888.0	3	6.1631	140.55
6	13888.5	1	4.8887	148.17
6	13889.0	2	5.2172	153.81
6	13889.5	1	5.6588	156.26
6	13890.0	1	6.7306	141.84
6	13890.5	1	7.581	131.95
6	13891.0	1	11.1284	121.54
6	13891.5	3	11.1693	127.07
6	13892.0	2	7.5811	133.7
6	13892.5	3	5.1961	142.18
6	13893.0	3	4.4324	150.46
6	13893.5	3	4.0862	153.71
6	13894.0	3	3.7196	158.59
6	13894.5	3	3.3345	160.31
6	13895.0	3	3.1306	157.09
6	13895.5	3	3.036	151.32
6	13896.0	3	3.0653	151.68
6	13896.5	3	3.2067	150.91
6	13897.0	3	3.2029	151.54
6	13897.5	2	3.1929	147.11
6	13898.0	1	4.0775	136.18
6	13898.5	2	5.662	130.42
6	13899.0	2	6.9496	119.89
6	13899.5	2	5.8643	128.34
6	13900.0	1	4.8127	138.28
6	13900.5	2	4.6	150.02
6	13901.0	3	4.5371	150.42

Table B.1 Gamma Ray and Deep Resistivity data from wells 1, 6 &amp; 7 (cont.).

6	13901.5	2	4.4426	148.97
6	13902.0	2	4.4018	150.85
6	13902.5	2	4.3439	154.9
6	13903.0	1	4.78	144.57
6	13903.5	2	5.9075	142.21
6	13904.0	2	6.2629	134.1
6	13904.5	2	5.7863	145.16
6	13905.0	2	4.639	151.81
6	13905.5	3	3.6878	162.47
6	13906.0	3	3.3333	162.82
6	13906.5	3	3.3443	163.31
6	13907.0	2	3.4109	160.36
6	13907.5	3	3.5813	156.91
6	13908.0	3	3.675	157.77
6	13908.5	3	3.5229	164.44
6	13909.0	3	3.4813	166.42
6	13909.5	3	3.4242	157.04
6	13910.0	3	3.4502	146.71
6	13910.5	3	3.5012	145.87
6	13911.0	3	3.5397	152.52
6	13911.5	3	3.6406	158.79
6	13912.0	3	3.1098	168.24
6	13912.5	2	3.1976	176.37
6	13913.0	1	4.3603	170.88
6	13913.5	1	6.9541	149.87
6	13914.0	1	12.0409	115.84
6	13914.5	2	17.8015	103.76
6	13915.0	3	14.9913	109.16
6	13915.5	3	8.0906	125.64
6	13916.0	2	5.7578	137.56
6	13916.5	3	5.3334	136.25
6	13917.0	3	4.6171	142.96
6	13917.5	3	4.1998	149.96
6	13918.0	2	3.5353	155.37
6	13918.5	3	3.3631	160.77
6	13919.0	2	3.4774	158.32
6	13919.5	2	4.0608	157.18
6	13920.0	2	5.0788	142.19
6	13920.5	3	5.8265	127.56

Table B.1 Gamma Ray and Deep Resistivity data from wells 1, 6 &amp; 7 (cont.).

6	13921.0	2	6.1251	126.09
6	13921.5	1	6.1943	130
6	13922.0	2	7.0836	140.83
6	13922.5	2	9.2703	142.86
6	13923.0	2	11.7431	145.71
6	13923.5	3	11.0078	138.09
6	13924.0	2	10.18	133.14
6	13924.5	2	8.4847	129.95
6	13925.0	2	7.4254	136.19
6	13925.5	3	6.3838	136.9
6	13926.0	3	6.0093	143.57
6	13926.5	2	7.0328	150.45
6	13927.0	1	7.8001	152.91
6	13927.5	1	8.4624	141.05
6	13928.0	1	8.5198	129.63
6	13928.5	1	9.2535	126.24
6	13929.0	1	11.2548	130.83
6	13929.5	1	14.0235	130.36
6	13930.0	2	16.326	132.98
6	13930.5	1	15.2387	129.3
6	13931.0	2	13.8975	127.34
6	13931.5	1	14.1043	123.56
6	13932.0	1	11.9914	121.7
6	13932.5	1	10.478	115.2
6	13933.0	1	8.7303	100.22
6	13933.5	1	8.5861	93.34
6	13934.0	1	8.5382	93.34
6	13934.5	1	9.0641	92.61
6	13935.0	1	9.6953	86.62
6	13935.5	1	10.7863	78.12
6	13936.0	1	12.1281	78.24
6	13936.5	1	16.7776	83.54
6	13937.0	1	19.1814	90.54
6	13937.5	1	14.5901	103.14
6	13938.0	1	10.0907	113.42
6	13938.5	1	7.6732	116.76
6	13939.0	1	6.2029	108.68
6	13939.5	1	5.7451	98.74
6	13940.0	1	4.9202	91.96

Table B.1 Gamma Ray and Deep Resistivity data from wells 1, 6 &amp; 7 (cont.).

6	13940.5	1	4.7892	95.04
6	13941.0	1	3.9193	84.22
6	13941.5	1	3.3982	78.93
6	13942.0	1	2.9125	70.21
6	13942.5	1	2.7977	68.6
6	13943.0	1	2.6728	63.35
6	13943.5	1	2.4144	56.22
6	13944.0	1	2.2295	57.71
7	12475.0	3	4.5166	108.95
7	12475.5	3	4.9058	100.13
7	12476.0	3	5.1457	110.85
7	12476.5	3	5.5705	83.19
7	12477.0	3	6.2324	109.38
7	12477.5	3	6.1885	112.06
7	12478.0	3	5.2889	100.53
7	12478.5	3	4.6812	89.37
7	12479.0	3	4.3571	81.76
7	12479.5	3	4.2231	96.78
7	12480.0	3	4.2478	92.42
7	12480.5	3	4.2119	88.66
7	12481.0	3	4.2014	91.6
7	12481.5	3	4.162	94.65
7	12482.0	1	4.2987	88.36
7	12482.5	3	4.2716	86.33
7	12483.0	2	4.1604	94.55
7	12483.5	2	4.422	84.6
7	12484.0	2	5.2332	92.93
7	12484.5	2	4.8178	93.53
7	12485.0	2	3.6873	95.66
7	12485.5	2	3.5422	97.93
7	12486.0	2	4.5445	105.4
7	12486.5	2	6.414	99.33
7	12487.0	2	8.1378	99.42
7	12487.5	3	9.3783	101.82
7	12488.0	3	8.5038	107.68
7	12488.5	3	6.4645	101.34
7	12489.0	3	5.9799	87.4
7	12489.5	3	5.6349	92.48
7	12490.0	3	4.9817	98.2

Table B.1 Gamma Ray and Deep Resistivity data from wells 1, 6 &amp; 7 (cont.).

7	12490.5	1	4.427	85.11
7	12491.0	3	5.5266	94.02
7	12491.5	3	6.9175	103.3
7	12492.0	3	7.059	104.17
7	12492.5	3	6.5881	93.54
7	12493.0	3	6.1477	95.13
7	12493.5	2	6.03	95.34
7	12494.0	2	6.0637	110.92
7	12494.5	2	4.8587	102.05
7	12495.0	2	5.1273	106.1
7	12495.5	2	5.5089	104.43
7	12496.0	3	6.9401	108.78
7	12496.5	3	8.3413	97.75
7	12497.0	3	8.4117	108.98
7	12497.5	3	7.7336	103.81
7	12498.0	3	7.8103	104.5
7	12498.5	3	6.4679	104.45
7	12499.0	3	6.2384	108.37
7	12499.5	1	6.1044	109.16
7	12500.0	3	5.6305	89.11
7	12500.5	3	4.809	97.69
7	12501.0	3	4.4491	98.3
7	12501.5	3	4.595	99.52
7	12502.0	3	4.0057	100.94
7	12502.5	3	4.1275	89.57
7	12503.0	2	4.1197	87.44
7	12503.5	3	4.6104	105.6
7	12504.0	3	5.4222	106.29
7	12504.5	3	5.6938	86.38
7	12505.0	3	5.7249	94.04
7	12505.5	3	5.752	89.37
7	12506.0	3	5.6463	90.83
7	12506.5	3	5.246	87.46
7	12507.0	3	5.2264	93.61
7	12507.5	3	5.3534	101.52
7	12508.0	3	5.1364	113.02
7	12508.5	3	5.0077	101.44
7	12509.0	3	4.8393	90.18
7	12509.5	3	4.4402	93.84

Table B.1 Gamma Ray and Deep Resistivity data from wells 1, 6 &amp; 7 (cont.).

7	12510.0	3	4.7058	96.47
7	12510.5	3	5.2639	89.38
7	12511.0	3	5.9806	88.95
7	12511.5	3	7.3837	82.42
7	12512.0	3	6.6816	101.8
7	12512.5	3	4.9747	99.59
7	12513.0	3	3.9963	100.73
7	12513.5	3	3.7763	83.59
7	12514.0	3	3.9441	91.51
7	12514.5	3	4.3093	87.04
7	12515.0	3	4.982	98.5
7	12515.5	3	5.5389	90.18
7	12516.0	3	6.8843	95.27
7	12516.5	3	7.948	110.4
7	12517.0	3	8.0632	102.69
7	12517.5	3	6.1924	108.12
7	12518.0	3	5.381	94.5
7	12518.5	3	4.3586	82.27
7	12519.0	3	5.2019	88.51
7	12519.5	3	6.9584	108.09
7	12520.0	3	7.173	81.29
7	12520.5	3	8.9588	102.17
7	12521.0	3	10.458	100.26
7	12521.5	3	11.96	103.12
7	12522.0	3	12.3468	103.3
7	12522.5	3	10.6985	105.73
7	12523.0	3	9.9438	104.26
7	12523.5	3	8.8912	107.83
7	12524.0	3	8.4395	108.98
7	12524.5	3	7.4884	105.22
7	12525.0	3	7.0729	103.35
7	12525.5	3	6.2858	109.98
7	12526.0	3	7.3035	97.99
7	12526.5	3	8.2035	91.6
7	12527.0	3	8.3979	105.06
7	12527.5	3	7.1725	75.17
7	12528.0	3	6.3721	103.92
7	12528.5	3	5.7592	99.19
7	12529.0	3	5.193	91.3

Table B.1 Gamma Ray and Deep Resistivity data from wells 1, 6 &amp; 7(cont.).

7	12529.5	3	4.7671	105.38
7	12530.0	3	4.1912	92.31
7	12530.5	3	3.8445	89.78
7	12531.0	3	3.9148	96.57
7	12531.5	3	4.9285	93.4
7	12532.0	3	5.6256	90.46
7	12532.5	1	4.6005	100.13
7	12533.0	4	3.9767	93.94
7	12533.5	3	4.6239	109.15
7	12534.0	3	4.6857	87.85
7	12534.5	3	4.4581	102.36
7	12535.0	3	3.8808	94.55
7	12535.5	3	4.3296	81.16
7	12536.0	4	4.4663	105.81
7	12536.5	4	4.6461	103.17
7	12537.0	4	5.6016	84.91
7	12537.5	4	7.7776	106.22
7	12538.0	4	6.1948	104.37
7	12538.5	4	4.7475	107.91
7	12539.0	4	3.9244	89.99
7	12539.5	4	3.9491	88.46
7	12540.0	3	4.4069	82.88
7	12540.5	3	5.1667	101.43
7	12541.0	3	5.5188	94.4
7	12541.5	3	5.3934	91.88
7	12542.0	3	5.4743	108.47
7	12542.5	3	5.6594	90.72
7	12543.0	3	5.6178	92.52
7	12543.5	3	5.6538	92.18
7	12544.0	3	5.6235	87.9
7	12544.5	3	5.5172	98.24
7	12545.0	3	5.908	94.4
7	12545.5	3	6.5527	98.06
7	12546.0	3	5.7114	95.88
7	12546.5	3	5.0048	104.39
7	12547.0	3	5.2234	91.3
7	12547.5	3	5.902	91.57
7	12548.0	3	5.5981	77.12
7	12548.5	3	5.7544	89.73

Table B.1 Gamma Ray and Deep Resistivity data from wells 1, 6 &amp; 7 (cont.).

7	12549.0	3	5.8313	97.72
7	12549.5	3	5.6956	90.05
7	12550.0	3	5.3665	100.08
7	12550.5	3	5.1158	109.37
7	12551.0	3	5.1748	95.24
7	12551.5	3	5.3042	100.72
7	12552.0	3	5.2608	85.92
7	12552.5	3	4.9925	102.35
7	12553.0	3	4.8578	94.95
7	12553.5	3	4.5364	109.25
7	12554.0	3	3.8155	89.47
7	12554.5	3	3.6277	89.38
7	12555.0	3	4.0962	85.52
7	12555.5	3	4.6171	109.15
7	12556.0	3	4.9893	101.44
7	12556.5	3	5.6068	88.62
7	12557.0	3	6.4069	101.16
7	12557.5	3	6.3411	108.74
7	12558.0	3	6.1976	105.93
7	12558.5	3	6.0631	110.83
7	12559.0	3	6.8681	90.66
7	12559.5	3	7.8633	106.56
7	12560.0	3	6.3643	97.16
7	12560.5	3	5.6662	89.36
7	12561.0	3	5.7585	94.54
7	12561.5	2	5.9653	93.36
7	12562.0	3	5.7193	102.18
7	12562.5	3	5.8972	88.36
7	12563.0	3	5.836	93.02
7	12563.5	3	6.1804	110.78
7	12564.0	3	6.637	103.23
7	12564.5	3	7.3256	90.17
7	12565.0	3	7.5036	104.81
7	12565.5	3	7.5824	96.35
7	12566.0	3	7.4286	102.29
7	12566.5	3	6.9956	103.44
7	12567.0	3	6.9597	107.37
7	12567.5	3	7.0643	101.79
7	12568.0	3	7.1927	94.43

Table B.1 Gamma Ray and Deep Resistivity data from wells 1, 6 &amp; 7 (cont.).

7	12568.5	4	7.0792	100.79
7	12569.0	4	7.3516	83.99
7	12569.5	4	7.6991	103.39
7	12570.0	3	10.3854	99.99
7	12570.5	3	9.0168	101.18
7	12571.0	3	6.2151	108.46
7	12571.5	3	5.021	97.08
7	12572.0	3	5.0457	104.74
7	12572.5	3	5.395	95.14
7	12573.0	3	6.0657	110.47
7	12573.5	3	6.7989	91.29
7	12574.0	3	7.6578	110.05
7	12574.5	4	8.0669	106.34
7	12575.0	4	7.641	100.61
7	12575.5	3	7.6511	105.85
7	12576.0	3	8.2784	94.31
7	12576.5	3	8.9355	106.86
7	12577.0	3	8.026	105.7
7	12577.5	4	7.2506	96.16
7	12578.0	4	7.4216	102.66
7	12578.5	4	7.9256	108.57
7	12579.0	3	9.1371	98.69
7	12579.5	3	8.5747	104.78
7	12580.0	3	6.4987	104.17
7	12580.5	2	4.8861	106.11
7	12581.0	2	5.8952	86.35
7	12581.5	3	7.4099	90.36
7	12582.0	3	7.6362	93.34
7	12582.5	3	7.1515	80.93
7	12583.0	3	6.1292	105.6
7	12583.5	4	5.2734	96.1
7	12584.0	3	4.7353	105.5
7	12584.5	3	5.4162	102.64
7	12585.0	3	6.3592	97.14
7	12585.5	4	6.6111	92.23
7	12586.0	4	7.2774	101.72
7	12586.5	3	7.3687	78.51
7	12587.0	3	7.1184	90.57
7	12587.5	4	6.6141	99.08

Table B.1 Gamma Ray and Deep Resistivity data from wells 1, 6 &amp; 7 (cont.).

7	12588.0	3	6.3829	104.65
7	12588.5	3	7.1762	86.25
7	12589.0	3	7.512	102.29
7	12589.5	3	7.2873	97.81
7	12590.0	3	8.0139	105.53
7	12590.5	3	10.1879	104.95
7	12591.0	3	10.3533	101.65
7	12591.5	3	9.0999	96.05
7	12592.0	3	6.2508	110.26
7	12592.5	3	4.9461	97.05
7	12593.0	3	6.3443	103.26
7	12593.5	3	9.0509	95.87
7	12594.0	3	14.3433	108.34
7	12594.5	3	13.7812	104.69
7	12595.0	3	11.0079	104.43
7	12595.5	3	9.1796	102.34
7	12596.0	3	8.0881	102.26
7	12596.5	3	7.7732	101.11
7	12597.0	3	10.6154	102.26
7	12597.5	2	13.0817	105.07
7	12598.0	2	15.9354	111.41
7	12598.5	3	11.8551	101.65
7	12599.0	3	9.8185	101.39
7	12599.5	3	8.7962	108.96
7	12600.0	3	6.3069	111.35
7	12600.5	2	4.3	86.84
7	12601.0	3	5.0213	97.8
7	12601.5	3	5.8744	86.79
7	12602.0	3	7.4143	98.4
7	12602.5	3	9.73	101.04
7	12603.0	3	7.8923	108.66
7	12603.5	3	6.0334	105.72
7	12604.0	3	5.9499	99.02
7	12604.5	3	6.1771	100.37
7	12605.0	2	5.1547	110.08
7	12605.5	2	4.0556	98.5
7	12606.0	1	3.6939	93.33
7	12606.5	2	4.2378	96.37
7	12607.0	3	5.0033	107.12

Table B.1 Gamma Ray and Deep Resistivity data from wells 1, 6 &amp; 7 (cont.).

7	12607.5	3	4.6835	85.52
7	12608.0	3	3.9736	89.47
7	12608.5	3	3.9262	90.09
7	12609.0	3	3.5544	95.09
7	12609.5	3	3.614	90.63
7	12610.0	3	3.7253	86.33
7	12610.5	2	4.0941	92.31
7	12611.0	2	4.7368	112.27
7	12611.5	1	4.9803	103.57
7	12612.0	1	5.714	103.57
7	12612.5	1	10.2647	105.73
7	12613.0	2	17.3349	117.27
7	12613.5	1	11.84	103.99
7	12614.0	2	8.7507	106.18
7	12614.5	3	6.6861	97.32
7	12615.0	2	4.8342	92.52
7	12615.5	2	4.1321	95.97
7	12616.0	3	4.2064	88.26
7	12616.5	1	4.2185	91.81
7	12617.0	1	4.1701	94.24
7	12617.5	1	4.0344	98.5
7	12618.0	1	4.7915	97.79
7	12618.5	2	5.5841	78.68
7	12619.0	2	5.9584	97.46
7	12619.5	2	5.0571	106.39
7	12620.0	2	4.6783	97.89
7	12620.5	3	4.434	89.88
7	12621.0	3	3.916	93.94
7	12621.5	1	3.3796	95.08
7	12622.0	1	3.2416	100.03
7	12622.5	3	3.3461	92.2
7	12623.0	3	3.7392	82.88
7	12623.5	3	3.4299	89.7
7	12624.0	3	2.8673	93.03
7	12624.5	3	2.6033	101.59
7	12625.0	3	2.5945	101.3
7	12625.5	3	2.7662	99.55
7	12626.0	3	2.9924	98.71
7	12626.5	3	2.9334	98.76

Table B.1 Gamma Ray and Deep Resistivity data from wells 1, 6 &amp; 7 (cont.).

7	12627.0	3	2.7718	101.4
7	12627.5	3	2.606	93.78
7	12628.0	3	2.534	103.61
7	12628.5	3	2.6744	94.66
7	12629.0	3	2.9078	92.52
7	12629.5	3	3.047	89.56
7	12630.0	3	2.9223	96.34
7	12630.5	3	2.8516	96.17
7	12631.0	2	3.1395	94.11
7	12631.5	2	3.2023	94.51
7	12632.0	2	3.4436	88.99
7	12632.5	1	3.6608	90.19
7	12633.0	3	5.4633	107.83
7	12633.5	3	6.132	96.1
7	12634.0	3	3.7491	83.79
7	12634.5	3	2.8534	93.94
7	12635.0	3	3.024	98.23
7	12635.5	3	3.1768	95.22
7	12636.0	3	3.0212	96.1
7	12636.5	3	2.9221	94.73
7	12637.0	2	3.0432	92.3
7	12637.5	2	3.2321	98.61
7	12638.0	2	3.4588	91.73
7	12638.5	3	3.6664	91.3
7	12639.0	3	3.4955	99.01
7	12639.5	1	3.3739	94.15
7	12640.0	3	3.3127	95.46
7	12640.5	3	3.2732	96.58
7	12641.0	3	3.1038	90.67
7	12641.5	3	2.9713	99.83
7	12642.0	1	3.0055	93.98
7	12642.5	3	3.1373	95.36
7	12643.0	3	3.354	92.4
7	12643.5	3	3.4161	91.53
7	12644.0	2	3.8127	89.88
7	12644.5	1	4.079	97.79
7	12645.0	1	3.7822	88.87
7	12645.5	3	3.7213	89.58
7	12646.0	3	3.8547	90.89

Table B.1 Gamma Ray and Deep Resistivity data from wells 1, 6 &amp; 7 (cont.).

7	12646.5	1	3.8143	91
7	12647.0	3	3.477	94.65
7	12647.5	3	3.0285	94.99
7	12648.0	3	3.0065	95.91
7	12648.5	3	2.9812	97.34
7	12649.0	3	3.1102	91.91
7	12649.5	3	3.2314	96.88
7	12650.0	1	3.223	95.05
7	12650.5	3	3.2557	97.3
7	12651.0	3	2.9296	99.64
7	12651.5	3	2.8464	98.86
7	12652.0	2	2.7187	93.3
7	12652.5	3	2.56	107.28

**APPENDIX C.  
LITHOFACIES DATA**

Table C.1. Lithofacies data from wells 1, 5-7, and 11. The following values are included in the table: well name, depth and lithofacies.

Table C.1 Lithofacies data.

Well name (#)	MD	LF
1	12099.0	3
1	12099.5	3
1	12100.0	3
1	12100.5	3
1	12101.0	3
1	12101.5	3
1	12102.0	3
1	12102.5	3
1	12103.0	3
1	12103.5	1
1	12104.0	1
1	12104.5	3
1	12105.0	3
1	12105.5	2
1	12106.0	3
1	12106.5	3
1	12107.0	3
1	12107.5	2
1	12108.0	3
1	12108.5	3
1	12109.0	3
1	12109.5	3
1	12110.0	3
1	12110.5	3
1	12111.0	3
1	12111.5	3
1	12112.0	3
1	12112.5	3
1	12113.0	3
1	12113.5	3
1	12114.0	3
1	12114.5	3
1	12115.0	3
1	12115.5	2
1	12116.0	3
1	12116.5	3
1	12117.0	3
1	12117.5	3

Table C.1 Lithofacies data (cont.).

1	12118.0	3
1	12118.5	3
1	12119.0	3
1	12119.5	2
1	12120.0	1
1	12120.5	3
1	12121.0	3
1	12121.5	3
1	12122.0	1
1	12122.5	1
1	12123.0	3
1	12123.5	3
1	12124.0	3
1	12124.5	3
1	12125.0	3
1	12125.5	3
1	12126.0	2
1	12126.5	3
1	12127.0	3
1	12127.5	2
1	12128.0	3
1	12128.5	3
1	12129.0	3
1	12129.5	2
1	12130.0	3
1	12130.5	3
1	12131.0	2
1	12131.5	1
1	12132.0	1
1	12132.5	3
1	12133.0	3
1	12133.5	3
1	12134.0	3
1	12134.5	3
1	12135.0	3
1	12135.5	3
1	12136.0	1
1	12136.5	3
1	12137.0	1

Table C.1 Lithofacies data (cont.).

1	12137.5	2
1	12138.0	3
1	12138.5	3
1	12139.0	3
1	12139.5	3
1	12140.0	3
1	12140.5	3
1	12141.0	3
1	12141.5	3
1	12142.0	3
1	12142.5	2
1	12143.0	3
1	12143.5	3
1	12144.0	3
1	12144.5	3
1	12145.0	3
1	12145.5	1
1	12146.0	3
1	12146.5	3
1	12147.0	3
1	12147.5	3
1	12148.0	3
1	12148.5	3
1	12149.0	3
1	12149.5	3
1	12150.0	2
1	12150.5	3
1	12151.0	3
1	12151.5	3
1	12152.0	3
1	12152.5	3
1	12153.0	3
1	12153.5	3
1	12154.0	3
1	12154.5	3
1	12155.0	3
1	12155.5	3
1	12156.0	3
1	12156.5	3

Table C.1 Lithofacies data (cont.).

1	12157.0	3
1	12157.5	3
1	12158.0	3
1	12159.5	3
1	12160.0	3
1	12160.5	3
1	12161.0	3
1	12161.5	3
1	12162.0	3
1	12162.5	3
1	12163.0	3
1	12163.5	3
1	12164.0	3
1	12164.5	3
1	12165.0	3
1	12165.5	1
1	12166.0	3
1	12166.5	3
1	12167.0	3
1	12167.5	3
1	12168.0	1
1	12168.5	1
1	12169.0	3
1	12169.5	3
1	12170.0	3
1	12170.5	3
1	12171.0	3
1	12171.5	3
1	12172.0	3
1	12172.5	3
1	12173.0	3
1	12173.5	1
1	12174.0	3
1	12174.5	3
1	12175.0	3
1	12175.5	1
1	12176.0	3
1	12176.5	3

Table C.1 Lithofacies data (cont.).

1	12177.0	3
1	12177.5	3
1	12178.0	2
1	12178.5	3
1	12179.0	1
1	12179.5	1
1	12180.0	3
1	12180.5	3
1	12181.0	2
1	12181.5	2
1	12182.0	2
1	12182.5	3
1	12183.0	3
1	12183.5	3
1	12184.0	3
1	12184.5	1
1	12185.0	1
1	12185.5	1
1	12186.0	3
1	12186.5	1
1	12187.0	1
1	12187.5	1
1	12188.0	1
1	12188.5	2
1	12189.0	1
1	12189.5	3
1	12190.0	1
1	12190.5	2
1	12191.0	1
1	12191.5	2
1	12192.0	2
1	12192.5	3
1	12193.0	3
1	12193.5	3
1	12194.0	3
1	12194.5	3
1	12195.0	3
1	12195.5	3

Table C.1 Lithofacies data (cont.).

1	12196.0	1
1	12196.5	1
1	12197.0	3
1	12197.5	3
1	12198.0	3
1	12198.5	3
1	12199.0	3
1	12199.5	1
1	12200.0	2
1	12200.5	1
1	12201.0	2
1	12201.5	2
1	12202.0	2
1	12202.5	2
1	12203.0	3
1	12203.5	3
1	12204.0	3
1	12204.5	1
1	12205.0	1
1	12205.5	1
1	12206.0	1
1	12206.5	1
1	12207.0	1
1	12207.5	2
1	12208.0	1
1	12208.5	1
1	12209.0	3
1	12209.5	3
1	12210.0	2
1	12210.5	3
1	12211.0	3
1	12211.5	3
1	12212.0	2
1	12212.5	1
1	12213.0	1
1	12213.5	1
1	12214.0	1
5	15149.0	3

Table C.1 Lithofacies data (cont.).

5	15149.1	3
5	15149.2	3
5	15149.3	3
5	15149.4	3
5	15149.5	3
5	15149.6	3
5	15149.7	3
5	15149.8	3
5	15149.9	3
5	15150.0	3
5	15150.1	3
5	15150.2	3
5	15150.3	3
5	15150.4	3
5	15150.5	2
5	15150.6	2
5	15150.7	2
5	15150.8	2
5	15150.9	2
5	15151.0	2
5	15151.1	2
5	15151.2	1
5	15151.3	1
5	15151.4	1
5	15151.5	3
5	15151.6	3
5	15151.7	3
5	15151.8	3
5	15151.9	3
5	15152.0	3
5	15152.1	3
5	15152.2	3
5	15152.3	3
5	15154.7	3
5	15154.8	3
5	15154.9	3
5	15155.0	3
5	15155.1	1

Table C.1 Lithofacies data (cont.).

5	15155.2	3
5	15155.3	3
5	15155.4	3
5	15155.5	3
5	15155.6	3
5	15155.7	3
5	15155.8	3
5	15155.9	1
5	15156.0	3
5	15156.1	3
5	15156.2	3
5	15156.3	3
5	15156.4	3
5	15156.5	3
5	15156.6	3
5	15156.7	3
5	15156.8	3
5	15156.9	1
5	15157.0	1
5	15157.1	1
5	15157.2	1
5	15157.3	1
5	15157.4	1
5	15157.5	1
5	15157.6	1
5	15157.7	1
5	15157.8	1
5	15157.9	1
5	15158.0	3
5	15158.1	3
5	15158.2	3
5	15158.3	3
5	15158.4	3
5	15158.5	3
5	15158.6	3
5	15158.7	3
5	15158.8	3
5	15158.9	3

Table C.1 Lithofacies data (cont.).

5	15159.0	3
5	15159.1	3
5	15159.2	3
5	15159.3	3
5	15159.4	3
5	15159.5	3
5	15159.6	3
5	15159.7	3
5	15159.8	3
5	15159.9	3
5	15160.0	3
5	15160.1	3
5	15160.2	3
5	15160.3	3
5	15160.4	3
5	15160.5	3
5	15160.6	3
5	15160.7	3
5	15160.8	3
5	15160.9	3
5	15161.0	2
5	15161.1	2
5	15161.2	2
5	15161.3	2
5	15161.4	2
5	15161.5	2
5	15161.6	2
5	15161.7	1
5	15161.8	1
5	15161.9	1
5	15162.0	1
5	15162.1	1
5	15162.2	1
5	15162.3	1
5	15162.4	2
5	15162.5	2
5	15162.6	2
5	15162.7	2

Table C.1 Lithofacies data (cont.).

5	15162.8	2
5	15162.9	2
5	15163.0	2
5	15163.1	2
5	15163.2	2
5	15163.3	2
5	15163.4	2
5	15163.5	3
5	15163.6	3
5	15163.7	1
5	15163.8	1
5	15163.9	1
5	15164.0	1
5	15164.1	2
5	15164.2	2
5	15164.3	2
5	15164.4	2
5	15164.5	2
5	15164.6	2
5	15164.7	2
5	15164.8	2
5	15164.9	2
5	15165.0	2
5	15165.1	2
5	15165.2	2
5	15165.3	2
5	15165.4	1
5	15165.5	1
5	15165.6	3
5	15165.7	3
5	15165.8	3
5	15165.9	3
5	15166.0	3
5	15166.1	3
5	15166.2	3
5	15166.3	3
5	15166.4	3
5	15166.5	3

Table C.1 Lithofacies data (cont.).

5	15166.6	3
5	15166.7	3
5	15166.8	2
5	15166.9	2
5	15167.0	2
5	15167.1	2
5	15167.2	2
5	15167.3	2
5	15167.4	3
5	15167.5	3
5	15167.6	3
5	15167.7	3
5	15167.8	3
5	15167.9	3
5	15168.0	3
5	15168.1	3
5	15168.2	3
5	15168.3	3
5	15168.4	3
5	15168.5	3
5	15168.6	3
5	15168.7	3
5	15168.8	3
5	15168.9	3
5	15169.0	3
5	15169.1	3
5	15169.2	3
5	15169.3	3
5	15169.4	3
5	15169.5	3
5	15169.6	3
5	15169.7	3
5	15169.8	3
5	15169.9	3
5	15170.0	3
5	15170.1	2
5	15170.2	2
5	15170.3	2

Table C.1 Lithofacies data (cont.).

5	15170.4	2
5	15170.5	2
5	15170.6	3
5	15170.7	3
5	15170.8	3
5	15170.9	3
5	15171.0	3
5	15171.1	3
5	15171.2	3
5	15171.3	3
5	15171.4	3
5	15171.5	3
5	15171.6	3
5	15171.7	1
5	15171.8	1
5	15171.9	3
5	15172.0	3
5	15172.1	3
5	15172.2	3
5	15172.3	3
5	15172.4	3
5	15172.5	1
5	15172.6	1
5	15172.7	3
5	15172.8	3
5	15172.9	3
5	15173.0	3
5	15173.1	3
5	15173.2	3
5	15173.3	3
5	15173.4	3
5	15173.5	3
5	15173.6	3
5	15173.7	2
5	15173.8	2
5	15173.9	3
5	15174.0	3
5	15174.1	3

Table C.1 Lithofacies data (cont.).

5	15174.2	3
5	15174.3	3
5	15174.4	3
5	15174.5	2
5	15174.6	2
5	15174.7	2
5	15174.8	2
5	15174.9	3
5	15175.0	3
5	15175.1	3
5	15175.2	3
5	15175.3	3
5	15175.4	3
5	15175.5	3
5	15175.6	3
5	15175.7	3
5	15175.8	3
5	15175.9	3
5	15176.0	3
5	15176.1	3
5	15176.2	3
5	15176.3	3
5	15176.4	3
5	15176.5	2
5	15176.6	2
5	15176.7	2
5	15176.8	3
5	15176.9	3
5	15177.0	3
5	15177.1	3
5	15177.2	3
5	15177.3	3
5	15177.4	3
5	15177.5	3
5	15177.6	3
5	15177.7	3
5	15177.8	1
5	15177.9	1

Table C.1 Lithofacies data (cont.).

5	15178.0	3
5	15178.1	3
5	15178.2	3
5	15178.3	3
5	15178.4	3
5	15178.5	3
5	15178.6	3
5	15178.7	3
5	15178.8	2
5	15178.9	2
5	15179.0	2
5	15179.1	2
5	15179.2	2
5	15179.3	2
5	15179.4	2
5	15179.5	2
5	15179.6	2
5	15179.7	2
5	15179.8	1
5	15179.9	1
5	15180.0	1
5	15180.1	3
5	15180.2	3
5	15180.3	3
5	15180.4	3
5	15180.5	3
5	15180.6	3
5	15180.7	3
5	15180.8	3
5	15180.9	3
5	15181.0	3
5	15181.1	3
5	15181.2	3
5	15181.3	3
5	15181.4	3
5	15181.5	3
5	15181.6	3
5	15181.7	3

Table C.1 Lithofacies data (cont.).

5	15181.8	3
5	15181.9	3
5	15182.0	3
5	15182.1	3
5	15182.2	3
5	15182.3	3
5	15182.4	3
5	15182.5	3
5	15182.6	3
5	15182.7	3
5	15182.8	3
5	15182.9	3
5	15183.0	3
5	15183.1	3
5	15183.2	3
5	15183.3	3
5	15183.4	3
5	15183.5	3
5	15183.6	3
5	15183.7	3
5	15183.8	3
5	15183.9	3
5	15184.0	3
5	15184.1	3
5	15184.2	3
5	15184.3	3
5	15184.4	3
5	15184.5	3
5	15184.6	3
5	15184.7	3
5	15184.8	3
5	15184.9	1
5	15185.0	3
5	15185.1	3
5	15185.2	2
5	15185.3	2
5	15185.4	3
5	15185.5	3

Table C.1 Lithofacies data (cont.).

5	15185.6	3
5	15185.7	3
5	15185.8	3
5	15185.9	3
5	15186.0	3
5	15186.1	3
5	15186.2	3
5	15186.3	3
5	15186.4	3
5	15186.5	3
5	15186.6	3
5	15186.7	3
5	15186.8	1
5	15186.9	1
5	15187.0	1
5	15187.1	1
5	15187.2	1
5	15187.3	2
5	15187.4	2
5	15187.5	2
5	15187.6	2
5	15187.7	2
5	15187.8	2
5	15187.9	2
5	15188.0	1
5	15188.1	1
5	15188.2	3
5	15188.3	3
5	15188.4	3
5	15188.5	3
5	15188.6	3
5	15188.7	3
5	15188.8	3
5	15188.9	3
5	15189.0	3
5	15189.1	3
5	15189.2	3
5	15189.3	3

Table C.1 Lithofacies data (cont.).

5	15189.4	3
5	15189.5	3
5	15189.6	3
5	15189.7	3
5	15189.8	3
5	15189.9	3
5	15190.0	2
5	15190.1	2
5	15190.2	2
5	15190.3	2
5	15190.4	2
5	15190.5	2
5	15190.6	2
5	15190.7	2
5	15190.8	2
5	15190.9	2
5	15191.0	2
5	15191.1	2
5	15191.2	2
5	15191.3	2
5	15191.4	2
5	15191.5	2
5	15191.6	2
5	15191.7	2
5	15191.8	2
5	15191.9	2
5	15192.0	2
5	15192.1	2
5	15192.2	2
5	15192.3	2
5	15192.4	2
5	15192.5	2
5	15192.6	2
5	15192.7	2
5	15192.8	1
5	15192.9	1
5	15193.0	3
5	15193.1	3

Table C.1 Lithofacies data (cont.).

5	15193.2	3
5	15193.3	3
5	15193.4	3
5	15193.5	3
5	15193.6	3
5	15193.7	3
5	15193.8	3
5	15193.9	3
5	15194.0	3
5	15194.1	3
5	15194.2	3
5	15194.3	3
5	15194.4	3
5	15194.5	3
5	15194.6	3
5	15194.7	3
5	15194.8	3
5	15194.9	3
5	15195.0	3
5	15195.1	3
5	15195.2	3
5	15195.3	3
5	15195.4	3
5	15195.5	3
5	15195.6	3
5	15195.7	3
5	15195.8	3
5	15195.9	3
5	15196.0	3
5	15196.1	3
5	15196.2	3
5	15196.3	3
5	15196.4	3
5	15196.5	3
5	15196.6	3
5	15196.7	3
5	15196.8	3
5	15196.9	3

Table C.1 Lithofacies data (cont.).

5	15197.0	3
5	15197.1	3
5	15197.2	3
5	15197.3	3
5	15197.4	3
5	15197.5	3
5	15197.6	3
5	15197.7	3
5	15197.8	3
5	15197.9	3
5	15198.0	3
5	15198.1	3
5	15198.2	3
5	15198.3	3
5	15198.4	3
5	15198.5	3
5	15198.6	3
5	15198.7	3
5	15198.8	3
5	15198.9	3
5	15199.0	3
5	15199.1	3
5	15199.2	3
5	15199.3	3
5	15199.4	3
5	15199.5	3
5	15199.6	3
5	15199.7	3
5	15199.8	3
5	15199.9	3
5	15200.0	3
5	15200.1	3
5	15200.2	3
5	15200.3	2
5	15200.4	2
5	15200.5	2
5	15200.6	2
5	15200.7	2

Table C.1 Lithofacies data (cont.).

5	15200.8	2
5	15200.9	2
5	15201.0	2
5	15201.1	2
5	15201.2	2
5	15201.3	2
5	15201.4	3
5	15201.5	3
5	15201.6	3
5	15201.7	3
5	15201.8	3
5	15201.9	3
5	15202.0	3
5	15202.1	3
5	15202.2	3
5	15202.3	3
5	15202.4	3
5	15202.5	3
5	15202.6	3
5	15202.7	3
5	15202.8	3
5	15202.9	3
5	15203.0	3
5	15203.1	3
5	15203.2	3
5	15203.3	3
5	15203.4	3
5	15203.5	3
5	15203.6	3
5	15203.7	3
5	15203.8	3
5	15203.9	3
5	15204.0	3
5	15204.1	3
5	15204.2	3
5	15204.3	3
5	15204.4	3
5	15204.5	3

Table C.1 Lithofacies data (cont.).

5	15204.6	3
5	15204.7	3
5	15204.8	3
5	15204.9	3
5	15205.0	3
5	15205.1	3
5	15205.2	3
5	15205.3	3
5	15205.4	3
5	15205.5	3
5	15205.6	3
5	15205.7	3
5	15205.8	3
5	15205.9	3
5	15206.0	3
5	15206.1	3
5	15206.2	3
5	15206.3	3
5	15206.4	2
5	15206.5	2
5	15206.6	2
5	15206.7	2
5	15206.8	2
5	15206.9	2
5	15207.0	2
5	15207.1	2
5	15207.2	2
5	15207.3	2
5	15207.4	2
5	15207.5	3
5	15207.6	3
5	15207.7	3
5	15207.8	3
5	15207.9	3
5	15208.0	3
5	15208.1	3
5	15208.2	3
5	15208.3	3

Table C.1 Lithofacies data (cont.).

5	15208.4	3
5	15208.5	3
5	15208.6	3
5	15208.7	3
5	15208.8	3
5	15208.9	3
5	15209.0	3
5	15209.1	3
5	15209.2	3
5	15209.3	3
5	15209.4	3
5	15209.5	3
5	15209.6	3
5	15209.7	3
5	15209.8	3
5	15209.9	3
5	15210.0	2
5	15210.1	2
5	15210.2	2
5	15210.3	2
5	15210.4	2
5	15210.5	2
5	15210.6	2
5	15210.7	2
5	15210.8	2
5	15210.9	2
5	15211.0	2
5	15211.1	2
5	15211.2	2
5	15211.3	2
5	15211.4	2
5	15211.5	3
5	15211.6	3
5	15211.7	3
5	15211.8	3
5	15211.9	3
5	15212.0	3
5	15212.1	3

Table C.1 Lithofacies data (cont.).

5	15212.2	3
5	15212.3	3
5	15212.4	3
5	15212.5	3
5	15212.6	2
5	15212.7	2
5	15212.8	3
5	15212.9	3
5	15213.0	3
5	15213.1	3
5	15213.2	3
5	15213.3	3
5	15213.4	3
5	15213.5	3
5	15213.6	3
5	15213.7	3
5	15213.8	3
5	15213.9	3
5	15214.0	3
5	15214.1	3
5	15214.2	3
5	15214.3	3
5	15214.4	3
5	15214.5	3
5	15214.6	3
5	15214.7	1
5	15214.8	1
5	15214.9	1
5	15215.0	3
5	15215.1	3
5	15215.2	3
5	15215.3	3
5	15215.4	3
5	15215.5	3
5	15215.6	3
5	15215.7	3
5	15215.8	3
5	15215.9	3

Table C.1 Lithofacies data (cont.).

5	15216.0	3
5	15216.1	3
5	15216.2	3
5	15216.3	3
5	15216.4	3
5	15216.5	2
5	15216.6	2
5	15216.7	2
5	15216.8	2
5	15216.9	2
5	15217.0	2
5	15217.1	2
5	15217.2	3
5	15217.3	3
5	15217.4	3
5	15217.5	3
5	15217.6	3
5	15217.7	3
5	15217.8	2
5	15217.9	2
5	15218.0	2
5	15218.1	2
5	15218.2	2
5	15218.3	2
5	15218.4	2
5	15218.5	2
5	15218.6	2
5	15218.7	2
5	15218.8	2
5	15218.9	2
5	15219.0	2
5	15219.1	2
5	15219.2	2
5	15219.3	2
5	15219.4	2
5	15219.5	2
5	15219.6	2
5	15219.7	1

Table C.1 Lithofacies data (cont.).

5	15219.8	1
5	15219.9	2
5	15220.0	2
5	15220.1	2
5	15220.2	2
5	15220.3	2
5	15220.4	2
5	15220.5	2
5	15220.6	1
5	15220.7	3
5	15220.8	3
5	15220.9	3
5	15221.0	3
5	15221.1	3
5	15221.2	3
5	15221.3	3
5	15221.4	3
5	15221.5	3
5	15221.6	3
5	15221.7	1
5	15221.8	3
5	15221.9	3
5	15222.0	3
5	15222.1	3
5	15222.2	3
5	15222.3	3
5	15222.4	1
5	15222.5	1
5	15222.6	1
5	15222.7	3
5	15222.8	3
5	15222.9	3
5	15223.0	3
5	15223.1	3
5	15223.2	3
5	15223.3	3
5	15223.4	1
5	15223.5	3

Table C.1 Lithofacies data (cont.).

5	15223.6	3
5	15223.7	3
5	15223.8	3
5	15223.9	3
5	15224.0	3
5	15224.1	3
5	15224.2	3
5	15224.3	2
5	15224.4	2
5	15224.5	2
5	15224.6	2
5	15224.7	2
5	15224.8	2
5	15224.9	2
5	15225.0	2
5	15225.1	2
5	15225.2	2
5	15225.3	1
5	15225.4	2
5	15225.5	2
5	15225.6	2
5	15225.7	1
5	15225.8	1
5	15225.9	1
5	15226.0	1
5	15226.1	3
5	15226.2	3
5	15226.3	3
5	15226.4	3
5	15226.5	3
5	15226.6	2
5	15226.7	2
5	15226.8	2
5	15226.9	2
5	15227.0	2
5	15227.1	2
5	15227.2	2
5	15227.3	2

Table C.1 Lithofacies data (cont.).

5	15227.4	2
5	15227.5	2
5	15227.6	2
5	15227.7	1
5	15227.8	1
5	15227.9	1
5	15228.0	3
5	15228.1	3
5	15228.2	1
5	15228.3	1
5	15228.4	1
5	15228.5	3
5	15228.6	3
5	15228.7	1
5	15228.8	2
5	15228.9	2
5	15229.0	2
5	15229.1	2
5	15229.2	2
5	15229.3	2
5	15229.4	1
5	15229.5	1
5	15229.6	1
5	15229.7	1
5	15229.8	3
5	15229.9	3
5	15230.0	3
5	15230.1	3
5	15230.2	3
5	15230.3	3
5	15230.4	3
5	15230.5	3
5	15230.6	3
5	15230.7	3
5	15230.8	3
5	15230.9	3
5	15231.0	3
5	15231.1	3

Table C.1 Lithofacies data (cont.).

5	15231.2	3
5	15231.3	3
5	15231.4	3
5	15231.5	3
5	15231.6	3
5	15231.7	3
5	15231.8	3
5	15231.9	3
5	15232.0	3
5	15232.1	3
5	15232.2	3
5	15232.3	3
5	15232.4	3
5	15232.5	3
5	15232.6	3
5	15232.7	3
5	15232.8	3
5	15232.9	3
5	15233.0	3
5	15233.1	3
5	15233.2	3
5	15233.3	3
5	15233.4	3
5	15233.5	3
5	15233.6	3
5	15233.7	3
5	15233.8	3
5	15233.9	3
5	15234.0	2
5	15234.1	3
5	15234.2	3
5	15234.3	3
5	15234.4	3
5	15234.5	3
5	15234.6	3
5	15234.7	3
5	15234.8	3
5	15234.9	1

Table C.1 Lithofacies data (cont.).

5	15235.0	3
5	15235.1	3
5	15235.2	3
5	15235.3	3
5	15235.4	3
5	15235.5	3
5	15235.6	3
5	15235.7	3
5	15235.8	3
5	15235.9	3
5	15236.0	3
5	15236.1	3
5	15236.2	3
5	15236.3	3
5	15236.4	1
5	15236.5	3
5	15236.6	3
5	15236.7	3
5	15236.8	3
5	15236.9	3
5	15237.0	3
5	15237.1	3
5	15237.2	3
5	15237.3	3
5	15237.4	3
5	15237.5	3
5	15237.6	1
5	15237.7	3
5	15237.8	3
5	15237.9	3
5	15238.0	3
5	15238.1	3
5	15238.2	3
5	15238.3	3
5	15238.4	3
5	15238.5	3
5	15238.6	3
5	15238.7	3

Table C.1 Lithofacies data (cont.).

5	15238.8	3
5	15238.9	3
5	15239.0	3
5	15239.1	3
5	15239.2	3
5	15239.3	3
5	15239.4	3
5	15239.5	3
5	15239.6	3
5	15239.7	3
5	15239.8	3
5	15239.9	3
5	15240.0	3
5	15240.1	3
5	15240.2	3
5	15240.3	3
5	15240.4	3
5	15240.5	3
5	15240.6	3
5	15240.7	3
5	15240.8	3
5	15240.9	3
5	15241.0	3
5	15241.1	3
5	15241.2	3
5	15241.3	3
5	15241.4	3
5	15241.5	3
5	15241.6	3
5	15241.7	3
5	15241.8	3
5	15241.9	3
5	15242.0	3
5	15242.1	3
5	15242.2	3
5	15242.3	3
5	15242.4	3
5	15242.5	3

Table C.1 Lithofacies data (cont.).

5	15242.6	2
5	15242.7	2
5	15242.8	2
5	15242.9	2
5	15243.0	2
5	15243.1	2
5	15243.2	2
5	15243.3	2
5	15243.4	2
5	15243.5	2
5	15243.6	2
5	15243.7	2
5	15243.8	2
5	15243.9	2
5	15244.0	2
5	15244.1	2
5	15244.2	2
5	15244.3	2
5	15244.4	2
5	15244.5	2
5	15244.6	2
5	15244.7	2
5	15244.8	2
5	15244.9	2
5	15245.0	2
5	15245.1	2
5	15245.2	2
5	15245.3	2
5	15245.4	2
5	15245.5	2
5	15245.6	2
5	15245.7	2
5	15245.8	2
5	15245.9	2
5	15246.0	2
5	15246.1	2
5	15246.2	2
5	15246.3	2

Table C.1 Lithofacies data (cont.).

5	15246.4	2
5	15246.5	2
5	15246.6	2
5	15247.4	1
5	15247.5	1
5	15247.6	1
5	15247.7	1
5	15247.8	1
5	15247.9	1
5	15248.0	1
5	15248.1	1
6	13763.5	3
6	13764.0	3
6	13764.5	3
6	13765.0	3
6	13765.5	3
6	13766.0	3
6	13766.5	2
6	13767.0	3
6	13767.5	2
6	13768.0	2
6	13768.5	2
6	13769.0	3
6	13769.5	2
6	13770.0	3
6	13770.5	1
6	13771.0	1
6	13771.5	2
6	13772.0	2
6	13772.5	2
6	13773.0	3
6	13773.5	3
6	13774.0	3
6	13774.5	3
6	13775.0	3
6	13775.5	3
6	13776.0	3
6	13776.5	3

Table C.1 Lithofacies data (cont.).

6	13777.0	3
6	13777.5	3
6	13778.0	3
6	13778.5	3
6	13779.0	3
6	13779.5	3
6	13780.0	3
6	13780.5	3
6	13781.0	3
6	13781.5	3
6	13782.0	3
6	13782.5	3
6	13783.0	3
6	13783.5	2
6	13784.0	3
6	13784.5	3
6	13785.0	3
6	13785.5	2
6	13786.0	3
6	13786.5	2
6	13787.0	3
6	13787.5	3
6	13788.0	3
6	13788.5	3
6	13789.0	3
6	13789.5	3
6	13790.0	1
6	13790.5	2
6	13791.0	2
6	13791.5	2
6	13792.0	2
6	13792.5	1
6	13793.0	3
6	13793.5	3
6	13794.0	3
6	13794.5	3
6	13795.0	3
6	13795.5	1

Table C.1 Lithofacies data (cont.).

6	13796.0	3
6	13796.5	3
6	13797.0	3
6	13797.5	3
6	13798.0	3
6	13798.5	3
6	13799.0	3
6	13799.5	3
6	13800.0	3
6	13800.5	3
6	13801.0	3
6	13801.5	3
6	13802.0	2
6	13802.5	2
6	13803.0	3
6	13803.5	3
6	13804.0	3
6	13804.5	3
6	13805.0	3
6	13805.5	3
6	13806.0	3
6	13806.5	3
6	13807.0	3
6	13807.5	3
6	13808.0	3
6	13808.5	3
6	13809.0	3
6	13809.5	1
6	13810.0	3
6	13810.5	3
6	13811.0	3
6	13811.5	3
6	13812.0	1
6	13812.5	3
6	13813.0	1
6	13813.5	3
6	13814.0	3
6	13814.5	3

Table C.1 Lithofacies data (cont.).

6	13815.0	3
6	13815.5	3
6	13816.0	3
6	13816.5	3
6	13817.0	3
6	13817.5	3
6	13818.0	3
6	13818.5	3
6	13819.0	3
6	13819.5	3
6	13820.0	3
6	13820.5	3
6	13821.0	3
6	13821.5	3
6	13822.0	3
6	13822.5	3
6	13823.0	3
6	13823.5	3
6	13824.0	3
6	13824.5	3
6	13825.0	3
6	13825.5	3
6	13826.0	3
6	13826.5	3
6	13827.0	3
6	13827.5	3
6	13828.0	2
6	13828.5	3
6	13829.0	3
6	13829.5	3
6	13830.0	3
6	13830.5	3
6	13831.0	3
6	13831.5	3
6	13832.0	3
6	13832.5	2
6	13833.0	2
6	13833.5	2

Table C.1 Lithofacies data (cont.).

6	13834.0	3
6	13834.5	3
6	13835.0	2
6	13835.5	3
6	13836.0	3
6	13836.5	3
6	13837.0	3
6	13837.5	3
6	13838.0	3
6	13838.5	3
6	13839.0	3
6	13839.5	3
6	13840.0	3
6	13840.5	1
6	13841.0	1
6	13841.5	1
6	13842.0	1
6	13842.5	1
6	13843.0	1
6	13843.5	3
6	13844.0	3
6	13844.5	3
6	13845.0	2
6	13845.5	3
6	13846.0	3
6	13846.5	1
6	13847.0	1
6	13847.5	3
6	13848.0	3
6	13848.5	3
6	13849.0	3
6	13849.5	3
6	13850.0	3
6	13850.5	3
6	13851.0	3
6	13851.5	3
6	13852.0	3
6	13852.5	1

Table C.1 Lithofacies data (cont.).

6	13853.0	3
6	13853.5	3
6	13854.0	3
6	13854.5	3
6	13855.0	3
6	13855.5	3
6	13856.0	3
6	13856.5	3
6	13857.0	3
6	13857.5	1
6	13858.0	3
6	13858.5	3
6	13859.0	3
6	13859.5	2
6	13860.0	3
6	13860.5	3
6	13861.0	3
6	13861.5	1
6	13862.0	1
6	13862.5	1
6	13863.0	1
6	13863.5	1
6	13864.0	1
6	13864.5	3
6	13865.0	3
6	13865.5	3
6	13866.0	3
6	13866.5	3
6	13867.0	3
6	13867.5	3
6	13868.0	3
6	13868.5	2
6	13869.0	3
6	13869.5	2
6	13870.0	2
6	13870.5	2
6	13871.0	3
6	13871.5	3

Table C.1 Lithofacies data (cont.).

6	13872.0	3
6	13872.5	3
6	13873.0	3
6	13873.5	3
6	13874.0	3
6	13874.5	2
6	13875.0	2
6	13875.5	3
6	13876.0	3
6	13876.5	3
6	13877.0	1
6	13877.5	3
6	13878.0	3
6	13878.5	3
6	13879.0	2
6	13879.5	1
6	13880.0	3
6	13880.5	1
6	13881.0	3
6	13881.5	3
6	13882.0	3
6	13882.5	3
6	13883.0	3
6	13883.5	3
6	13884.0	3
6	13884.5	3
6	13885.0	1
6	13885.5	2
6	13886.0	2
6	13886.5	2
6	13887.0	1
6	13887.5	3
6	13888.0	3
6	13888.5	1
6	13889.0	2
6	13889.5	1
6	13890.0	1
6	13890.5	1

Table C.1 Lithofacies data (cont.).

6	13891.0	1
6	13891.5	3
6	13892.0	2
6	13892.5	3
6	13893.0	3
6	13893.5	3
6	13894.0	3
6	13894.5	3
6	13895.0	3
6	13895.5	3
6	13896.0	3
6	13896.5	3
6	13897.0	3
6	13897.5	2
6	13898.0	1
6	13898.5	2
6	13899.0	2
6	13899.5	2
6	13900.0	1
6	13900.5	2
6	13901.0	3
6	13901.5	2
6	13902.0	2
6	13902.5	2
6	13903.0	1
6	13903.5	2
6	13904.0	2
6	13904.5	2
6	13905.0	2
6	13905.5	3
6	13906.0	3
6	13906.5	3
6	13907.0	2
6	13907.5	3
6	13908.0	3
6	13908.5	3
6	13909.0	3
6	13909.5	3

Table C.1 Lithofacies data (cont.).

6	13910.0	3
6	13910.5	3
6	13911.0	3
6	13911.5	3
6	13912.0	3
6	13912.5	2
6	13913.0	1
6	13913.5	1
6	13914.0	1
6	13914.5	2
6	13915.0	3
6	13915.5	3
6	13916.0	2
6	13916.5	3
6	13917.0	3
6	13917.5	3
6	13918.0	2
6	13918.5	3
6	13919.0	2
6	13919.5	2
6	13920.0	2
6	13920.5	3
6	13921.0	2
6	13921.5	1
6	13922.0	2
6	13922.5	2
6	13923.0	2
6	13923.5	3
6	13924.0	2
6	13924.5	2
6	13925.0	2
6	13925.5	3
6	13926.0	3
6	13926.5	2
6	13927.0	1
6	13927.5	1
6	13928.0	1
6	13928.5	1

Table C.1 Lithofacies data (cont.).

6	13929.0	1
6	13929.5	1
6	13930.0	2
6	13930.5	1
6	13931.0	2
6	13931.5	1
6	13932.0	1
6	13932.5	1
6	13933.0	1
6	13933.5	1
6	13934.0	1
6	13934.5	1
6	13935.0	1
6	13935.5	1
6	13936.0	1
6	13936.5	1
6	13937.0	1
6	13937.5	1
6	13938.0	1
6	13938.5	1
6	13939.0	1
6	13939.5	1
6	13940.0	1
6	13940.5	1
6	13941.0	1
6	13941.5	1
6	13942.0	1
6	13942.5	1
6	13943.0	1
6	13943.5	1
6	13944.0	1
7	12475.0	3
7	12475.5	3
7	12476.0	3
7	12476.5	3
7	12477.0	3
7	12477.5	3
7	12478.0	3

Table C.1 Lithofacies data (cont.).

7	12478.5	3
7	12479.0	3
7	12479.5	3
7	12480.0	3
7	12480.5	3
7	12481.0	3
7	12481.5	3
7	12482.0	1
7	12482.5	3
7	12483.0	2
7	12483.5	2
7	12484.0	2
7	12484.5	2
7	12485.0	2
7	12485.5	2
7	12486.0	2
7	12486.5	2
7	12487.0	2
7	12487.5	3
7	12488.0	3
7	12488.5	3
7	12489.0	3
7	12489.5	3
7	12490.0	3
7	12490.5	1
7	12491.0	3
7	12491.5	3
7	12492.0	3
7	12492.5	3
7	12493.0	3
7	12493.5	2
7	12494.0	2
7	12494.5	2
7	12495.0	2
7	12495.5	2
7	12496.0	3
7	12496.5	3
7	12497.0	3

Table C.1 Lithofacies data (cont.).

7	12497.5	3
7	12498.0	3
7	12498.5	3
7	12499.0	3
7	12499.5	1
7	12500.0	3
7	12500.5	3
7	12501.0	3
7	12501.5	3
7	12502.0	3
7	12502.5	3
7	12503.0	2
7	12503.5	3
7	12504.0	3
7	12504.5	3
7	12505.0	3
7	12505.5	3
7	12506.0	3
7	12506.5	3
7	12507.0	3
7	12507.5	3
7	12508.0	3
7	12508.5	3
7	12509.0	3
7	12509.5	3
7	12510.0	3
7	12510.5	3
7	12511.0	3
7	12511.5	3
7	12512.0	3
7	12512.5	3
7	12513.0	3
7	12513.5	3
7	12514.0	3
7	12514.5	3
7	12515.0	3
7	12515.5	3
7	12516.0	3

Table C.1 Lithofacies data (cont.).

7	12516.5	3
7	12517.0	3
7	12517.5	3
7	12518.0	3
7	12518.5	3
7	12519.0	3
7	12519.5	3
7	12520.0	3
7	12520.5	3
7	12521.0	3
7	12521.5	3
7	12522.0	3
7	12522.5	3
7	12523.0	3
7	12523.5	3
7	12524.0	3
7	12524.5	3
7	12525.0	3
7	12525.5	3
7	12526.0	3
7	12526.5	3
7	12527.0	3
7	12527.5	3
7	12528.0	3
7	12528.5	3
7	12529.0	3
7	12529.5	3
7	12530.0	3
7	12530.5	3
7	12531.0	3
7	12531.5	3
7	12532.0	3
7	12532.5	1
7	12533.0	4
7	12533.5	3
7	12534.0	3
7	12534.5	3
7	12535.0	3

Table C.1 Lithofacies data (cont.).

7	12535.5	3
7	12536.0	4
7	12536.5	4
7	12537.0	4
7	12537.5	4
7	12538.0	4
7	12538.5	4
7	12539.0	4
7	12539.5	4
7	12540.0	3
7	12540.5	3
7	12541.0	3
7	12541.5	3
7	12542.0	3
7	12542.5	3
7	12543.0	3
7	12543.5	3
7	12544.0	3
7	12544.5	3
7	12545.0	3
7	12545.5	3
7	12546.0	3
7	12546.5	3
7	12547.0	3
7	12547.5	3
7	12548.0	3
7	12548.5	3
7	12549.0	3
7	12549.5	3
7	12550.0	3
7	12550.5	3
7	12551.0	3
7	12551.5	3
7	12552.0	3
7	12552.5	3
7	12553.0	3
7	12553.5	3
7	12554.0	3

Table C.1 Lithofacies data (cont.).

7	12554.5	3
7	12555.0	3
7	12555.5	3
7	12556.0	3
7	12556.5	3
7	12557.0	3
7	12557.5	3
7	12558.0	3
7	12558.5	3
7	12559.0	3
7	12559.5	3
7	12560.0	3
7	12560.5	3
7	12561.0	3
7	12561.5	2
7	12562.0	3
7	12562.5	3
7	12563.0	3
7	12563.5	3
7	12564.0	3
7	12564.5	3
7	12565.0	3
7	12565.5	3
7	12566.0	3
7	12566.5	3
7	12567.0	3
7	12567.5	3
7	12568.0	3
7	12568.5	4
7	12569.0	4
7	12569.5	4
7	12570.0	3
7	12570.5	3
7	12571.0	3
7	12571.5	3
7	12572.0	3
7	12572.5	3
7	12573.0	3

Table C.1 Lithofacies data (cont.).

7	12573.5	3
7	12574.0	3
7	12574.5	4
7	12575.0	4
7	12575.5	3
7	12576.0	3
7	12576.5	3
7	12577.0	3
7	12577.5	4
7	12578.0	4
7	12578.5	4
7	12579.0	3
7	12579.5	3
7	12580.0	3
7	12580.5	2
7	12581.0	2
7	12581.5	3
7	12582.0	3
7	12582.5	3
7	12583.0	3
7	12583.5	4
7	12584.0	3
7	12584.5	3
7	12585.0	3
7	12585.5	4
7	12586.0	4
7	12586.5	3
7	12587.0	3
7	12587.5	4
7	12588.0	3
7	12588.5	3
7	12589.0	3
7	12589.5	3
7	12590.0	3
7	12590.5	3
7	12591.0	3
7	12591.5	3
7	12592.0	3

Table C.1 Lithofacies data (cont.).

7	12592.5	3
7	12593.0	3
7	12593.5	3
7	12594.0	3
7	12594.5	3
7	12595.0	3
7	12595.5	3
7	12596.0	3
7	12596.5	3
7	12597.0	3
7	12597.5	2
7	12598.0	2
7	12598.5	3
7	12599.0	3
7	12599.5	3
7	12600.0	3
7	12600.5	2
7	12601.0	3
7	12601.5	3
7	12602.0	3
7	12602.5	3
7	12603.0	3
7	12603.5	3
7	12604.0	3
7	12604.5	3
7	12605.0	2
7	12605.5	2
7	12606.0	1
7	12606.5	2
7	12607.0	3
7	12607.5	3
7	12608.0	3
7	12608.5	3
7	12609.0	3
7	12609.5	3
7	12610.0	3
7	12610.5	2
7	12611.0	2

Table C.1 Lithofacies data (cont.).

7	12611.5	1
7	12612.0	1
7	12612.5	1
7	12613.0	2
7	12613.5	1
7	12614.0	2
7	12614.5	3
7	12615.0	2
7	12615.5	2
7	12616.0	3
7	12616.5	1
7	12617.0	1
7	12617.5	1
7	12618.0	1
7	12618.5	2
7	12619.0	2
7	12619.5	2
7	12620.0	2
7	12620.5	3
7	12621.0	3
7	12621.5	1
7	12622.0	1
7	12622.5	3
7	12623.0	3
7	12623.5	3
7	12624.0	3
7	12624.5	3
7	12625.0	3
7	12625.5	3
7	12626.0	3
7	12626.5	3
7	12627.0	3
7	12627.5	3
7	12628.0	3
7	12628.5	3
7	12629.0	3
7	12629.5	3
7	12630.0	3

Table C.1 Lithofacies data (cont.).

7	12630.5	3
7	12631.0	2
7	12631.5	2
7	12632.0	2
7	12632.5	1
7	12633.0	3
7	12633.5	3
7	12634.0	3
7	12634.5	3
7	12635.0	3
7	12635.5	3
7	12636.0	3
7	12636.5	3
7	12637.0	2
7	12637.5	2
7	12638.0	2
7	12638.5	3
7	12639.0	3
7	12639.5	1
7	12640.0	3
7	12640.5	3
7	12641.0	3
7	12641.5	3
7	12642.0	1
7	12642.5	3
7	12643.0	3
7	12643.5	3
7	12644.0	2
7	12644.5	1
7	12645.0	1
7	12645.5	3
7	12646.0	3
7	12646.5	1
7	12647.0	3
7	12647.5	3
7	12648.0	3
7	12648.5	3
7	12649.0	3

Table C.1 Lithofacies data (cont.).

7	12649.5	3
7	12650.0	1
7	12650.5	3
7	12651.0	3
7	12651.5	3
7	12652.0	2
7	12652.5	3
11	13479.0	3
11	13479.5	3
11	13480.0	3
11	13480.5	3
11	13481.0	3
11	13481.5	3
11	13482.0	3
11	13482.5	3
11	13483.0	1
11	13483.5	1
11	13484.0	1
11	13484.5	3
11	13485.0	3
11	13485.5	1
11	13486.0	1
11	13486.5	1
11	13487.0	1
11	13487.5	1
11	13488.0	3
11	13488.5	3
11	13489.0	3
11	13489.5	3
11	13490.0	2
11	13490.5	3
11	13491.0	3
11	13491.5	3
11	13492.0	1
11	13492.5	3
11	13493.0	3
11	13493.5	2
11	13494.0	2

Table C.1 Lithofacies data (cont.).

11	13494.5	2
11	13495.0	2
11	13495.5	2
11	13496.0	2
11	13496.5	2
11	13497.0	2
11	13497.5	3
11	13498.0	1
11	13498.5	1
11	13499.0	2
11	13499.5	2
11	13500.0	2
11	13500.5	3
11	13501.0	3
11	13501.5	3
11	13502.0	3
11	13502.5	3
11	13503.0	1
11	13503.5	1
11	13504.0	1
11	13504.5	1
11	13505.0	2
11	13505.5	1
11	13506.0	2
11	13506.5	3
11	13507.0	3
11	13507.5	3
11	13508.0	2
11	13508.5	2
11	13509.0	1
11	13509.5	3
11	13510.0	3
11	13510.5	3
11	13511.0	3
11	13511.5	3
11	13512.0	3
11	13512.5	3
11	13513.0	1

Table C.1 Lithofacies data (cont.).

11	13513.5	1
11	13514.0	2
11	13514.5	1
11	13515.0	1
11	13515.5	2
11	13516.0	2
11	13516.5	2
11	13517.0	2
11	13517.5	2
11	13518.0	2
11	13518.5	1
11	13519.0	1
11	13519.5	1
11	13520.0	1
11	13520.5	1
11	13521.0	1
11	13521.5	2
11	13522.0	2
11	13522.5	1
11	13523.0	3
11	13523.5	3
11	13524.0	3
11	13524.5	3
11	13525.0	3
11	13525.5	3
11	13526.0	3
11	13526.5	3
11	13527.0	1
11	13527.5	2
11	13528.0	1
11	13528.5	1
11	13529.0	1
11	13529.5	3
11	13530.0	3
11	13530.5	3
11	13531.0	2
11	13531.5	2
11	13532.0	2

Table C.1 Lithofacies data (cont.).

11	13532.5	2
11	13533.0	2
11	13533.5	2
11	13534.0	2
11	13534.5	3
11	13535.0	3
11	13535.5	3
11	13536.0	3
11	13536.5	3
11	13537.0	3
11	13537.5	3
11	13538.0	3
11	13538.5	3
11	13539.0	3
11	13539.5	1
11	13540.0	3
11	13540.5	3
11	13541.0	3
11	13541.5	3
11	13542.0	2
11	13542.5	2
11	13543.0	2
11	13543.5	2
11	13544.0	2
11	13544.5	2
11	13545.0	3
11	13545.5	3
11	13546.0	3
11	13546.5	3
11	13547.0	3
11	13547.5	3
11	13548.0	3
11	13548.5	2
11	13549.0	3
11	13549.5	3
11	13550.0	3
11	13550.5	3
11	13551.0	3

Table C.1 Lithofacies data (cont.).

11	13551.5	3
11	13552.0	3
11	13552.5	3
11	13553.0	3
11	13553.5	3
11	13554.0	3
11	13554.5	3
11	13555.0	3
11	13555.5	3
11	13556.0	3
11	13556.5	3
11	13557.0	3
11	13557.5	3
11	13558.0	3
11	13558.5	3
11	13559.0	1
11	13559.5	3
11	13560.0	3
11	13560.5	3
11	13561.0	3
11	13561.5	3
11	13562.0	3
11	13562.5	3
11	13563.0	3
11	13563.5	3
11	13564.0	2
11	13564.5	1
11	13565.0	3
11	13565.5	1
11	13566.0	3
11	13566.5	3
11	13567.0	3
11	13567.5	1
11	13568.0	3
11	13568.5	1
11	13569.0	3
11	13569.5	3
11	13570.0	3

Table C.1 Lithofacies data (cont.).

11	13570.5	3
11	13571.0	3
11	13571.5	3
11	13572.0	3
11	13572.5	3
11	13573.0	3
11	13573.5	2
11	13574.0	2
11	13574.5	2
11	13575.0	2
11	13575.5	3
11	13576.0	3
11	13576.5	3
11	13577.0	3
11	13577.5	3
11	13578.0	3
11	13578.5	3
11	13579.0	3
11	13579.5	3
11	13580.0	3
11	13580.5	3
11	13581.0	3
11	13581.5	3
11	13582.0	3
11	13582.5	3
11	13583.0	1
11	13583.5	2
11	13584.0	2
11	13584.5	3
11	13585.0	3
11	13585.5	3
11	13586.0	3
11	13586.5	2
11	13587.0	3
11	13587.5	3
11	13588.0	3
11	13588.5	3
11	13589.0	2

Table C.1 Lithofacies data (cont.).

11	13589.5	2
11	13590.0	2
11	13590.5	2
11	13591.0	3
11	13591.5	3
11	13592.0	3
11	13592.5	3
11	13593.0	3
11	13593.5	3
11	13594.0	3
11	13594.5	3
11	13595.0	3
11	13595.5	3
11	13596.0	2
11	13596.5	1
11	13597.0	3
11	13597.5	3
11	13598.0	1
11	13598.5	3
11	13599.0	3
11	13599.5	3
11	13600.0	2
11	13600.5	2
11	13601.0	2
11	13601.5	2
11	13602.0	2
11	13602.5	3
11	13603.0	3
11	13603.5	3
11	13604.0	3
11	13604.5	2
11	13605.0	3
11	13605.5	3
11	13606.0	2
11	13606.5	1
11	13607.0	3
11	13607.5	3
11	13608.0	3

Table C.1 Lithofacies data (cont.).

11	13608.5	3
11	13609.0	3
11	13609.5	3
11	13610.0	3
11	13610.5	3
11	13611.0	3
11	13611.5	3
11	13612.0	3
11	13612.5	3
11	13613.0	3
11	13613.5	3
11	13614.0	3
11	13614.5	3
11	13615.0	3
11	13615.5	3
11	13616.0	3
11	13616.5	3
11	13617.0	3
11	13617.5	3
11	13618.0	3
11	13618.5	3
11	13619.0	2
11	13619.5	2
11	13620.0	2
11	13620.5	3
11	13621.0	3
11	13621.5	3
11	13622.0	3
11	13622.5	3
11	13623.0	3
11	13623.5	3
11	13624.0	3
11	13624.5	3
11	13625.0	3
11	13625.5	3
11	13626.0	3
11	13626.5	3
11	13627.0	3

Table C.1 Lithofacies data (cont.).

11	13627.5	3
11	13628.0	3
11	13628.5	3
11	13629.0	3
11	13629.5	3
11	13630.0	3
11	13630.5	3
11	13631.0	3
11	13631.5	3
11	13632.0	3
11	13632.5	3
11	13633.0	3
11	13633.5	3
11	13634.0	3
11	13634.5	3
11	13635.0	3
11	13635.5	3
11	13636.0	3
11	13636.5	3
11	13637.0	3
11	13637.5	2
11	13638.0	2
11	13638.5	2
11	13639.0	3
11	13639.5	3
11	13640.0	3
11	13640.5	3
11	13641.0	3
11	13641.5	3
11	13642.0	3
11	13642.5	3
11	13643.0	3
11	13643.5	3
11	13644.0	3
11	13644.5	3
11	13645.0	3
11	13645.5	3
11	13646.0	3

Table C.1 Lithofacies data (cont.).

11	13646.5	3
11	13647.0	3
11	13647.5	3
11	13648.0	3
11	13648.5	3
11	13649.0	3
11	13649.5	3
11	13650.0	3
11	13650.5	3
11	13651.0	3
11	13651.5	3
11	13652.0	3
11	13652.5	3
11	13653.0	3
11	13653.5	3
11	13654.0	3
11	13654.5	3
11	13655.0	3
11	13655.5	3
11	13656.0	3
11	13656.5	3
11	13657.0	1
11	13657.5	1
11	13658.0	1
11	13658.5	1
11	13659.0	3
11	13659.5	1
11	13660.0	3
11	13660.5	3
11	13661.0	3
11	13661.5	3
11	13662.0	2
11	13662.5	2
11	13663.0	3
11	13663.5	3
11	13664.0	3
11	13664.5	2
11	13665.0	3

Table C.1 Lithofacies data (cont.).

11	13665.5	3
11	13666.0	3
11	13666.5	3
11	13667.0	1
11	13667.5	3
11	13668.0	3
11	13668.5	1
11	13669.0	3
11	13669.5	3
11	13670.0	3
11	13670.5	3
11	13671.0	3
11	13671.5	2
11	13672.0	3
11	13672.5	1
11	13673.0	3
11	13673.5	3
11	13674.0	1
11	13674.5	1
11	13675.0	3
11	13675.5	3
11	13676.0	2
11	13676.5	2
11	13677.0	2
11	13677.5	1
11	13678.0	1
11	13678.5	2
11	13679.0	2
11	13679.5	3
11	13680.0	3
11	13680.5	3
11	13681.0	3
11	13681.5	3
11	13682.0	2
11	13682.5	2
11	13683.0	2
11	13683.5	3
11	13684.0	3

Table C.1 Lithofacies data (cont.).

11	13684.5	3
11	13685.0	3
11	13685.5	2
11	13686.0	2
11	13686.5	2
11	13687.0	2
11	13687.5	2
11	13688.0	3
11	13688.5	3
11	13689.0	3
11	13689.5	3
11	13690.0	3
11	13690.5	3
11	13691.0	3
11	13691.5	3
11	13692.0	3
11	13692.5	3
11	13693.0	3
11	13693.5	3
11	13694.0	3
11	13694.5	3
11	13695.0	3
11	13695.5	3
11	13696.0	3
11	13696.5	3
11	13697.0	3
11	13697.5	3
11	13698.0	2
11	13698.5	2
11	13699.0	3
11	13699.5	3
11	13700.0	3
11	13700.5	3
11	13701.0	3
11	13701.5	3
11	13702.0	3
11	13702.5	3
11	13703.0	3

Table C.1 Lithofacies data (cont.).

11	13703.5	3
11	13704.0	3
11	13704.5	3
11	13705.0	3
11	13705.5	3
11	13706.0	3
11	13706.5	3
11	13707.0	3
11	13707.5	3
11	13708.0	3
11	13708.5	3
11	13709.0	3
11	13709.5	3
11	13710.0	3
11	13710.5	3
11	13711.0	3
11	13711.5	3
11	13712.0	1
11	13712.5	3
11	13713.0	3
11	13713.5	3
11	13714.0	3
11	13714.5	3
11	13715.0	1
11	13715.5	2
11	13716.0	2
11	13716.5	2
11	13717.0	3
11	13717.5	3
11	13718.0	2
11	13718.5	2
11	13719.0	2
11	13719.5	3
11	13720.0	3
11	13720.5	3
11	13721.0	3
11	13721.5	3
11	13722.0	3

Table C.1 Lithofacies data (cont.).

11	13722.5	2
11	13723.0	2
11	13723.5	2
11	13724.0	2
11	13724.5	2
11	13725.0	2
11	13725.5	2
11	13726.0	1
11	13726.5	1
11	13727.0	2
11	13727.5	3
11	13728.0	3
11	13728.5	2
11	13729.0	1
11	13729.5	3
11	13730.0	3
11	13730.5	2
11	13731.0	2
11	13731.5	3
11	13732.0	3
11	13732.5	3
11	13733.0	3
11	13733.5	3
11	13734.0	3
11	13734.5	2
11	13735.0	1
11	13735.5	1
11	13736.0	3
11	13736.5	3
11	13737.0	2
11	13737.5	1
11	13738.0	2
11	13738.5	2
11	13739.0	3
11	13739.5	3
11	13740.0	3
11	13740.5	3
11	13741.0	3

Table C.1 Lithofacies data (cont.).

11	13741.5	2
11	13742.0	2
11	13742.5	3
11	13743.0	3
11	13743.5	3
11	13744.0	3
11	13744.5	3
11	13745.0	3
11	13745.5	3
11	13746.0	3
11	13746.5	3
11	13747.0	3
11	13747.5	3
11	13748.0	3
11	13748.5	3
11	13749.0	3
11	13749.5	1
11	13750.0	1
11	13750.5	1
11	13751.0	1
11	13751.5	3
11	13752.0	1
11	13752.5	1
11	13753.0	1
11	13753.5	1
11	13754.0	1
11	13754.5	1
11	13755.0	1
11	13755.5	1
11	13756.0	1
11	13756.5	1
11	13757.0	1
11	13757.5	1
11	13758.0	1
11	13758.5	1
11	13759.0	1
11	13759.5	1
11	13760.0	1

Table C.1 Lithofacies data (cont.).

11	13760.5	1
11	13761.0	1
11	13761.5	1
11	13762.0	1
11	13762.5	3
11	13763.0	3
11	13763.5	3
11	13764.0	3
11	13764.5	3
11	13765.0	3
11	13765.5	1
11	13766.0	2
11	13766.5	3
11	13767.0	3
11	13767.5	3
11	13768.0	3
11	13768.5	3
11	13769.0	3
11	13769.5	3
11	13770.0	3
11	13770.5	3
11	13771.0	3
11	13771.5	3
11	13772.0	3
11	13772.5	3
11	13773.0	3
11	13773.5	3
11	13774.0	1
11	13774.5	1
11	13775.0	1
11	13775.5	1
11	13776.0	1
11	13776.5	1
11	13777.0	1
11	13777.5	1
11	13778.0	1
11	13778.5	1
11	13779.0	1

Table C.1 Lithofacies data (cont.).

11	13779.5	1
11	13780.0	1
11	13780.5	1
11	13781.0	1
11	13781.5	1
11	13782.0	1
11	13782.5	1
11	13783.0	1
11	13783.5	1
11	13784.0	1
11	13784.5	2
11	13785.0	2
11	13785.5	2
11	13786.0	2
11	13786.5	2
11	13787.0	1
11	13787.5	2
11	13788.0	1
11	13788.5	1
11	13789.0	1

**BIBLIOGRAPHY**

- Allen Jr., J.E., Meylan, M.A., Heitmuller, F.T., 2014, Determining hydrocarbon distribution using resistivity, Tuscaloosa marine shale, southwestern Mississippi: ' Gulf Coast Assoc. Geol. Soc. Trans. 64, 41-57.
- Alnahwi, A., & Loucks, R.G. (2019). Mineralogical composition and total organic carbon quantification using x-ray fluorescence data from the Upper Cretaceous Eagle Ford Group in southern Texas. *AAPG Bulletin*, 103, 2891-2907.
- Barrell, K. A., 1997, Sequence stratigraphy and structural trap styles of the Tuscaloosa Trend: Gulf Coast Association of Geological Societies Transactions, v. 47, p. 27–34.
- Beitel, Hayley Roxana, "Relationships among mineralogy, geochemistry, and oil and gas production in the Tuscaloosa marine shale" (2021). *Masters Theses*. 7975.  
[https://scholarsmine.mst.edu/masters\\_theses/7975](https://scholarsmine.mst.edu/masters_theses/7975)
- Borrok, D.M., Yang, W., Wei, M., Mokhtari, M., 2019, Heterogeneity of the mineralogy and organic content of the Tuscaloosa marine shale: *Mar. Petrol. Geol.* 109, 717–731. <https://doi.org/10.1016Zj.marpetgeo.2019.06.056>.
- Bouma, A.H., 1964. Turbidites. *Dev. Sedimentol.* 3, 247–256.  
[https://doi.org/10.1016/S0070-4571\(08\)70967-1](https://doi.org/10.1016/S0070-4571(08)70967-1).
- Berch, Hunter, "Predicting Potential Unconventional Production in the Tuscaloosa Marine Shale Play Using Thermal Modeling and Log Overlay Analysis" (2013). *LSU Master's Theses*. 3676.  
[https://digitalcommons.lsu.edu/gradschool\\_theses/3676](https://digitalcommons.lsu.edu/gradschool_theses/3676)
- Berg, R. R., & Cook, B. C. (1968). Petrography and origin of Lower Tuscaloosa sandstones, Mallalieu field, Lincoln County, Mississippi. *Gulf Coast Association of Geological Societies Transactions*, 18, 242–255.
- Chasteen, H.R., 1983, Re-evaluation of the Lower Tuscaloosa and Dantzer Formations (Mid-Cretaceous) with emphasis on depositional environments and time-stratigraphic relationships: *Gulf Coast Association of Geological Societies Transactions*, v. 33, p. 31-40.
- Colorado Plateau Geosystems: <https://deeptimemaps.com/western-interior-seaway/>

- Dale, A. W., S. R. Meyers, D. R. Aguilera, S. Arndt, and K. Wallmann, 2011, Controls on organic carbon and molybdenum accumulation in Cretaceous marine sediments from the Cenomanian-Turonian interval including Oceanic Anoxic Event 2: *Chemical Geology*, p. 324-325.
- Drennen, C.W., 1953, Reclassification of outcropping Tuscaloosa group in Alabama: *American Association of Petroleum Geologists Bulletin*, v. 37, p. 522-538.
- Dockery, D. T., 1996, Toward a revision of the generalized stratigraphic column of Mississippi: *Mississippi Geology*, v. 17, p. 1-9.
- Dockery, D. T., and D. E. Thompson, 2016, Cretaceous geology, in D. T. Dockery, and D. E. Thompson, eds., *The geology of Mississippi: Mississippi Department of Environmental Quality, Office of Geology, University Press of Mississippi, Jackson*, p. 133-245.
- Energy Information Administration, 2016 Lower 48 states shale plays: [https://www.eia.gov/maps/images/shale\\_gas\\_lower48.pdf](https://www.eia.gov/maps/images/shale_gas_lower48.pdf)
- Eldrett, J.S., Ma, C., Bergman, S.C., Ozkan, A., Minisini, D., Lutz, B.P., Jackett, S., Macaulay, C.I., & Kelly, A.E. (2015). Origin of limestone-marlstone cycles: Astronomic forcing of organic-rich sedimentary rocks from the Cenomanian to early Coniacian of the Cretaceous Western Interior Seaway, USA. *Earth and Planetary Science Letters*, 423, 98-113.
- Enomoto, C.B., Hackley, P.C., Valentine, B.J., Rouse, W.A., Dulong, F.T., Lohr, C.D., Hatcherian, J.J., 2017, Geologic characterization of the hydrocarbon resource potential of the Upper Cretaceous Tuscaloosa marine shale in Mississippi and Louisiana, U.S.A: *Gulf Coast Assoc. Geol. Soc. Trans.* 67, 95-109.
- Fearn, M. K., 2019, A Petrographic Core Analysis of the Upper Cretaceous Tuscaloosa Marine Shale (TMS), Eads Poitevent et al., No. 1, St. Tammany Parish, Louisiana, 50 USA, Master's thesis, University of Louisiana at Lafayette, Lafayette, Louisiana, 117 p.
- Galloway, W., 2008, Chapter 15 Depositional Evolution of the Gulf of Mexico Sedimentary Basin: *Sedimentary Basins of the World* 5. 10.1016/S1874-5997(08)00015-4.
- Gamero-Diaz, H., Miller, C., Lewis, R., 2013, Core: A Mineralogy Based Classification Scheme for Organic Mudstones. *Proceedings - SPE Annual Technical Conference and Exhibition*. 3. 10.2118/166284-MS.
- Gruebel, R. D., 1985, Exploring the Lower Tuscaloosa in Southwest Mississippi: *G.C.A.G.S. Transactions*, Vol. 35, p. 87-89.

- Hackley, P.C., Enomoto, C.B., Valentine, B.J., Rouse, W.A., Lohr, C.D., Dulong, F.T., Hatcherian, J.J., Brennan, S.T., Craddock, W.H., Finn, T.M., Gaswirth, S.B., Le, P.A., Leathers-Miller, H.M., Marra, K.R., Mercier, T.J., Paxton, S.T., Whidden, K. J., Woodall, C.A., Schenk, C.J., 2018, Assessment of undiscovered continuous oil and gas resources in the Upper Cretaceous Tuscaloosa marine shale of the U.S: Gulf Coast, 2018. U.S. Geol. Surv. Fact Sheet.  
<https://doi.org/10.3133/fs20183043>, 2018-3043.
- Hackley, P.C., Dennen, K.O., Garza, D., Lohr, C.D., Valentine, B.J., Hatcherian, J.J., Enomoto, C.B., Dulong, F.T., 2020, Oil-source rock correlation studies in the unconventional Upper Cretaceous Tuscaloosa marine shale (TMS) petroleum, Mississippi and Louisiana, USA: *Journal of Petroleum Science and Engineering*, Volume 190 (July 2020), 107015.
- Hamilton, W.S. and Cameron, C.P., 1986, Facies relationships and depositional environments of lower Tuscaloosa Formation reservoir sandstones in McComb and Little Creek Field areas, Southwest Mississippi: *American Association of Petroleum Geologists Bulletin*, v. 70, p. 1182-1182.
- Harding, D.P. Mineral identification using a scanning electron microscope. *Mining, Metallurgy & Exploration* 19, 215–219 (2002).  
<https://doi.org/10.1007/BF03403272>
- Hogg, M.D., 1988, Newtonia Field: a model for mid-dip lower Tuscaloosa retrograde deltaic sedimentation: *Gulf Coast Association of Geological Societies Transactions*, v. 38, p. 461–471.
- Holmden, C., A. D. Jacobson, B. B. Sageman, and M. T. Hurtgen, 2016. Response of the Cr isotope proxy to Cretaceous Ocean Anoxic Event 2 in a pelagic carbonate succession from the Western Interior Seaway: *Geochimica et Cosmochimica Acta*, 186, p. 277- 295.
- John, C.J., Jones, B.L., Moncrief, J.E., Bourgeois, R., Harder, B.J., 1997, An Unproven Unconventional Seven Billion Barrel Oil Resource—The Tuscaloosa Marine Shale: vol. 7. Louisiana State University Basin Research Institute Bulletin, Baton Rouge, pp. 22.
- Karges, H.E., 1962, Significance of Lower Tuscaloosa sand patterns in Southwest Mississippi: *Gulf Coast Association of Geological Societies Transactions*, v. 12, p. 171-185.

- Guo, W., Chen, G., Li, Y., Li, Y., Zhang, Y., Zhou, J., Han, W., Xu, X., Ma, Y., & Dang, H. (2021). Factors Controlling the Lower Radioactivity and Its Relation with Higher Organic Matter Content for Middle Jurassic Oil Shale in Yuqia Depression, Northern Qaidam Basin, China: Evidence from Organic and Inorganic Geochemistry. *ACS omega*, 6(11), 7360–7373. <https://doi.org/10.1021/acsomega.0c05618>
- Lazar, O.R., Bohacs, K.M., Macquaker, J.H.S., Schieber, J. & Demko, T.M. (2015a) Capturing key attributes of fine-grained sedimentary rocks in outcrops, cores and thin sections: nomenclature and description guidelines. *Journal of Sedimentary Research*, 85(3), 230–246.
- Lazar, O.R., Bohacs, K.M., Schieber, J., Macquaker, J.H. & Demko, T.M. 2015b. Mudstone Primer: Lithofacies Variations, Diagnostic Criteria, and Sedimentologic-stratigraphic Implications at Lamina to Bedset Scales. SEPM (Society for Sedimentary Geology), Tulsa, OK, doi:<https://doi-org.libproxy.mst.edu/10.2110/sepmcsp.12>.
- Liu, K., 2005, Upper Cretaceous sequence stratigraphy, sea-level fluctuations, and Oceanic Anoxic Events 2 and 3, northeastern Gulf of Mexico: *Stratigraphy* 2, 147-166.
- Lohr, C. D., P. C. Hackley, B. J. Valentine, and C. B. Enomoto, 2016, Thermal gradient trends in the Tuscaloosa marine shale play area: Preliminary results from studies to support oil and natural gas resource assessments: *Gulf Coast Association of Geological Societies Transactions*, v. 66, p. 1099-1108.
- Lohr, C.D., Valentine, B.J., Hackley, P.C., Dulong, F.T., 2020, Characterization of the unconventional Tuscaloosa marine shale reservoir in southwestern Mississippi, USA: Insights from optical and SEM petrography: *Marine and Petroleum Geology*, Volume 121, November 2020, 104580.
- Lowery, C.M., Cunningham, R., Barrie, C.D., Bralower, T., Snedden, J.W., 2017, The northern Gulf of Mexico during OAE2 and the relationship between water depth and black shale development: *Paleoceanography* 32, 1316-1335.
- Mancini, E.A., Smith, C.C., and Payton, J.W., 1980, Geologic age and depositional environment of the 'Pilot sand' and 'Marine Shale' Tuscaloosa Group, South Carlton Field, South Alabama, in *Geology of the Woodbine and Tuscaloosa formations; First annual research conference, Society of Economic Paleontologists and Mineralogists, Gulf Coast Section*, p. 24-25.
- Mancini, E. A., and Puckett, T.M., 2003, Integrated biostratigraphic and sequence stratigraphic approach for correlation and basin interpretation: *Gulf Coast Association of Geological Societies Transactions*, v. 53, p. 517–526.

- Mancini, E.A., Obid, J.A., Badalí, M., Liu, K., & Parcell, W.C. (2008). Sequence-stratigraphic analysis of Jurassic and Cretaceous strata and petroleum exploration in the central and eastern Gulf coastal plain, United States. *AAPG Bulletin*, 92, 1655-1686.
- Macquaker, J.H.S., Bentley, S.J., and Bohacs, K.M., 2010, Wave-enhanced sediment-gravity flows and mud dispersal across the continental shelves: reappraising sediment transport processes operation in ancient mudstone successions: *Geology*, v. 38, p. 947 – 950.
- Minter, L.L., Cameron, C.P., Thomas, A.R., and Ward, W.C., 1992, Carbonate-cemented zones in the Lower Tuscaloosa Formation (Upper Cretaceous), southwestern Mississippi: *Gulf Coast Association of Geological Societies Transactions*, v. 42, p. 279-304.
- O'Brien N R. Significance of lamination in Toarcian (Lower Jurassic) shales from Yorkshire, Great Britain. *Sedimentary Geology*, 1990, 67: 25–34.
- Pair, J. D., 2017, The Tuscaloosa Marine Shale: Geologic History, Depositional Analysis, and Exploration Potential [Master of Science thesis]: Stephen F Austin State University, Electronic Theses and Dissertations. 68.  
<https://scholarworks.sfasu.edu/etds/68>
- Scott, R. 2010. Cretaceous Stratigraphy, Depositional Systems, and Reservoir Facies of the northern Gulf of Mexico. *The Gulf Coast Association of Geological Societies*. V. 60, pp. 597-609
- Spooner Jr., H.V., 1964, Basal Tuscaloosa sediments, east-central Louisiana: *AAPG (Am. Assoc. Pet. Geol.) Bull.*, 48 (1) (1964), pp. 1-21
- Snedden, J. W., Virdell, J., Whiteaker, T. L., & Ganey-Curry, P. (2016). A basin-scale perspective on Cenomanian-Turonian (Cretaceous) depositional systems, greater Gulf of Mexico (USA). *Interpretation*, 4(1), SC1–SC22.  
<https://doi.org/10.1190/INT-2015-0082.1>
- Warner, A. J., 1993, Regional geologic framework of the Cretaceous, offshore Mississippi: final report: Jackson, MS, Mississippi Dept. of Environmental Quality, Office of Geology, Open File Report 21.
- Weitkunat, S., 2015, Facies and Log Analysis of the Tuscaloosa Marine Shale, Master's thesis, University of Louisiana at Lafayette, Lafayette, Louisiana, 65 p.
- Woolf, K. S., 2012, Regional character of the lower Tuscaloosa formation depositional systems and trends in reservoir quality: Ph.D. Dissertation, University of Texas at Austin, 227 p.

Yang, W., Borrok, D.M., Mokhtari, M., 2020, Depositional Environments and Stratigraphic Hierarchy of Upper Cretaceous Tuscaloosa Marine Shale in Central U.S. Gulf Coast – A Core observation: Geological Society of America Abstracts with Programs. Vol 52, No. 6, 2020. doi: 10.1130/abs/2020AM-358947.

## VITA

Efren Mendez is originally from San Antonio, Texas, but resides in Houston, Texas. He attended Sam Houston State University (SHSU) where he was active in various clubs and organizations such as the American Association of Petroleum Geologist student chapter, SHSU Quidditch Club, Geology student chapter, and more. While at SHSU, he interned for Precision Well Logging Inc. as a mudlogger intern, he logged unconventional wells across the Permian Basin, Eagle Ford Shale, and conventional wells in the Frio System in South Texas. He then went on to pursue a Masters degree at Missouri University of Science and Technology (Missouri S&T) in Rolla, MO as a recipient of the Torie Vanderven Fellow. During his time at Missouri S&T, he held leadership roles in the National Association of Environment & Engineering Geologists. He also competed in the AAPG Imperial Barrel Award competition and earned 2<sup>nd</sup> place in the Mid-continent section. While at Missouri S&T, Efren had the opportunity to intern for Pioneer Natural Resources and Chevron North America Exploration and Production. He was able to gain knowledge in the Midland Basin and the San Joaquin Basin – Kern River Field in Bakersfield, CA. He learned new skillsets ranging from machine learning, unconventional and conventional reservoir characterization, oil geochemistry, facies modelling, subsurface mapping, and statistical analyses through high level technical projects that were presented to upper management. He has accepted a full time offer to work for Chevron as a Development Geologist working in Houston, Texas upon graduation. Efren received his master's degree in Geology & Geophysics in December 2022 from Missouri S&T.